Understanding the translation regulation of Fragile X Mental Retardation Protein (FMRP) through its interaction with the ribosome

---

A THESIS TO BE SUBMITTED TO

THE UNIVERSITY OF TRANS-DISCIPLINARY HEALTH SCIENCES AND TECHNOLOGY

FOR THE AWARD OF THE DEGREEOF
DOCTOR OF PHILOSOPHY

BY

MICHELLE NINOCHKA D'SOUZA

UNDER THE GUIDANCE OF

DR.DASARADHI PALAKODETI

INSTITUTE FOR STEM CELL SCIENCE AND REGENERATIVE MEDICINE, GKVK CAMPUS, BELLARY ROAD, BANGALORE -560065

AUGUST,2023

THE UNIVERSITY OF TRANS-DISCIPLINARY HEALTH SCIENCES AND TECHNOLOGY

Private University Established in Karnataka by ACT 35 of 2013

BENGALURU - 560064

DECLARATION BY THE CANDIDATE

I declare that this thesis entitled "***Understanding the translation regulation of Fragile X Mental Retardation Protein through its interaction with the ribosome***" submitted for the award of Doctor of Philosophy to THE UNIVERSITY OF TRANS-DISCIPLINARY HEALTH SCIENCES AND TECHNOLOGY, Bengaluru, is my original work, conducted under the supervision of my guide ***Dr. Dasaradhi Palakodeti*** and co-guide, ***Dr. Ravi S Muddashetty.*** I also wish to inform that no part of the research has been submitted for a degree or examination at any university. References, help and material obtained from other sources have been duly acknowledged

I hereby confirm the originality of the work and that there is no plagiarism in any part of the dissertation.

Place: Bangalore **Signature of the Candidate**

Date: 04.08.2023

Name of candidate: *Michelle Ninochka D'Souza*

Reg. No.: *21018021192*

(November 2019)

THE UNIVERSITY OF TRANS-DISCIPLINARY HEALTH SCIENCES AND TECHNOLOGY

Private University Established in Karnataka by ACT 35 of 2013

BENGALURU - 560064

CERTIFICATE

This is to certify that the work incorporated in this thesis **"*Understanding the translation regulation of Fragile X Mental Retardation Protein through its interaction with the ribosome*"** submitted by ***Michelle Ninochka D'Souza*** was carried out under my supervision. No part of this thesis has been submitted for a degree or examination at any university. References, help and material obtained from other sources have been duly acknowledged. I hereby confirm the originality of the work and that there is no plagiarism in any part of the dissertation.

Research Supervisor:

Date: 04.08.2023

Name, designation & address details:

Dr. Dasaradhi Palakodeti

Associate professor

Institute for Stem cell science and Regenerative Medicine (InStem)

GKVK campus, Bellary road

Bangalore -560065

THE UNIVERSITY OF TRANS-DISCIPLINARY HEALTH SCIENCES AND TECHNOLOGY

Private University Established in Karnataka by ACT 35 of 2013

BENGALURU - 560064

CERTIFICATE

This is to certify that the work incorporated in this thesis **""*Understanding the translation regulation of Fragile X Mental Retardation Protein through its interaction with the ribosome*"** submitted by ***Michelle Ninochka D'Souza*** was carried out under my supervision. No part of this thesis has been submitted for a degree or examination at any university. References, help and material obtained from other sources have been duly acknowledged. I hereby confirm the originality of the work and that there is no plagiarism in any part of the dissertation.

Co-Supervisor

Date: 04.08.2023

Name, designation & address details:

Dr. Ravi S Muddashetty

Associate professor

Centre for Brain Research (CBR), IISc campus

Bangalore -560012

ACKNOWLEDGEMENT

My thesis would not have been possible without the support of many people. Firstly, I extend my gratitude to my PhD mentors Dr.Ravi Muddashetty and Dr. Dasaradhi Palakodeti. Along with being supportive mentors, they have been a great friends and confidants. I sincerely thank my thesis committee member Dr.Vinothkumar Kutti Ragunath whose suggestions and perspectives opened new thinking arenas for me and helped in directing my work towards what it is now. I extend my deepest thanks to our collaborators Dr. Deepak Nair, Dr. James Chelliah, Dr. Arati Ramesh and Dr Shona Chatterjee.

There are many people who contributed in different ways to the completion of this work. I sincerely thank Vishal Tiwari who mentored me during the start of my doctoral work, Dr. Maki Muratahori who taught me everything about stem cell culture.

No number of words are sufficient to express my gratitude and love for my lab mates. I was lucky to have one of the most enriching lab environments where each one was co- operative and helpful, yet constructively critical which improved the quality of my work tremendously. I have learnt many things from each one of them and they contributed the most towards my development, as a researcher and as a person. I thank every lab mate, present and past – Preeti, Vishal, Sreenath, Sudhriti, Bharti, Michelle, Naveen, Vishwaja, Bindu, Sukanya, Sumita, Subhajit, Reena, Abhik and Nisa.

I acknowledge all the funding sources, which have generously supported my work. I thank DST for providing my PhD fellowship for five years and for supporting this work through the Indo-Danish NeuroStem Grant . I had the opportunity to attend several national and international conferences during my PhD, which have expanded my outlook towards research. This would not have been possible without the travel grants I got from DMM and Brain Prize 2023 from FENS, IBRO-PERC. I also thank TDU for my PhD registration, which made the completion of this work possible. I specially acknowledge Mr. Ravi Kumar, the academic coordinator at TDU, for being the point of contact and helping me with all the formalities at TDU. I extend my sincere gratitude to in the BLiSC (Bangalore Life Science Cluster) campus. It truly has one of the best environments for research where everyone is encouraged to think freely and discuss openly. Lastly I'd like to thank my family and friends who have supported me during every step of this journey.

List of figures

Chapter 1

Chapter 3

Chapter 4

Chapter 5

Chapter 6

Chapter 7

Chapter 8

List of tables

Chapter 2

List of contents

Chapter 4 :Contribution of FMRP domains in regulating puncta formation and microtubule association

Chapter 5: Validating the role of FMRP domains through pathogenic FMRP mutations

Chapter 6:Role of nuclear FMRP in regulating protein synthesis

ABSTRACT

Fragile X Syndrome (FXS) is a trinucleotide repeats expansion disorder of the FMR1 gene resulting in intellectual disability. The silencing of the gene due to the expansion of CGG repeat in its 5'UTR results in the loss of the encoded protein Fragile X Messenger Ribonucleoprotein (FMRP). FMRP is nucleo-cytoplasmic located and structurally comprises of protein-interacting, RNA-binding and intrinsically disordered domains, which contribute to its versatile role in a range of biological processes such as chromatin remodeling, ion channel stability, RNA transport and ribosome heterogeneity. Most importantly, FMRP regulates the translation of mRNAs essential for synaptic development and plasticity making it critical for neuronal function and development. The function of FMRP is complex and the contribution of FMRP to FXS pathology is mostly investigated in the absence of the protein. Studying the localization and role of individual domains is beneficial in understanding FMRP-mediated regulation of protein synthesis. Hence I systematically investigated the contribution of FMRP and its individual domains in the dynamic processes of ribosome binding, mRNP granule formation, and microtubule association. I also emphasize the role of phosphorylation of FMRP at Serine 500 in these processes. Additionally, I elucidate the functional consequences of pathogenic point mutations on regulatory mechanisms controlled by FMRP. Lastly, my work also describes a novel role for nuclear FMRP and how its interaction with nuclear small RNA can regulate the ribosome and thus protein synthesis. This is important to understand FMRP domains and their role in coordinating the mechanisms leading to translation regulation.

Chapter 1

Introduction

Plasticity in biological tissues allows organic components to adapt to various conditional changes. The brain is one organ that is considered to possess an unlimited degree of plasticity and this phenomenon is seen to stabilize with age. Neuroplasticity ensures neural synapses and brain pathways to be modified by altered emotions, environmental, behavioral as well as neural stimuli. On a cellular scale, the long-term maintenance of many forms of this plasticity requires the synthesis of new proteins. The regulation of somatic mRNA expression has been extensively studied in the context of neuronal plasticity. But it is very evident that many mRNAs are trafficked to dendrites, suggesting a role for local protein synthesis in maintaining synaptic plasticity. Subcellular protein synthesis is a well conserved mechanism controlling rapid expression of mRNA in response to localized cues[43]. mRNAs are aided for transport by various trans-acting factors like RNA-Binding proteins (RBPs) and non-coding RNAs to form ribonucleoparticles (RNPs).

RNA-Binding Proteins are important cellular effectors of post transcriptional gene expression. Through alternate splicing and translational control of existing mRNAs, they are responsible for generating proteome diversity in the cell. RBPs recognize and bind mRNAs through regulatory elements present in the Untranslated regions (UTRs) and occasionally in the coding regions and transport them to their subcellular localizations [44,45]. This feature is important in polarized cells like neurons where mRNAs are transported to dendrites and axons for localized translation. Apart from directly influencing target metabolism which includes splicing, localization and degradation, neuronal RBPs can also regulate targets indirectly. This is done so through an interaction with other regulatory RNA species such as small nuclear RNAs (snRNA) , small nucleolar RNAs (snoRNA), small cytoplasmic RNAs and microRNAs [46]. The binding of RBPs to various RNA species is mediated through well-known RNA Binding motifs in the proteins. These are often present in multiple copies and multiple forms in the same protein. [47]. This property of RBPs to potentially interact with various species of RNA makes them critical for developmental regulation.

RBP dysregulation has been implicated in a number of neurological diseases and neurodevelopmental disorders. The Hu/ Embryonic lethal abnormal vision-like (ELAVL) family of proteins constitute multiple RNA Recognition Motifs (RRMs) which binds to AU rich regions located in the 3'UTRs of mRNAs that are implicated in learning and memory [48,49]. This interaction facilitates mRNA stability and post-transcriptional regulation of transcripts. However Hu proteins serve as antigens for auto-antibodies generated against them in a neurological disorder called Paraneoplastic subacute sensory neuropathy which is characterized by loss of RNA metabolism and turnover leading to neuronal degeneration in multiple regions of the brain simultaneously [50]. TDP43 is another RRM-containing nuclear RBP that plays a role in RNA processing. The levels of TDP43 in a cell are self-regulated through the destabilization of its own transcript. However in the neurodegenerative disorder Amyotrophic Lateral sclerosis (ALS), this autoregulation is lost, leading to a mis-localization of the protein and consequential loss in gene stability and expression [51]. Not all RBP-based neurological disorders involve dysregulation in mRNA stability. Studies have shown certain neuronal RBPs play a role in splicing as well. Studies indicate that the Survival Motor Neuron protein (SMN) is essential for the maturation of U-snRNPs which are important components of the spliceosome. Reduced expression of this RBP results in Spinal muscular atrophy which is characterized by the degeneration of α-motor neurons in the lower spinal cord followed by progressive muscle weakness[52].

A handful of RBPs are known to form dynamic RNP complexes with other protein partners. RBPs such as Fused in Sarcoma (FUS) and TDP43 are known to form a subtype of RNA granules called Stress granules which alternate between rapid assembly and disassembly thereby controlling translation of the bound transcripts. Both these proteins are known to constitute protein deposits in patients affected by Frontotemporal Dementia (FTD) and ALS [53,54]. Mutations in FUS and TDP43 are known to alter the dynamics of RNA granule assembly which initiate aggregate formation in these neurodegenerative disorders [55]. Evidence also suggests that RBPs such as Staufen1, in its wild-type unmutated form, can be found within neuronal stress granules containing mutated Ataxin2 which is a hallmark of Spinocerebellar Ataxia type 2. In addition to this, multiple neurodegenerative disorders involving mutations of Ataxin2 , TDP43 or even C9orf2 display elevated levels of Staufen1 protein[56]. Taken together it is clear that RBPs play a crucial role in

maintaining normal neuronal physiology and alterations in RBP functioning and RNP assembly can contribute to neurodegeneration.

The Fragile X Mental Retardation Protein (FMRP) is one such RBP that has been widely studied for its diverse cellular roles. FMRP regulates the expression of its target mRNAs which are necessary for neuronal functioning and synaptic plasticity[8]. The loss of FMRP results in Fragile X Syndrome (FXS), a monogenic neurodevelopmental disorder that causes autism in the affected individual. Majority of FMRP's cellular functions have been studied in the context of its absence but the key question is to biochemically assess its role in a normal functioning paradigm. In my thesis project, I have studied the structural contribution of FMRP's domains in regulating neuronal protein synthesis. In this chapter, I will briefly review the properties and functions of FMRP's individual domains and their role in regulating various aspects of translation regulation.

1.1 Fragile X Syndrome

Fragile X syndrome is a classic example of a disorder caused primarily due to translation dysregulation. FXS is the most common form of inherited intellectual disability and is primarily caused due to the silencing of the *FMR1* gene on the X chromosome [57]. Under normal circumstances, the *FMR1* gene contains about 50 CGG repeats in the 5'UTR[58]. However, FXS individuals, who express a full mutation in the gene, display more than 200 CGG repeats leading to its hypermethylation and a consequential transcriptional silencing of the gene [58] (**Figure 1.1A**). FXS afflicts 1 in 7000 males and 1 in 11000 females and also has a strong association with Autism Spectrum Disorder [59]. The complex genetics of FXS has made it difficult to diagnose and determine the prevalence of the disorder. Further, there exists a huge variation in the severity of symptoms between males and females owing to the X-linked nature of the disorder. Due to a compensation from the normal X chromosome, females show a lesser tendency of being affected. [60].

The FMRP protein is ubiquitously expressed in most tissues, with maximum expression in the brain [3,61,62]. To be precise, FMRP is expressed in neural progenitor cells , neurons and in glial cells [63,64].The loss of FMRP in these cell types can partially explain the difficulties in learning, social behavior, hypersensitivity and uncoordinated motor skills , which is captured in FXS-affected individuals [65]. FMRP is also abundantly expressed in the testes consistent with macroorchidism, a predominant phenotype of FXS [62]. However due to the extreme defects seen in

learning and memory, much of FMRP research has been focused on its role in the nervous system.

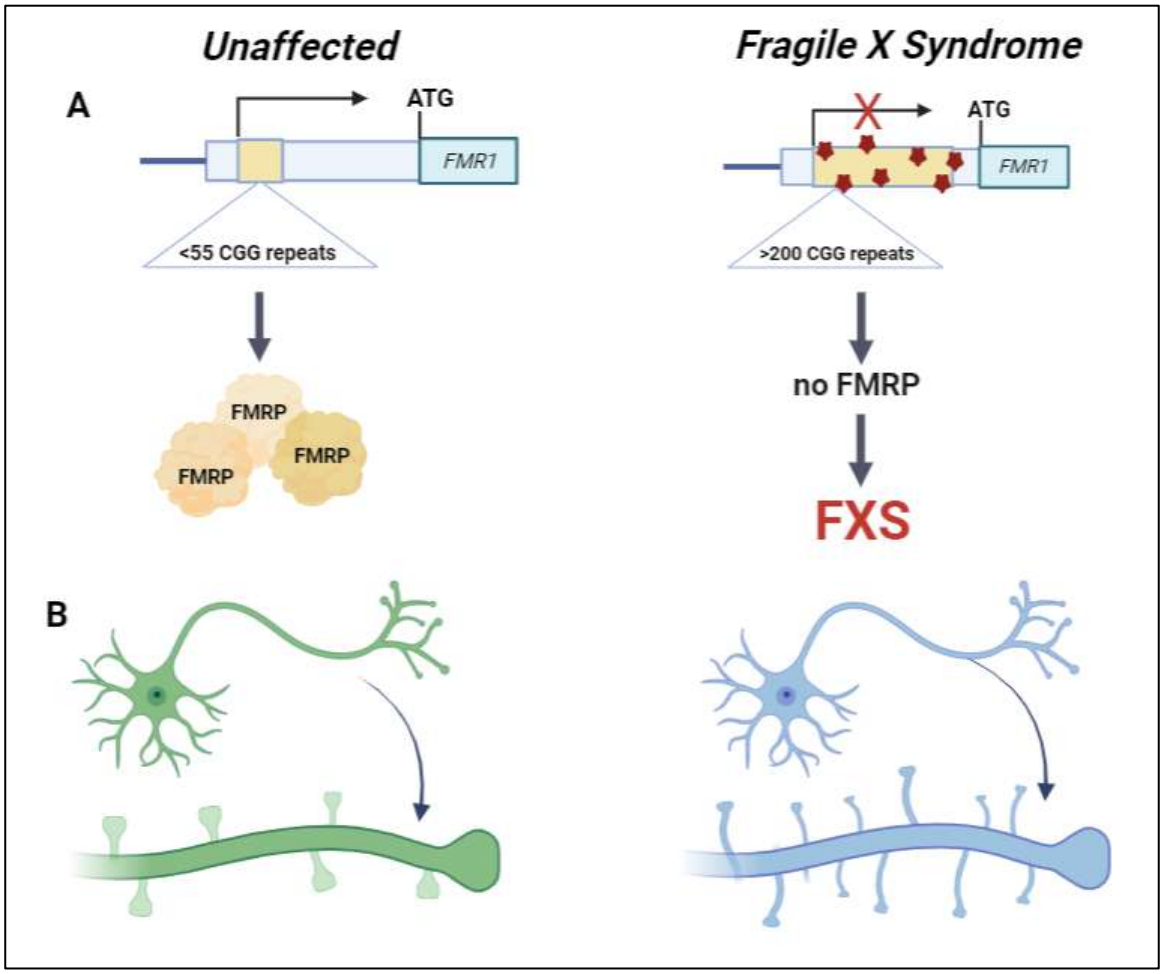

Figure 1.1: Features of canonical Fragile X Syndrome. A- *FMR1 alleles displaying <55 CGG repeats allow for normal transcription and expression of the FMRP protein. However full mutation alleles displaying >200 CGG repeats undergo epigenetic silencing leading to the absence of FMRP which is the primary feature of individuals affected by canonical FXS.* ***B-*** *neurons in FXS affected individuals display increased dendritic branching and immature dendritic spines.*

On a physiological scale, the inactivation of *FMR1* leads to an impairment in brain and cellular function at multiple levels including neurogenesis , dendritic growth, integration of neural circuits and axon guidance[3,8,61]. In particular, FXS neurons display developmental abnormalities such as thin, immature spines and dysregulated dendritic branching [66] (**Figure 1.1B**). Evidences from *Fmr1* KO mice suggest that altered brain development is a consequence of disrupted synaptic plasticity [14]. As a brain-enriched RNA binding protein, FMRP targets a vast variety of

mRNAs and non-coding RNAs such as microRNAs and Long non-coding RNAs both in vivo and *in-vitro*[8,67–69]. In particular, FMRP regulates the expression of a defined set of mRNA targets required for the maintenance of neuronal function and synaptic plasticity [8]. FMRP dynamically transports RNA in the form of granules from the cell body to the synapses in an activity dependent manner through the association with microtubules and their motors[16,70]. The localization of mRNAs such as PSD-95 and MAP1b to the synapse is altered in the absence of FMRP[70,71]. Consequently, the loss in FMRP-mediated translational control of these candidates and many such mRNAs is one of the biggest factors contributing to the pathogenic phenotypes in FXS. However, the precise mechanism underlying dysregulated protein synthesis in FXS is yet to be elucidated.

Majority of FMRP's cellular functions have been studied in the context of its absence but the key question is to biochemically assess its role in a normal functioning paradigm. In my thesis project, I have studied the structural contribution of FMRP's domains in regulating neuronal protein synthesis. In this chapter, I will briefly review the properties and functions of FMRP's individual domains and their role in regulating various aspects of translation regulation.

1.2 Structural organization of FMRP's domains

As an RBP, FMRP has three functionally distinct RNA-binding motifs: two K-homology domains and one RGG Box motif which mediate interactions with RNAs and facilitate mRNA stability, storage, transport and expression [2,61]. But there also exists a series of protein-protein interacting motifs in the amino terminal of FMRP [2]. The emerging concept of translation regulation by FMRP is that it involves a complex network of protein-RNA and protein-protein interactions. However, there is very little structural information available on FMRP to understand its function. The following section will outline the characteristics of FMRP's domains and how the combination and synchronization of domains can contribute to the functional diversity of FMRP in a cell.

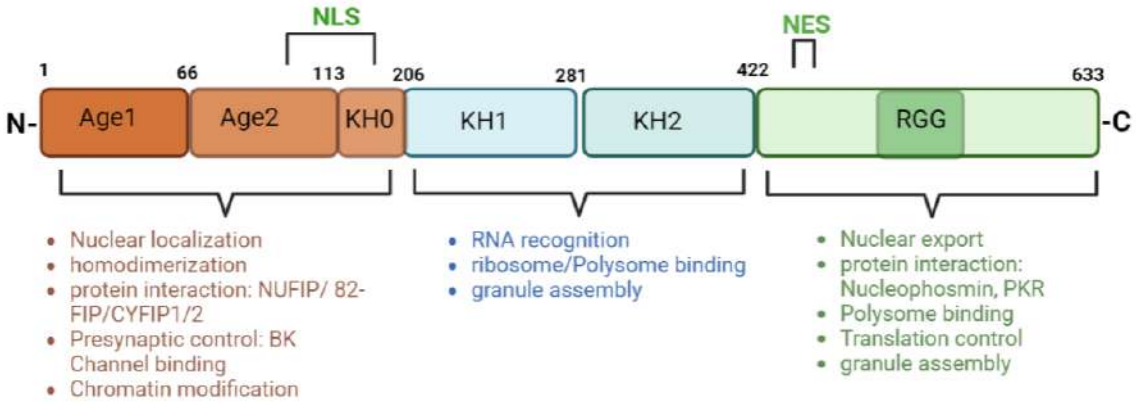

Figure 1.2: Functional organization of FMRP's domains*. FMRP comprises multiple structural domains that add to its functional diversity. These include two Tudor domains that aid in DNA and protein interactions followed by RNA-Binding domains KH1, KH2 and RGG. Each domain is implicated to play a role in specific cellular processes as depicted in the schematic.*

1.2.1 Amino (N)-terminus of FMRP.

The N-terminus of FMRP shows the highest degree of conservation within the FMRP family of proteins[72]. Biochemical characterization of the N-terminus indicates that this independently folded domain can bind RNA as well as homodimerize and interact with other protein partners [73]. Further , structural analysis revealed the presence of two Tudor/ Agenet motifs within this region facilitating protein-protein interactions [74]. FMRP localizes to both the nucleus and the cytoplasm and the sequence which serves as an NLS is located within this region [33]. The N-terminal domain has been shown to interact with multiple nuclear partners of FMRP such as NUFIP and 82-FIP though the consequence of this interaction has not been elucidated [75,76]. Recently, the N-terminus has been linked to FMRP's role in presynaptic functioning through its interaction with large conductance calcium-activated BK channels [77–79]. Further, the Agenet domains have been shown to interact with chromatin and modulate DNA damage response [6]. One prime study indicated that FMRP also interacts with CYFIP1/2 through the N-terminus to regulate synaptic translation [80]. Except for a few studies, majority of the functions described so far portray a translation-independent role of FMRP's N-terminus. The FXS causing R138Q mutation was identified to occur within this N-terminal domain of FMRP[30]. A study showed that the mutant protein elutes earlier from the anion exchange column during purification in comparison to the WT protein[30]. The

positively charged arginine residue maybe critical for specific protein-protein interactions and the shift to a non-polar glutamine may hamper this function.

Very few studies have started to explore the RNA-binding ability of this domain. The amino terminus of FMRP was shown to bind to a few targets: BC1 RNA being one among them [68,69]. Computational analysis revealed that specific residues downstream of the Agenet domains were responsible for this binding. Crystal structure of these residues identified it as a novel KH motif (termed KH0) which could assist in RNA recognition and could potentially explain the RNA binding capacity of the N-terminal domain[2].

1.2.2 K-Homology domains

The N-terminal domain of FMRP is followed by a series of tandem KH1-KH2 domains which perform the typical function of RNA recognition. Crystal structure of FMRP's KH domains revealed that they consist of 3 anti-parallel β-sheets followed by 3 α-helices with a sequence of hydrophobic residues present between the α-helices and β-sheets. This structure enables the association of various RNA targets through varying degrees of affinity [81,82]. However, this structural characteristic was only examined after the discovery of the pathogenic FXS-causing I304N mutation which occurs in the KH2 domain. Importantly, this study showcased the importance of the KH domains to polysome association through the use of the KH2-I304N mutant[83,84]. Nevertheless, this study and many such others described the essential role of KH domains in RNA binding and strengthened the connection between FXS and the loss of RNA-binding characteristic of FMRP [82,85,86]. The KH domains have been shown to interact with mRNAs such as Neurofibromatosis Type1 (NF1), *FMR1*, PPP2CA and UBE3A [87]. It is worth noting that although KH domain-specific targets have been identified, there is no precise mechanism explaining their selective binding and regulation. Initial reports claim that FMRP interacts with targets containing a 'pseudoknot' or 'kissing complex' motifs particularly through the KH2 domain. This interaction was found to compete out FMRP's association with polysomes, a feature that was also KH domain dependent [17,84]. Further Ascano et al described the recognition of ACUK/WGGA motifs within FMRP mRNA targets through the KH1 domain [87]. Suhl et al later discovered that GACR was the only RNA-recognition Element (RRE) that was common among all the predicted FMRP-mRNA datasets [88]. However these previously identified sequences were further taken into question when Athar et al observed that neither of the KH domains , including KH0,

were capable of recognizing the WGGA, ACUK or GACR recognition motifs [89]. These contradictory findings suggest that the KH domain-RNA interactions maybe more complex than just simple recognition of short sequences.

A recent study also showed that FMRP recognizes transcripts that possess m6A modified 'AGACU' motifs through its KH domains [90] .It is uncertain if the KH domains work independently or co-operatively to regulate the expression of FMRP's target mRNAs. Further the aforementioned recognition sequences are present in almost all mRNAs[88]. It is evident that alternate mechanisms of FMRP-mediated translation regulation exist independent of mRNA recognition by the KH domains. A recent Cryo-EM structure suggested that in FMRP-mediated translation repression, the KH1 and KH2 domains bind directly to the ribosome while the RGG motif of the C-terminus interacts with mRNA [91]. Further through the use of FXS-causing missense mutations (G266E and I304N) , the KH domains have also been implicated to regulate the formation and dynamics of neuronal granules [92]. The lack of consensus in the functioning of the KH domains suggests that there are yet more undiscovered mechanisms that can explain their contribution to FMRP-mediated translation regulation.

1.2.3 Intrinsically disordered C-terminus domain.

The C-terminal region of FMRP contributes to the maximum versatility in FMRP's functions. Structurally the C-terminus of FMRP encompasses an RNA-binding RGG box motif present next to the Intrinsically Disordered region (IDR) with low-complexity sequences[93,94]. The C-terminus of FMRP is also shown to harbor a well characterized Nuclear Export Signal (NES) and 2 putative Nucleolar Localization Sequences (NoLS). This is suggested to permit the shuttling of FMRP between the nucleus and the Cytoplasm to facilitate mRNA transport [36,74,95]. Although there is no evidence to support the export of target mRNAs via this NES, the biochemical binding between FMRP-C-term and its mRNAs has been extensively studied. Initial *in-vitro* studies identified FMRP-target mRNAs to be guanine rich RNAs which were capable of forming G-quadruplexes[96–98]. mRNAs such as PSD-95, MAP1B, SEMA3F, NAP22 and serine/threonine protein kinase LMTK1 are some of the few candidates that were found associated with the C-terminal of FMRP and majority of these possess G-quadruplex structures within their 3'UTR [97,99–102].

The RGG box has also been shown to be essential for polysome association of FMRP since deletion of the RGG Box results in its accumulation in lighter non-ribosomal complexes [103,104]. A recent *in-vitro* study showed that together with the C-terminal domain, the RGG Box was capable of inhibiting the translation of both 5'm7G capped as well as uncapped mRNAs that employ the IRES-route of translation initiation [105]. Further, key arginines of this motif are essential for polysome binding and this interaction is heavily regulated by PRMT1-mediated methylations of the arginines [103]. However, the study does not explain why this RNA-binding-feature of the RGG domain is essential for binding to the ribosome. Evidently a large number of FMRP-interacting mRNAs show a prevalence of G-quadruplexes but it is also interesting that G-quadruplexes exist in the expansion segments of 18S and 28S rRNA of the ribosome[89,106,107]. The recent Cryo-EM structure shows that FMRP can directly bind to the ribosome through the RGG-C-terminus tail, suggesting that translation inhibition may depend on the interaction of FMRP with potential G-quadruplexes of rRNA.

The striking presence of unstructured regions within the C-terminus has made it possible to unravel novel functions of FMRP. A recent *in-vitro* study involving pulldown with recombinant FMRP C-term showed that proteins such as Nucleophosmin1 and Protein Kinase R can interact with the C-terminus of FMRP independent of RNA.[108]. This Protein-interacting function of FMRP's C-terminus is interesting since this region was presumed to be predominantly involved in RNA binding. Because of the intrinsically disordered nature of the Low Complexity Regions of FMRP and many other such RBPs, it is now possible to understand their contribution to many cellular mechanisms such as phase separation and granule formation as well.

1.3 Non-canonical FXS mutations

So far, it is evident that the majority of FMRP's functions have been uncovered, particularly by studying them in the background of FXS which results due to the expansion of CGG repeats in the 5'UTR region of *FMR1* gene. Despite this, there is evidence indicating that several conventional mutations in the coding region of *FMR1* gene, apart from CGG-repeat expansions, can cause developmental defects with symptoms similar to FXS. These single point mutations generate both coding and non-coding variants of FMRP that impair FMRP's expression and function. In this study, we chose to employ several mutations present with the coding region of FMRP that would help us understand the structure-function contribution of the domains to protein synthesis regulation (**Figure 1.3)**

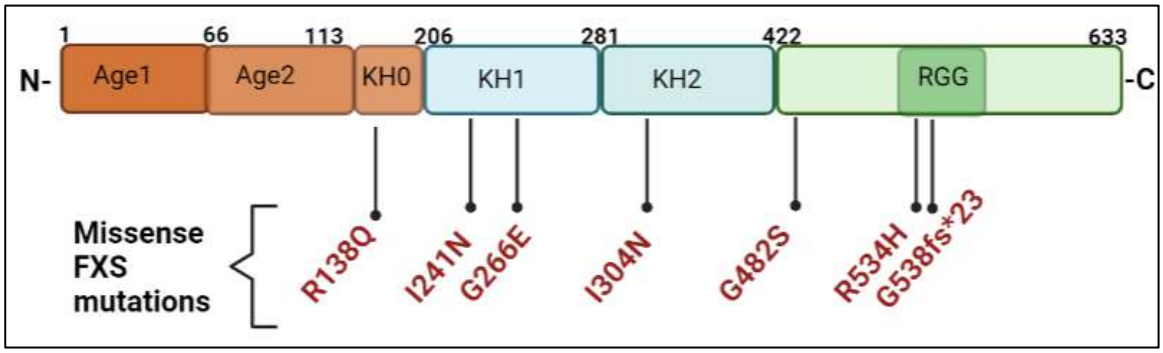

Figure 1.3: Non-canonical mutations of FXS. *Individuals displaying missense mutations in the coding sequence of FMR1 gene also develop FXS like phenotypes. Missense mutations in the domains of FMRP used in this study are highlighted here*

1.3.1 I304N and I241N

The I304N mutation is the first and most widely studied mutation in FMRP known to cause a severe form of FXS [83]. Isoleucine 304 is a highly conserved hydrophobic residue in the KH2 domain of FMRP predominantly playing a role in RNA recognition [109]. This feature of hydrophobicity is also well displayed in other RBPs like hnRNPs which also contain KH2 domains. The initial study of the I304N mutation investigated the importance of the KH2 domains in RNA Binding[83]. Additionally, a structurally equivalent mutation of isoleucine in the KH1 domain was simultaneously generated (I241N) and this also displayed a similar impairment in binding to PolyG and PolyU RNA oligomers [83]. In-silico studies indicate that the substitution of isoleucine to asparagine in either of the FMRP's KH domains results in a complete unfolding of the hydrophobic platform suggesting the importance of both isoleucine and KH

domains in FMRP-mediated RNA-binding [110]. However, this impairment in RNA-recognition by either I241 or I304N has been refuted by multiple studies. Darnell et al demonstrate that I304N and not I241N can affect the binding to kcRNA by full length FMRP[17]. Later studies showed that the I304N mutation affects FMRP-polysome association without affecting mRNA binding [84]. A general characteristic of RBPs containing KH domains is their incorporation into mRNP complexes [111]. But Feng et al clearly indicated that the I304N mutation retains the ability to associate with cytoplasmic mRNAs and even RNA homopolymers[84]. Importantly, this is the first study that suggested the KH domains of FMRP might be associating with ribosomal components instead, since the I304N mutation affected distribution of FMRP in the polysomal fraction. This key observation has been identified repeatedly across multiple studies involving I304N mutation [86]. Moreover it is the translation of a subset of mRNAs that gets affected due to this mutation and not their transport [112]. Hence the I304N mutation can help explain alternate mechanisms that contribute to the pathophysiology of FXS, especially mechanisms that do not purely depend on RNA binding.

1.3.2 R138Q

The R138Q mutation was a novel missense mutation identified in a cohort of developmentally delayed males without CGG- repeat expansion. The mutation codes for an Arginine to glutamine substitution and was identified to affect the conserved residue located within the nuclear localization signal and KH0 domain of FMRP. Arginine 138 is one of the basic residues constituting the NLS and is conserved in the drosophila variant of FMRP as well [33,76]. Studies indicate that this mutation does not affect RNA binding , polysome association or AMPA receptor internalization [113,114]. However, further presynaptic roles of FMRP were tested in the context of this mutation. The absence of FMRP results in a lengthened action potential duration in both mouse hippocampal and cortical neurons however this phenotype cannot be rescued with the R138Q N-terminal domain fragment of FMRP. This study later showed that the N-terminal domain binds to β4 subunit of the BK (Big Potassium) channels located in the presynaptic membrane and that the R138Q mutant severely impairs this association [77,113]. Further the R138Q mutation was also found to impair the role of FMRP in mediating DNA Damage Response by affecting chromatin binding. Although the R to Q mutation does not alter the general structure of the

protein, it is likely to influence the interaction with physiological partners. Further in-silico studies predict that the R138Q mutation can cause destabilization of the protein leading to an increased fibrillogenic tendency [115]. Taken together the R138Q mutation seems to affect cellular mechanisms related to chromatin remodeling and presynaptic functioning and overall it indicates that the role of the N-terminus domain is independent of RNA-binding and translation regulation.

1.3.3 G266E

The G266E mutation is another pathogenic mutation occurring within the KH1 domain of FMRP and results in a Glycine to Glutamate change at amino acid 266 [116]. The positioning of Glycine266 is highly conserved with respect to both KH domain amino acid sequences. The 266th amino acid position of FMRP structurally requires a small, flexible and non-polar amino acid making Glycine the best amino acid candidate in the context of secondary structure of KH domain. In-silico experiments showed that since Glutamate is large and negatively charged, there is likely a chance of it sterically clashing with the surrounding amino acids in the KH domain. This can disrupt several canonical functions of the KH2 domain leading to FXS [114]. The G266E variant of FMRP results in the loss of binding to several known FMRP targets such as Map1b, PSD-95 and CamKII [116]. Further this mutation also results in the loss of polysome binding of FMRP[116]. Additionally, it was also observed that the defect in AMPA receptor internalization could not be rescued by G266E-FMRP when overexpressed in *FMR1* KO mouse hippocampal neurons[116]. The G266E mutation was also demonstrated to affect the formation and dynamic stability of FMRP containing granules in drosophila motor neurons [92]. Similar to the I304N mutation, the consequential increase in size of the mutated residue at amino acid 266 alters the hydrophobicity and affects multimer interactions which explains the numerous cellular processes that get affected downstream of G266E-causing FXS [29]. Together these data suggest that the G266E mutation can disrupt the structure of FMRP and likewise several canonical functions of FMRP.

1.3.4 G482S and R534H

The G482S and R534H missense mutations are located in the C-terminus domain of FMRP and were first discovered together from a cohort of developmental delayed males who also met the criteria for FXS-like phenotype [31]. In-silico analysis of the

two mutations classified them as pathogenic however there is very little experimental evidence in support of this [31]. The G482S and R534H mutations are located within the low complexity region of FMRP making it very difficult to predict their functional outcomes using conventional sequence analysis techniques. The generation of a new Serine residue due to the G482S mutation can possibly affect the phosphorylation of FMRP. Further the R534H mutation is located in the center of the well-studied RNA-binding RGG domain of FMRP suggesting that R534H-FMRP could have hampered recognition and binding.

1.3.5 G-insert / G538 fs*23

The G538fs*23 mutation was identified from a small cohort of developmentally delayed individuals who showed FXS-like phenotypes but with normal CGG repeat lengths [32]. This mutation is the result of an insertion of a guanine in Exon 15 of the *FMR1* gene at position 1457.This single nucleotide insertion in the C-terminus of FMRP, generates a frameshift and a consequent addition of 22 novel amino acids downstream of the insertion followed by a premature termination codon. This also leads to the generation of a truncated form of the mutant FMRP protein which shows reduced expression in the affected individual. The most striking feature of this mutation is the disruption of the RGG domain and a shift in the cellular localization of the expressed mutant protein primarily to the nucleus. To explain this, computational analysis revealed that the novel 22 amino acids can give rise to a motif which resembles a Nucleolar localization sequence. Overall, due to the retention of the mutant protein in the nucleus, there is lesser FMRP available to regulate functions occurring in the synapse. Drosophila neurons overexpressing G538fs*23-hFMRP displayed misguided axonal phenotypes[32]. Nevertheless, the frameshift mutation is a novel platform to understand FXS pathology in the background of lowered protein expression and a gain-of-function property. Specific endogenous isoforms of FMRP have been shown to exist in trace amounts in the nucleolus where they interact with proteins such as Nucleolin to regulate rRNA transcription and ribosome biogenesis[36]. Hence there is a likelihood of this frameshift FMRP mutant affecting ribosome assembly and function. Moreover, this novel C-terminus mutant can give us a clear understanding of the nucleolar role of FMRP in various cell types.

1.4 Role of post translational modifications in modulating FMRP's function

Given the multifarious roles of FMRP in guiding various processes of a cell, it is essential to have spatiotemporal regulation over its functions. Post translational Modifications (PTMs) on various proteins, especially RBPs, govern these functions through the regulation of protein assembly, cellular localization, maintaining activity kinetics , stability and protein turnover rates [117]. These PTMs can act independently or cooperatively to guide complex biological processes and studies indicate that dysregulated PTM dynamics can also lead to a large number of neurological disorders [118,119]. FMRP is a protein that is known to get extensively modified after it is synthesized in the cytoplasm. A growing body of evidence also shows a regulation of FMRP-PTM homeostasis in response to various forms of synaptic signaling and plasticity [15,22,120,121].

The signaling downstream of Group 1 mGluRs plays a significant role in modulating FMRPs function throughout various cell types. DHPG mediated activation of Gp1 mGluRs in hippocampal neurons leads to mGluR-dependent Long Term Depression (LTD) a type of plasticity that is highly regulated through protein synthesis[122]. mGluR-dependent LTD leads to the translation of various mRNAs including that of FMRP itself[123]. FMRP is majorly an inhibitor of translation, repressing the synthesis of proteins that are needed to sustain LTD. However this 'brake' in translation is lifted in the absence of FMRP leading to exaggerated mGluR-LTD, a characteristic which is evident in FXS neurons[13,117]. The following section outlines the common PTMs that play a role in regulating FMRP-mediated protein synthesis.

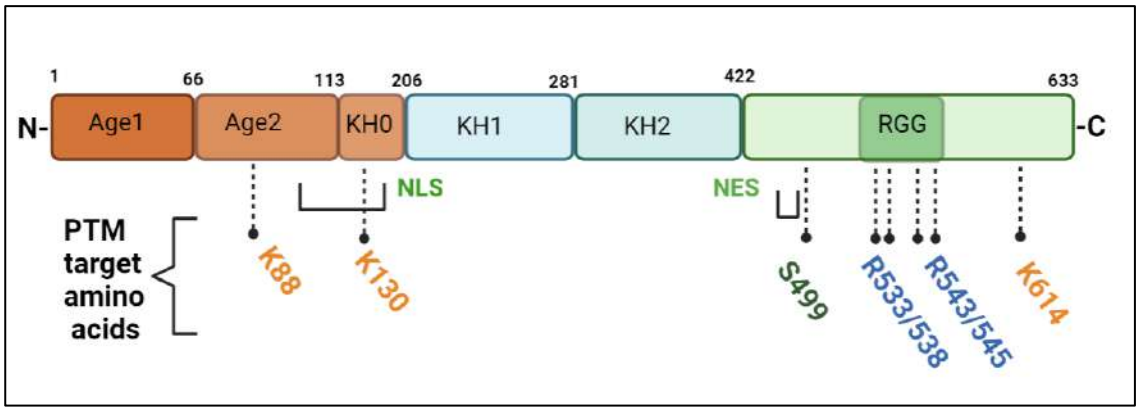

Figure 1.4: Post Translational Modifications alter functions of FMRP's domains. *Schematic depicting the protein-interacting Agenet domains, K-homology KH1 and KH2 domains and RGG box containing C-terminus domain. The schematic*

also depicts the putative Nuclear Localization Signal (111-152aa) and Nuclear Export Signal (425-441aa) along with amino acids that are Post translationally modified (Sumoylation- orange; Phosphorylation- green; Methylation- blue). Although FMRP is known to be ubiquitinated and acetylated, target amino acids for these modifications have not yet been established.

1.4.1 Ubiquitination:

Multiple studies have reported a transient and rapid increase in translation of certain targets such as FMRP, PSD-95 and CamKII downstream of mGluR activation [123]. The increase in FMRP levels is followed by a concomitant drop in its expression back to basal levels, indicating a degradation of the protein. The degradation of the FMRP is mediated through its polyubiquitination and processing via the Ubiquitin-Proteasome system (UPS) and later phase of mGluR-LTD is shown to be hampered if the proteasome activity is blocked. The ubiquitin ligase containing CdH1-APC complex is essential for the polyubiquitination of FMRP during mGluR-LTD. Mice lacking CdH1 display impaired mGluR-LTD in the hippocampus confirming the role of ubiquitination in regulating the dynamics of FMRP-mediated plasticity [124] .

1.4.2 Phosphorylation:

Phosphorylation is one of the most extensively studied PTM of FMRP and occurs within the C-terminal region of the protein. Site-directed mutagenesis in the mouse ortholog of FMRP established that Serine499 was the primary phosphorylation site which triggered the hierarchical autophosphorylation of neighboring serine residues[22] (**Figure 1.4**). The phosphorylation of FMRP results in its accumulation with non-translating and stalled polysomal fractions consistent with its role as a translation repressor. Conversely the dephosphorylation of FMRP increases the translation of its target mRNAs such as Arc and SAPAP3 [10,21,22,125]. The phosphorylation of FMRP also promotes the assembly of the FMRP-AGO2-miR125a complex to inhibit PSD-95 mRNA while mGluR mediated dephosphorylation of FMRP signals the dissociation of this complex allowing PSD-95 mRNA to be translated [126]. Studies show that the dephosphorylation of FMRP downstream of mGluR signaling is transient (1min) and PP2A-dependent.

However, the sustained activation of mGluRs (1-5mins) leads to the inactivation of PP2A followed by the re-phosphorylation of FMRP [21]. PP2A is the major phosphatase targeting FMRP however the kinases that regulate this PTM are many. S6 kinase is a major kinase in hippocampal neurons and S6K knockout (S6K-/-) mice have undetectable levels of phosphorylated FMRP [21]. Importantly the activity of PP2A and S6 Kinase are regulated simultaneously by mTOR signaling. A short activation of mGluR triggers the dephosphorylation of FMRP and inhibition of S6 Kinase in a PP2A-dependent manner [21,23]. An interesting observation by Bartley et al elucidated that the amino acids surrounding the primary phosphorylation site Serine 500, does not constitute the consensus motif for S6 Kinase binding [127]. This suggests that Serine 500 might also be a site for other FMRP-based kinases. Casein Kinase II(CKII) , a constitutively active kinase, was also proposed to phosphorylate FMRP at Serine 500 and promote the consequent phosphorylation on secondary residues [128,129]. The *in-vitro* phosphorylation of FMRP via CKII was observed to induce a reversible phase separation of FMRP containing granules further elucidating the importance of phosphorylation in FMRP-mediated translation repression[130].

1.4.3 Methylation:

Besides Phosphorylation, the methylation of arginines within the RGG motif has also been shown to regulate FMRP-mediated protein synthesis [103]. Arginines R533, R538, R543 and R545 were the primary residues identified to be targets for both symmetric and asymmetric methylation [103] (**Figure 1.4**). This PTM alters the side chain of arginine, increasing its hydrophobicity and steric hindrance and thus has shown to modulate functions such as RNA-binding as well as protein-protein interactions of FMRP[131]. Protein arginine methyltransferase 1 (PRMT1) was shown to methylate specific arginines in the RGG box of FMRP although the role of other PRMTs cannot be ruled out[103]. Methylation of FMRP arginines results in the loss of binding to RNA G-quadruplex structures [103]. This characteristic could potentially explain the loss in translation inhibition of certain FMRP-target mRNAs. This characteristic loss of translation repression was also observed in *in-vitro* translation assays involving methylated FMRP-C-term [130] . Tsang et al also observed that arginine methylation decreases the phase

separating propensity of FMRP in vitro[130]. This particular finding implied that methylation of FMRP inhibits the formation of higher order assemblies which can potentially explain the mechanism behind disassembly of neuronal granules when FMRP gets methylated [130]. Although methylation decreases the RNA-binding ability of FMRP, its precise mechanism in protein synthesis regulation is unclear. Further the need for partial or completely methylated arginines to regulate FMRP interactions is yet to be determined. Hence it would be interesting to dissect the mechanism of FMRP methylation and its contribution to FMRP's functioning in a cell.

1.4.4 Sumoylation:

A wide variety of neurodevelopmental processes are known to be guided by Sumoylation[132,133]. FMRP as a target for sumoylation was only discovered recently. Sumoylation involves the covalent enzymatic conjugation of a small ubiquitin-like modifier (SUMO) protein to lysine residues of the substrate [134]. This process is reversible and guided by a E2-conjugating enzyme Ubc9 and de-sumoylating enzymes called Sentrin proteases (SENPs) [134]. The role of protein sumoylation has been demonstrated to spatiotemporally play a role in the developing rat brain. Additionally, sumoylation is also implicated in many neuronal functions such as synaptic signaling, neurotransmitter release and in regulating spine dynamics [132,133,135,136]. The role of FMRP sumoylation has also been studied downstream of mGluR5 signaling in neurons [134]. A study with rat cortical neurons showed that activation of mGluR5 with DHPG resulted in the Ubc9-mediated sumoylation of N-terminal K33 and K130 and C-terminal K614 residues of FMRP which led to the dissociation of FMRP from neuronal granules[134] (Figure 1.4). An intriguing fact is that the R138Q missense mutation of FMRP is located close to the N-terminal lysines which are targeted for sumoylation[113]. Although the R138Q mutation does not hamper RNA binding, it would be interesting to understand the effect of this mutation on mGluR5 mediated sumoylation of FMRP at these residues which could impact mGluR-dependent protein synthesis.

1.4.5 Acetylation:

The acetylation of FMRP was first detected on the N-terminal Met1 of the protein and has been the most understudied PTM so far. Mass spectrometric analysis of purified recombinant FMRP revealed that the N-terminal MEELVVEVR peptide was primarily acetylated [137]. This is a common feature for around 85% of all human proteins and has been shown to be essential for synthesis, stability and localization of the protein [138]. Since FMRP is known to be nucleo-cytoplasmic shuttling protein, it would be interesting to examine the role of acetylation in guiding the subcellular distribution of FMRP.

1.5 FMRP regulates mRNA expression at various stages of translation

Through subcellular fractionation, it is evident that FMRP sediments with polysomes in neuronal as well as non-neuronal cells[19,139,140]. FMRP is a selective RNA binding protein with over 800 predicted mRNA targets and its association with polysomes supports the hypothesis that it regulates the translation of these mRNAs via this interaction[8,87,96]. As pointed out earlier, the I304N mutation disrupts FMRP's interaction with actively translating polysomes generating a severe phenotype, indicating that this interaction is extremely crucial to the normal functioning of FMRP[18].

On the contrary, FMRP is also found in RNA granules, complexes which supposedly suppress the expression of mRNAs[16,141] (**Figure 1.5**). These RNA transport granules constituting FMRP localize to both dendrites and axons and display both oscillatory and directional transport [7,142,143]. Actin-based and microtubule- based motor proteins have been implicated in the transport of FMRP-granules in neurons, although there is a large evidence in support of the latter [16,144–148]. Understanding the biochemical constituents of FMRP-containing granules and their transport helps to characterize the spatio-temporal control in dynamics of the associated mRNAs. For e.g. FMRP associating with miRISC proteins in RNA processing bodies (P-bodies) promotes the degradation of mRNAs via miRNA guided silencing[67,126]. Simultaneously FMRP granules comprising of ribosomal machinery along with mRNAs have been proposed to regulate local translation of those mRNAs[149]. Hence there is a dynamic hold over the inhibition and expression of FMRP's mRNA targets (**Figure 1.5)**.

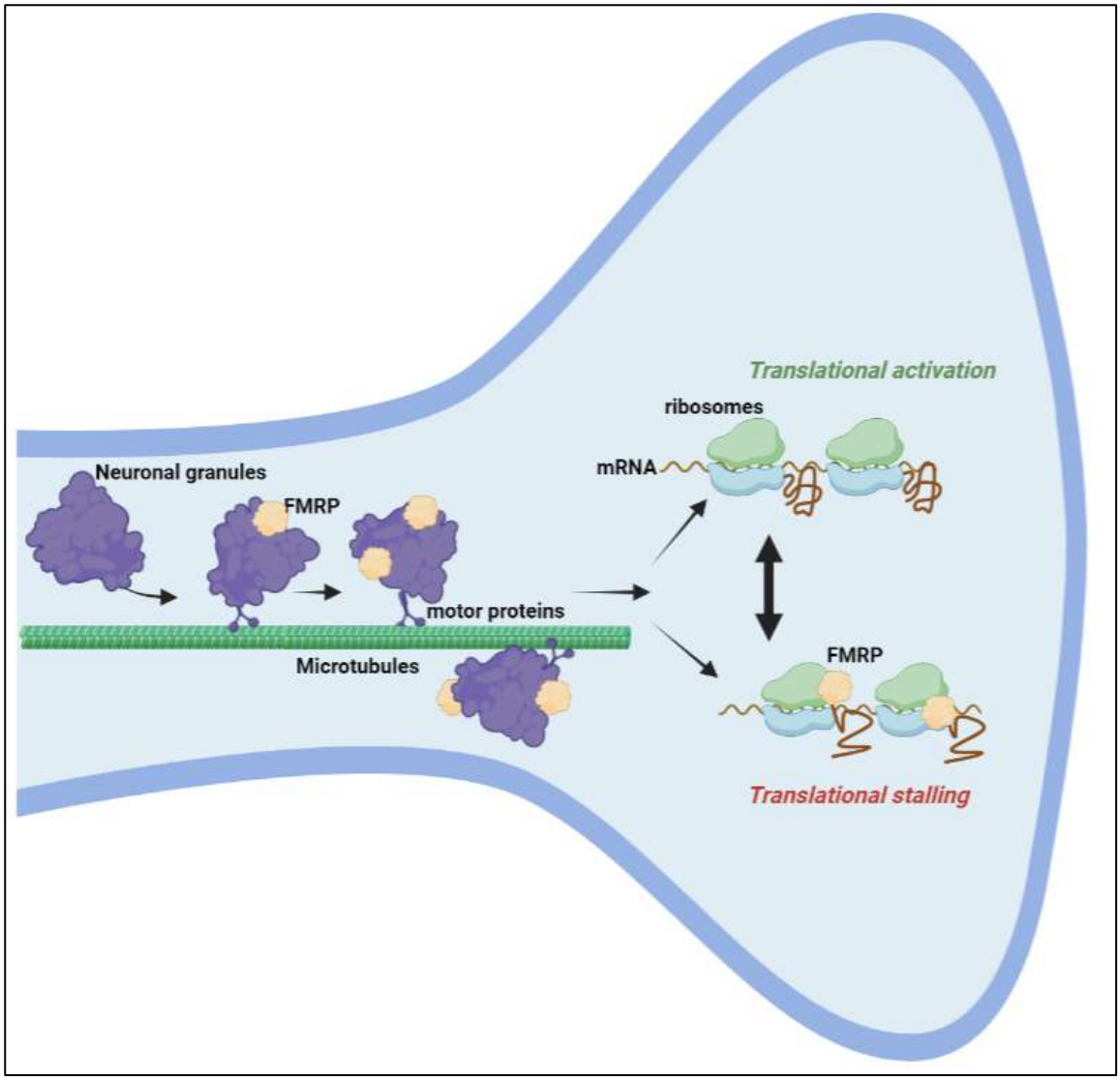

Figure 1.5: Regulated transport and translation of FMRP-target mRNAs at the synapse. *FMRP sequesters mRNAs into membrane-less mRNP granules for microtubule mediated transport towards the synapse. At the synapse, mRNAs that are translationally repressed are in dynamic equilibrium with mRNAs that are actively translated and these two processes are controlled spatially by FMRP.*

A large amount of experimental evidence suggests that FMRP is a translational repressor[8,26]. Though its predicted targets are many, only a few mRNAs have been validated to show a direct biochemical interaction [1]. Nevertheless, it is necessary to understand the modes of translational repression adopted by FMRP in a cell.

Mammalian protein synthesis is a complex symphony of multiple regulatory molecules that can display their control at the stages of initiation, elongation or termination. One model suggests that FMRP represses translation initiation[150]. Cap

dependent translation of transcripts involves the formation of the eIF4F complex (eIF4A-eIFE-eIF4G) to bind to the m7GTP cap at the 5' end of the mRNA for initiation. 4E-binding proteins (4EBPs) interfere with the formation of the initiation complex by binding to eIF4E-eIF4G[151]. Cytoplasmic FMRP-interacting protein (CYFIP1) is a 4EBP and a well-studied protein interactor of FMRP which was found to co-precipitate with FMRP and the eIF4E protein in vivo[150]. The formation of the CYFIP1-FMRP-eIF4E complex in presence of capped FMRP-target Arc mRNA suggested that FMRP might play a role in inhibiting translation initiation by recruiting CYFIP to eIF4E to consequently block the assembly of the translation initiation complex[150] (**Figure 1.6A**). In line with this model, mice expressing reduced levels of CYFIP1 display increased levels of FMRP-targets such as APP, CamKIIα and MAP1b[150]. Additionally, DHPG-mediated activation of protein synthesis in cultured mouse cortical neurons showed reduced levels of eIF4E bound to FMRP-CYFIP complex suggesting that CYFIP1-FMRP-eIF4E complex formation inversely controls translation activation[150].

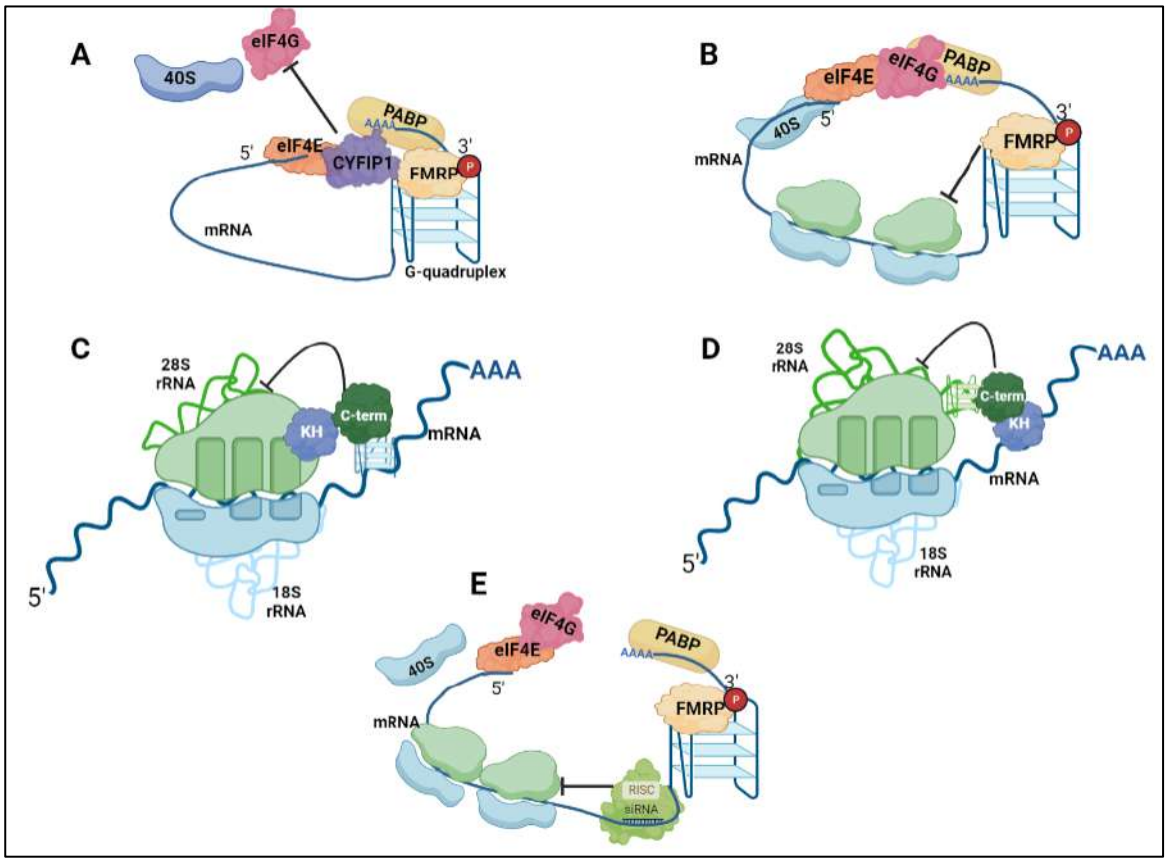

***Figure 1.6:* Mechanisms of translation regulation by FMRP. *A*-** *Translation initiation is blocked by the recruitment of CYFIP1 by FMRP to prevent the formation of the eif4E-eIF4G-eIF4A complex,* ***B*-** *FMRP also blocks translation by stalling*

elongating ribosomes. ***C****- At elongation, FMRP KH domains associate with components of the ribosome while C-terminus RGG box stabilizes the inhibition by binding to mRNA G-quadruplexes.* ***D****- Alternatively RGG box of FMRP binds to the G-quadruplexes of rRNA to block translation elongation.* ***E****- FMRP can also recruit the miRISC complex to inhibit translation.*

Studies have also demonstrated that FMRP can regulate translation at the elongation phase of protein synthesis. Treatment of cells with sodium azide, a nonspecific inhibitor of translation initiation, leads to ribosome run off without affecting ribosomes that are stalled during translation elongation. FMRP was found to co-sediment with such stalled polysomes where it binds to the coding sequence of the associated transcripts[8,22] (**Figure 1.6B**). The stalling of ribosomes during elongation has been examined to occur for multiple reasons: lack of available tRNAs, specific subcellular localization, regulation of peptide folding and presence of secondary structures such as G-quadruplexes in the transcript [152] . Chen et al further illustrated through Cryo-EM that during elongation-phase stalling, the KH domains of FMRP dock on to the 80S ribosome peptidyl (P-site) site and block the entry/exit of amino-acyl tRNAs and elongation factors. Further since the C-terminus of FMRP was found near the A-site of the ribosome in this structure, it was suggested that the RGG domain would control mRNA binding through the recognition of putative mRNA G-quadruplex structures [91] (**Figure 1.6C)**. Contradictory to this hypothesis, the recent Cryo-EM structure which depicted the RGG-C-terminus tail of FMRP in close proximity to the ribosome functional site suggested that the RGG domain might regulate FMRP-mediated translation inhibition by directly binding to the G-quadruplexes in the expansion segment of ribosomal RNA while the KH domains associate with the mRNA transcript in the complex [105] **(Figure 1.6D)**

FMRP's interaction with components of the microRNA silencing Complex (miRISC) has also been studied in the context of translation regulation. FMRP is known to interact with a distinct set of microRNAs across development and under synaptic activation. The process of FMRP-mediated RNA interference is strongly dependent on its interaction with Argonaute2 (AGO2) and this plays an important role in maintaining synaptic plasticity [67,153] (**Figure 1.6E)**. Similarly, FMRP was also shown to interact with mir125 and mir132 to regulate mGluR1 and NMDAR signaling [154] . The 3'UTR of PSD-95 mRNA is a target for both miR125a and FMRP. Together a putative model for translation inhibition was proposed where FMRP binds the

3'UTR of PSD-95 mRNA and recruits the complementary miRNA containing RISC complex to stabilize and clock translation [126]. Muddashetty et al also observed a shift in mir125a from the mRNP fraction to polysomal fractions on DHPG-mediated activation of translation. This could potentially imply that FMRP-miRISC works at the level of translation initiation to inhibit protein synthesis but one cannot rule out the role of FMRP-miRISC at the step of translation elongation.

It is possible that the above-mentioned mechanisms could be adopted at specific spatio-temporal events of an FMRP-target mRNA. FMRP might act at the translation initiation stage when an mRNA is transported towards dendritic spines in the form of mRNP granules. mRNP granules harboring FMRP and target mRNAs such as Arc, APP etc. are also known to contain CYFIP1. It is conceivable that through its association with CYFIP1 in these granules, FMRP prevents the assembly of the initiation eIF4F complex and represses translation of these mRNAs. However, the CYFIP1- mediated block in translation initiation is not the major mechanism employed by FMRP to control protein synthesis [155]. mRNP granules are known to constitute ribosome-associated mRNAs which are stalled from active translation. Since the consensus binding motif for FMRP spans the UTR and coding regions of its target mRNAs, it is also possible that FMRP can block translation elongation depending on the relative positioning of FMRP recognition sites. FMRP might repress translation through the recruitment of the miRNA-RISC complex if its cognate site on the mRNA lies within the 3'UTR. On the other hand, FMRP might act directly on the ribosome through either KH or RGG domains and inhibit protein synthesis of its target mRNAs.

The details available in literature on the mechanisms explaining FMRP-mediated translation regulation are vast but still incomplete. Most of these hypotheses explain translation control of only a handful of FMRP-target mRNAs. Moreover, cells lacking FMRP display dysregulated protein synthesis globally and not just for a few candidate mRNAs. There is a need to dissect out a precise yet common mechanism of translational control since FMRP constitutes structurally complex domains that functionally respond to different cues. Further it is important to establish a unifying hypothesis of how FMRP regulates overall protein synthesis, especially in cells such as neurons.

Chapter 2

Materials and Methodology

2.1 Ethics statement:

All the work was done with due approval from the Institutional Animal Ethics committee (IAEC) and the institutional biosafety committee (IBSC), InStem, Bangalore, India.

2.2 Animals:

Sprague Dawley (SD) rats were used in all animal experiments. Rodents were maintained at conditions with 20-22°C temperatures, 50-60 relative humidity, 0.3µm HEPA-filtered air supply at 15-20 ACPH and 14h/10h light/ dark cycle maintained.

2.3 Cell line culture:

HEK293T cells were cultured in Dulbecco's Modified Eagle Medium (#21331–020 Thermo) containing 10% Fetal Bovine Serum (#F2442 Sigma) at 37°C and 5% CO2 (**Table 2**). Cells were passaged with 0.25% Trypsin solution (#15090046 Thermo) for 2 min and neutralized using the same culture medium. HeLa and Neuro2A cells were maintained in DMEM containing 10% FBS and 1% Penicillin- Streptomycin at 37°C in a 5% CO2 environment passaged using 0.05% trypsin-EDTA solution (**Table 2**)

2.4 Primary neuronal cultures:

Primary neuronal cultures were obtained from E18 rat embryos. Primary cultures were processed as previously described [10]. Briefly, cortices from both the hemispheres were dissected out from E18 embryos in ice cold Hank's Balanced Salt Solution (#H6648-1L Sigma). The tissues were incubated with 0.25% Trypsin solution for 5min at 37°C to enzymatically dissociate the cells and finally manually triturated in Minimum Eagles Medium (#11095080 Thermo) containing 10% FBS (#F2442 Sigma) to generate a single cell suspension (**Table 2**). Cells were plated at a density of 6x104 cells / cm2 on glass coverslips coated with 0.2mg/ml Poly-L-lysine (#P2636-100MG Sigma) made in Borate buffer pH 8.5 (**Table 1**). Neurons were cultured for in MEM medium for 4h after plating following which they were cultured in Neurobasal Medium (#21103-049 Thermo) containing B27 Supplement (#17504-044

Thermo) and 1x Glutamax (#35050061 Thermo) for 11 days at 37°C and 5% CO2 (**Table 2**).

For nuclear localization experiments primary neurons were cultured for 5 days at 37°C in a 5% CO2 incubator (low density 2500 cells per sq.cm). Astroglia were obtained from the same animal as that of the neurons and grown in MEM supplemented with 10% FBS and 1X Glutamax for 2 weeks.

2.5 Embryonic Stem Cell culture:

H9 hESCs, Shef4 WT ESCs and Shef4 *FMR1* KO ESCs were cultured on Matrigel (#3545277 BD Biosciences,) coated plates containing mTeSR1 medium (#5850,StemCell Technologies) at 37°C in a 5% CO2 environment. Cells were further passaged with an enzyme cocktail containing 1 mg/ml of Collagenase type IV (#17104019, Invitrogen), 20% KOSR (#10828010,Gibco), 0.25% Trypsin and 1 mM CaCl2 dissolved in 1X PBS without CaCl2 or MgCl2 pH 7.2. For immunostaining experiments, H9 hESC colonies were plated on Matrigel coated glass coverslips and cultured as mentioned above. H9 hESCs were further differentiated to Neural Precursor Cells (hNPCs) by inducing them with Neural Induction Medium for 14 days (**Table 2**). The hNPCs were further expanded in Neural Expansion medium [156]. Shef4 WT and Shef4 *FMR1* KO hESCs were maintained on Matrigel coated plates containing Essential 8™ Medium (#A15169-01,ThermoFisher Scientific) and passaged with a 1:1 solution of 2 mg/ml Collagenase type IV (#17104-019, Gibco) and 1 mg/ml Dispase (#17105-041,Gibco). Collagenase and Dispase stock solutions were prepared in Advanced DMEM-F12 (#12634- 010, Gibco).

2.6 Immunoprecipitation:

Cells were lysed in a 1 % NP40 containing lysis buffer (**Table 1**) with protease (#S8830-20TAB, Sigma) and RNase inhibitors (#4906837001, Roche) and spun at 18000 rcf (12500 rpm) for 20 min at 4°C. Precleared supernatant was used for immunoprecipitation with Protein G Dynabeads (#10004D, ThermoFisher Scientific). 5µg of anti-FMRP/ AGO2/ Fibrillarin/Flag antibody was coupled to the Protein G Dynabeads. Similar amount of normal mouse/rabbit IgG antibody was used as a control. Lysate was incubated with the beads for 1h at RT on a rotor. The beads were washed thrice with fresh lysis buffer and protein/ RNA was isolated using Lamelli buffer / Trizol LS.

2.7 Cellular fractionation:

H9 hESCs and HeLa cells were trypsinised (0.25 % trypsin) and centrifuged down at 1000 rpm for 5 min at 25°C. The pellet was lysed with a 0.1% NP40 containing lysis buffer with gentle trituration (**Table 1**). 1/3rd of the volume was spun down at 10,000 rpm and the supernatant was used as the cytoplasmic input. The remaining 2/3rd of the lysate was gently layered over a 1 M sucrose cushion and spun at 2800 g for 20 min at 4°C. The final nuclear pellet was suspended in a 1 % NP40 containing lysis buffer and used for further experiments.

2.8 Small-RNA sequencing

H9 hESC and H9 hNPC lysates were subjected to FMRP and AGO2 immunoprecipitation. Whole cell lysates from these two samples were also used to generate input libraries for each cell line. RNA was isolated from the FMRP and AGO2 IP samples using the Trizol method of RNA extraction. A corresponding IgG IP was also performed simultaneously as a control from each cell line. The extracted RNA was used for small RNA library preparation using the Illumina TruSeq library kit (#RS-930-1013, Illumina). The libraries were resolved on a 6% TBE PAGE gel and bands corresponding to 140 bp and 200bp were excised and sequenced by HiSeq1000.

Raw reads of the libraries were uniformly processed. Adapter reads (5' TGGAATTCTCGGGTGCCAAGG 3') were removed using the Cutadapt tool with -q30 (quality score) and -minum length 36 (minimum length of the reads) parameters. The trimmed reads were processed to filter out ribosomal RNA sequences using the GencodeV19 and hg19 genome version. Remaining sequences were aligned to the genome with '-q --best -m 1 -k 1 --chunkmbs 200' parameters ensuring unique reads are only mapped. The read counts were derived using the 'Homo_sapiens.GRCh37.75.gtf' annotation using HTSeq. MDS plot for the samples was derived using edgeR package in R. 33% of the total reads from FMRP IP libraries were associated with snoRNAs. The bam files were converted to bed and the overlap for each annotated snoRNA was analyzed using bedtools with UCSC genome browser as the database.

2.9 Constructs

2.9.1 Bacterial expression:

Human FMRP gene was amplified (1900bp) from Addgene plasmid (#48690,Addgene) with EcoR1 and Sal1 restriction sites and sub cloned into pET28a+ bacterial expression vector along with a 6XHis tag located at the N-terminal of FMRP. This construct was transformed into Rosetta DE3 cells and purified protein was used for EMSA experiments. Plasmids generated for recombinant protein were constructed as follows. Sequences corresponding to N-terminus (1-216aa), KH (217-425aa) and C-terminus (425-632aa) of FMRP were PCR amplified from plasmid pFRT-TODestFLAGHAhFMRPiso1 and cloned into PGEX6P1 vector (#GE28-9546-48, Cytiva) with N-terminus GST tag and PreScission protease site. These constructs were transformed into Rosetta D3 cells and purified protein was used for *in-vitro* binding assays and polysome –spiking assays.

2.9.2 Mammalian cell expression:

In plasmids generated for cell line and neuronal transfection, all truncations and site directed mutations (SDM) of FMRP were performed in the original plasmid pFRT-TODestFLAGHAhFMRPiso1 (#48690,Addgene) containing full-length human *FMR1* gene with N-terminal Flag-HA tag. Site directed mutagenesis was performed using overlapping PCR with Phusion® High-Fidelity DNA Polymerase (#M0530S, NEB) and primer sequences mentioned in **Table 3**.

2.9.3 Insect cell expression:

Full-length *FMR1* sequence was PCR amplified along with N-terminal 6XHis tag and cloned into PFastBac-HtB (#10712024, ThermoFisher Scientific) for Baculoviral protein expression.

2.10 Overexpression and protein purification experiments:

2.10.1 For mammalian cell expression:

HEK293T cells/ DIV11 primary neurons were transfected with Flag-HA tagged FMRP constructs using Lipofectamine 2000 (#11668027, ThermoFisher Scientific) for 24h as per the reagent's protocol. His-GFP was also used as a control and transfection was performed in a similar manner as mentioned before. All constructs were transfected at equal concentrations. Flag-HA FMRP G538fs*23 showed very

less transfection efficiency and hence was doubled in concentration with every transfection.

2.10.2 For bacterial cell expression:

The N-terminus (1-216aa), KH (217-425aa) and C-terminus (425-632aa) of FMRP bearing GST tag at the N-terminal was transformed into Escherichia coli (E.coli) Rosetta DE3 cells and grown at 37 °C in LB. Protein expression was induced with 0.5 mM IPTG at an OD600nm ~0.6 and grown overnight at 25 °C. Cells were harvested and pelleted via centrifugation. Pellets were stored at -20 °C or used immediately. Cells were lysed in buffer containing protease inhibitor and sonicated for 30 min (10s ON, 10s OFF) (**Table 1**). Lysed cells were spun down and lysate was then loaded onto Glutathione Sepharose beads equilibrated with lysis buffer. Resin was washed with 10 column volumes of lysis buffer followed by 5 column volumes of lysis buffer with 100mM KCl. Elution buffer (**Table 1**) was used to elute the GST-tagged domains of FMRP. The flow-through was concentrated and further purified using a Superdex 75 column (GE Healthcare) equilibrated with buffer containing 50 mM Tris pH 8, 100mM KCl, 1mM DTT and 10% glycerol. Protein containing fractions were pooled together. The purity of protein was confirmed with SDS-PAGE gel.

Human FMRP with 6X His tag was cloned in a pET28a vector and transformed into Rosetta DE3 competent cells. Cells were incubated overnight in the presence of kanamycin (50ug/ml). The expression of FMRP ISO1 was induced in 4lt of culture with isopropyl β-D-1-thiogalactopyranoside (IPTG) at a final concentration of 0.5 mM for 16 hours at 18^{o}C. The final bacterial pellet was lysed and clarified bacterial lysate was added on to an equilibrated Ni-NTA column (#R90115, Life Technologies) (**Table 1**). Purified His-FMRP was eluted in fractions using buffer containing a gradient of 100 mM to 500 mM imidazole (#288-32-4, Sigma) (**Table 1**). Protein stocks were dialyzed to remove the imidazole, concentrated and flash frozen with 10% glycerol

2.10.3 For Insect cell expression:

Full-length FMRP was cloned into a Baculoviral pFastHTb vector with His-tag located towards the N-terminus of the protein. Sf21 insect cells were transfected with the construct with PEI and maintained at 26 °C at 120 rpm in SF900II medium (#10902088, Thermo) until virus supernatant P0 was harvested 5 days post-

transfection. Cell number, viability and diameter of the cells were monitored for Baculoviral infection. P1 virus supernatant was further harvested from a larger scale culture. P1 virus was used to infect a fresh culture of Sf21 cells. Baculoviral infection was monitored by recording cell number, viability and diameter prior to harvesting of cells. Cells were lysed and sonicated for 1min (10s ON, 10s OFF) **(Table 1**). Lysed cells were spun down and lysate was loaded onto Ni-NTA beads equilibrated with lysis buffer. Resin was washed with 10 column volumes of lysis buffer followed by 5 column volumes of lysis buffer. His-FMRP was eluted in buffer containing 100mM Imidazole (**Table 1**). The flow through was further dialyzed in the same buffer to eliminate imidazole.

2.11 Electro Mobility Shift Assay:

2.11.1 hFMRP expression and purification:

Human FMRP with 6X His tag was cloned in a pET28a vector and transformed into Rosetta DE3 competent cells. Cells were incubated overnight in the presence of kanamycin (50ug/ml). The expression of FMRP ISO1 was induced in 4lt of culture with isopropyl β-D-1-thiogalactopyranoside (IPTG) at a final concentration of 0.5 mM for 16 hours at 18^{o}C. The final bacterial pellet was lysed in buffer containing 20 mM HEPES pH 8.0, 500 mM NaCl, 10 mM MgCl2, 10 mM β-Mercaptoethanol, 10% glycerol **(Table 1)**. Clarified bacterial lysate was added on to an equilibrated Ni-NTA column (#R90115, Life Technologies). Purified His-FMRP was eluted in fractions using buffer containing a gradient of 100 mM to 500 mM imidazole **(Table 1)**. Protein stocks were dialyzed to remove the imidazole, concentrated and flash frozen with 10% glycerol.

2.11.2 *In-vitro* transcription of snoRNA and radiolabeling:

SNORD80 was *in-vitro* transcribed using recombinant T7 RNA polymerase purified in the lab. First, SNORD80 was amplified by PCR using respective forward and reverse primers. Forward primer contained the T7 promoter sequence. SNORD80 was transcribed using the following reaction mix

10x transcription buffer	2ul
T7 Polymerase	2ul
NTPs	2ul

SNORD80 template	2ug
TIPP	1ul
Water	up to 20ul

This mixture was incubated for 4h at 37°C followed by DNase I (# M0303S, NEB) treatment at 37°C for 15min. RNA was ethanol precipitated overnight and run on an agarose gel to purify the band of the approximate size. RNA was treated with Calf Intestinal alkaline Phosphatase (#M0290S, NEB) and 5'end labeled with γ-[32P] ATP. Nonspecific bacterial RNA was *in-vitro* transcribed in a similar manner.

2.11.3 EMSA reaction

Radiolabeled RNA (~10 fmol @ 20 CPS/µl) was incubated with increasing amounts of His-FMRP in EMSA buffer in the presence of 2.5 ng/µl yeast tRNA and 10 U of RNAseOUT for 1 h at RT. 10 M (280 pmoles) excess of unlabeled SNORD80 was used in a reaction to compete out the binding between radiolabeled SNORD80 and the maximum concentration of His-FMRP (14.6 µM). 7 µl of the reaction mixture were loaded in IX TBE / 5% native gel (5% acrylamide: bis (80:1). and run at 100V for approximately 40 minutes in cold. The gel was dried and exposed overnight using Typhoon FLA 7000 Phosphorimager.

2.12 FUNCAT Assay:

2.12.1 Metabolic labeling:

For metabolic labeling of transfected neurons, neurons were incubated in methionine-free Dulbecco's Modified Essential Medium (Thermo# 21013024) for 30min followed by addition of azidohomoalanine (AHA; 1µM #C10102, Thermo) in the same medium. This was incubated for 30min further and later fixed with 4%PFA. Cells were then permeabilized in PBS+0.3% Triton X-100 solution (**Table 1)** and blocked with buffer containing PBS+0.1% Triton X-100 + 2%BSA + 4% FBS solution (**Table 1**). Newly synthesized proteins were then labeled with Alexa-Fluor-555–alkyne [Alexa Fluor 555 5-carboxamido-(propargyl), bis (triethylammonium salt) (#A20013, ThermoFisher scientific], by allowing the fluorophore alkyne to react with AHA azide group through click chemistry. All reagents were from Thermo Fisher, and stoichiometry of reagents was calculated according to the manufacture manual (CLICK-iT cell reaction buffer kit, #C10269). The neurons were subjected to

immunostaining for MAP2B to identify neurons and HA to identify FMRP transfections (**Table 4**). with Mowiol® 4-88 mounting media was used to mount the coverslips (#81381 Sigma).

2.12.2 Imaging:

Mounted coverslips were imaged on Olympus FV3000 confocal laser scanning inverted microscope with 60X objective. The pinhole was kept at 1 Airy Unit and the optical zoom at 2X to satisfy Nyquist's sampling criteria in XY direction. The objective was moved in Z-direction with a step size of 1 µM (~8-10 Z-slices) to collect light from the planes above and below the focal plane. The transfected neurons were identified using the HA channel. Images of transfected and untransfected neurons were taken from each coverslip of every biological replicate. The image analysis was performed using ImageJ software and the maximum intensity projection of the slices was used for quantification of the mean fluorescent intensities. The region of interest (ROI) was drawn around the transfected and untransfected neurons using the MAP2 channel for their respective analyses. The mean fluorescent intensity of the FUNCAT channel was normalized to the MAP2 channel for each ROI. For each construct, the FUNCAT/MAP2 intensity ratio of the transfected neurons was normalized to the untransfected neurons from the corresponding biological replicate. Data is represented as box plots indicating the quantification of the FUNCAT fluorescent intensity normalized to MAP2 fluorescent intensity. The box extends from 25th to 75th percentile. The middlemost line represents the median of the dataset and whiskers of the box plot range from minimum to maximum data points.

2.13 Linear sucrose density centrifugation

Polysome assay was done from HEK293T cell lysate as described previously in Kute et al [10]. In brief, HEK293T cells were lysed **(Table 1)** and lysate was separated on 15%–45% linear sucrose gradient in presence of 0.1mg/ml Cycloheximide (CHX) (#C7698-5G, Sigma) and Phosphatase inhibitor (#4906837001, Roche) by centrifugation at 39,000 rpm in SW41 rotor for 90 min. The sample was fractionated into 12 1.0 mL fractions with continuous UV absorbance measurement (A254). Fractions were further analyzed by western blots. For quantification of FMRP distribution, Fractions were pooled (F3 and F4–11) according to subunit distribution based on RPLP0 and RPS6 immunoblotting. Similar protocol was followed with

purified recombinant full-length and domains of FMRP. 150pmoles of recombinant protein was spiked into pre-cleared HEK293T cell lysate and incubated for 10min on ice prior to separation on sucrose gradient.

2.14 *In-vitro* binding assays:

50pmoles of recombinant GST-tagged domains of FMRP was incubated with pre-cleared HEK293T cell lysate. Ribosome protein complexes were formed for 30min on ice and later incubated with 10µl of GST-Sepharose beads for 2h at 4°C. After incubation, beads were pelleted (30s at 1000 rpm.). The beads were then washed twice with 50 µl of ice-cold binding buffer **(Table 1)**. The amount of ribosome in cell lysate bound to beads was eluted with 1X Lamelli buffer and checked on a western blot. Ribosomes from HEK293T cells were purified as described in Khatter et al [157]. 5pmoles of purified 80S was incubated with 50 pmoles of recombinant protein in 50µl of Binding buffer for 30min on ice **(Table 1)**. Ribosome-protein complexes were incubated with 10µl of GST-Sepharose beads for 2h at 4°C, eluted and quantified as mentioned previously. For quantification of rRNA, Trizol (#15596018,ThermoFisher Scientific) was added to the beads after the last wash and RNA was eluted as per manufacturer's protocol. Total RNA was reverse transcribed into cDNA using MMLV Reverse transcriptase enzyme and random hexamers.

2.15 Quantitative PCR:

2.15.1 snoRNA quantification:

CDNA of snoRNA was prepared from RNA using reverse primers specific to individual snoRNA candidates (Table 3) . CDNA was prepared using the following reaction mixture

Total RNA	100ng
Specific reverse primer	1ul
Water	up to 10ul

Reaction mixture was heated to 65°C for 5 min followed by cooling on ice for 1 min. To this mixture the following components were added.

10x MMLV RT buffer	2ul
MMLV reverse transcriptase	1ul
dNTPs	2ul
Water	up to 10ul

This was incubated at 42°C for 1hr followed by enzyme inactivation at 85°C for 10 min. CDNA was amplified using SYBR premix by qPCR. Arbitrary copy numbers were calculated from a standard curve drawn from Ct values obtained from serial dilutions of cDNA for snoRNA candidate HBII99. Copy numbers for various snoRNA candidates were obtained using the equation generated from the standard curve.

2.15.2 rRNA quantification:

rRNA was quantified using specific primers (**Table 3**) designed against human 18SrRNA and 28SrRNA. Arbitrary copy numbers were calculated from a standard curve drawn from Ct values obtained from serial dilutions of cDNA for each candidate.

2.16 Microtubule enrichment assay:

To separate microtubule polymers from free tubulin, HEK293T cells were treated with 10 nM paclitaxel (#PHL89806-10MG, Sigma) for 1 h to stabilize microtubules. Cells were later lysed in buffer containing protease inhibitor cocktail (#S8830-20TAB, Sigma), and 10 U of RNase-out (# 10777019, ThermoFisher Scientific) at room temperature for 5 min **(Table 1)**. To analyze microtubule association of the Flag HA-tagged wild type and mutant FMRP variants, HEK293T cells were transfected with these constructs 24h prior to paclitaxel treatment. For RNase treatment, the lysate buffer contained 1.2 µg/µl RNase A1 and 30 units of RNase T1 but no RNase-out. Nuclei were pelleted at 700 g for 1 min at room temperature, and the cytoplasmic supernatant was centrifuged for 10 min at 16,000 g at room temperature to pellet microtubule polymers. The microtubule pellet and the post microtubule supernatant were denatured in 1X Laemmli buffer followed by SDS-PAGE analysis. For microtubule-destabilizing experiments, HEK293Tcells were incubated with 2 µg/ml Nocodazole (# M1404, Merck) for 15min prior to lysis with the same buffer containing Nocodazole and no paclitaxel. Data is represented as box plots indicating the enrichment of overexpressed FMRP variants in the pellet/supernatant on Taxol treatment of HEK293T cells. The box extends from 25th to 75th percentile. The middlemost line represents the median of the dataset and whiskers of the box plot range from minimum to maximum data points.

2.17 Western blotting and densitometry analysis:

2.17.1 Immunoblotting:

The elutes from *in-vitro* binding pull-downs, immunoprecipitations, fractions of polysome profiling experiments and fractions from microtubule enrichment assay were analyzed through western blotting. Briefly, the denatured lysates were run on 12% resolving and 5% stacking acrylamide gels and subjected to overnight transfer onto PVDF membrane (**Table 1**). The blots were subjected to blocking for 1h at room temperature using 5% BSA prepared in TBST (TBS with 0.1% Tween-20) **(Table 1**). This was followed by primary antibody (prepared in blocking buffer) incubation at 4°C overnight. HRP tagged secondary antibodies were used for primary antibody detection. The secondary antibodies (prepared in blocking buffer) were incubated with the blots for 1h at room temperature. Three washes of TBST solution were given after primary and secondary antibody incubation . Details of primary and secondary antibody dilutions are provided in **Table 4**. The blots were subjected to chemiluminescent-based detection of the HRP tagged proteins.

2.17.2 Densitometry quantification:

For the analysis of microtubule enrichment, the samples were probed with FMRP/GFP/HA antibody followed by α-Tubulin as the loading control. In cases where the over-expressed protein shared the same molecular weight as α-Tubulin, the blots were probed with FMRP/GFP/HA antibody first. The same blots were stripped and re-probed with α-Tubulin antibody later. For sucrose gradient fractions, distribution of overexpressed protein and RPLP0/RPS6 were analyzed from the same blot. The details of the antibodies used and their dilutions are given in **Table 4**. Western blot quantifications were performed using densitometry analysis on ImageJ software.

2.18 Immunostaining and image analysis:

2.18.1 Nuclear FMRP immunostaining

Cells were fixed with 4% PFA before staining. The cells were permeabilized with TBS-50T (0.3%) followed by treatment with Tris-Glycine solution. The cells were blocked with buffer containing 2% BSA and 4 % FBS. Cells were incubated with primary antibody overnight at 4°C and Alexa fluor coupled anti-mouse 488 and anti-rabbit 555 secondary antibodies at room temperature for 2h. The cells were finally incubated with DAPI for 5min before being mounted with Mowiol® 4-88 mounting

medium. For quantification of FMRP in hESCs, Images were acquired on Olympus FLUOVIEW 3000 confocal laser scanning microscope (Olympus Corporation) with 60X PlanApoN, NA- 1.42, oil immersion objective. For maximum resolution both in the XY direction and Z direction, Images were acquired using optical zooming of 2.5x to satisfy the sampling theorem of Nyquist, pinhole was kept at 1 Airy unit and stacks in the Z direction were acquired with a step size of 0.3µm. Imaging conditions were kept constant across experiments and across different data sets.

2.18.3 Image Analysis for Nuclear FMRP

Image analysis was done with Bitplane IMARIS 9.0 (Bitplane, oxford Instrument Company) software. For quantifying intensity within the nucleus, DAPI Channel was used to make volumetric nuclear mask and FMRP channel was used to make volumetric mask the entire cell. Local background correction was done using a radius of 5-10 µm while making the masks. Subsequently, integrated intensity was calculated for FMRP channel within both nuclear mask and whole cell mask and was plotted as a ratio of nuclear and cytoplasmic intensity for multiple cells from 3 independent experiments. The distribution was then checked for normality.

2.18.4 FMRP Puncta immunostaining

Rat primary cortical neurons were transfected with HA-FMRP constructs on DIV11 followed by fixation with 4% PFA on DIV12. The fixed neurons were subjected to immunostaining for MAP2 and HA (**Antibody details in Table 4**). The coverslips were mounted with Mowiol® 4-88 mounting media (#81381, Sigma) and imaged on Olympus FV300 confocal laser scanning inverted microscope with 60X objective.

2.18.5 FMRP Puncta analysis

The pinhole was kept at 1 Airy Unit and the optical zoom at 2X to satisfy Nyquist's sampling criteria in XY direction. The objective was moved in Z-direction with a step size of 0.5 µM (~8-10 Z-slices) to collect light from the planes above and below the focal plane. The images were analyzed using ImageJ software and the maximum intensity projection of the slices was used for quantification. The MAP2 channel was used to draw the ROI around each dendritic segment and subjected to thresholding. The ROI created using the MAP2 channel was selected on the HA-FMRP image. The area the selected ROI in the HA-FMRP channel was measured to obtain the

total area of the dendritic ROI (a). Further, the ROI was subjected to particle analysis in the HA-FMRP image. Particles in the range of 3-30 pixels were considered for the analysis. The sum of the area of all the particles or the puncta area (b) and the number of particles or puncta (c) were the two parameters obtained using particle analysis. The ratio of puncta area (b) to total area (a) was calculated to measure the area occupied by the puncta in the given ROI. The ratio of puncta number (c) to total area (a) was calculated to measure the number of puncta per μm2. The ratios of puncta area/total area and number of puncta/ μm2 were compared among dendritic segment ROIs expressing different FMRP constructs. Data is represented as box plots indicating (I) the quantification of puncta area by total dendritic area for FMRP constructs and (II) quantification of the number of puncta per unit area of the dendrite FMRP constructs. The box extends from 25th to 75th percentile. The middlemost line represents the median of the dataset and whiskers of the box plot range from minimum to maximum data points.

2.18.6 Colocalization analysis

For colocalization, cortical neurons were co-transfected with RPL10-GFP and HA-FMRP simultaneously at DIV11 followed by Puromycin treatment at DIV12 for 1hr. The images were analysed using ImageJ software and the maximum intensity projection of the slices was used for quantification. The ROI was created using the MAP2 channel and was selected on the HA-FMRP image. Particle analysis was conducted on the selected ROI to identify the FMRP puncta. The mean intensity of FMRP and RPL10 was measured in these punctae. The mean intensity of FMRP and RPL10 in the puncta was normalized to the total intensity of FMRP and RPL10 in the ROI respectively. Data is represented as a scatter plot that includes normalized FMRP intensity on X-axis and normalized RPL10 intensity on Y-axis for both Untreated and Puromycin treatment conditions. A regression analysis was performed for the same data to test the linear dependency of RPL10 and FMRP

2.19 RiboMethSequencing

2μg of total RNA extracted from Shef4 WT and Shef *FMR1* KO ESCs was used for library preparation. RNA was hydrolyzed with alkaline Tris buffer pH10 95°C for 5 minutes further ethanol precipitated. Isolated RNA was run on a 12% TBE PAGE gel and band corresponding to 30-50 bp was excised out. Libraries were prepared from

the hydrolyzed RNA using TruSeq small RNA library kit and samples were sequenced using HiSeq 3000. Adapters were trimmed using Cutadapt v1.8.3 with parameters average quality: 30, minimum length: 17 bp, maximum length: 45 bp. Bowtie1.1.2 was used for alignment of the reads to the rRNA reference sequence using the parameters: : -v=2 (end-to-end mode) and k-1 (one good alignment per read). Bedtools v2.25.0 was used to compute the number of 5'end and 3'end reads that were mapped to the reference rRNA. The 5'end and 3'end read counts had to be shifted to exactly align with the methylated nucleotides in the reference rRNA sequence. Ultimately two separate datasets were obtained i.e. 5' read end count and 3' read end counts , and these were combined and used for calculation of RiboMeth scores . Optimal cut-off values to detect the methylations were analyzed using Matthew's correlation coefficient in the ROCR package.

2.20 Statistical analysis:

All statistical analyses were performed using Graph Pad Prism software. The normality of the data was tested using the Kolmogorov-Smirnov test. For experiments with less than 5 data points, parametric statistical tests were applied. Data were represented as mean ± SEM in all *in-vitro* and polysome experiment graphs. FUNCAT and puncta data was represented as boxes and whiskers with all the individual data points. Data from colocalization experiments were plotted as scatter plots and a linear regression analysis was performed. Statistical significance was calculated using Unpaired Student's t-test (2 tailed with equal variance) in cases where 2 groups were being compared. One-way ANOVA was used for multiple group comparisons, followed by Tukey's multiple comparison tests, Bonferroni's multiple comparison test or Dunnett's multiple comparison test. Unpaired Student's t-test was used to calculate statistical significance for all snoRNA qPCR assays. For nuclear imaging quantifications, distribution of data points was assessed using Shapiro-Wilk's test. P-value less than 0.05 was considered to be statistically significant.

2.21 Tables

2.21.1. Buffer composition

Lysis buffer	

Tris-HCl pH 7.5	20mM
NaCl	150 mM
MgCl2	5mM
NP40	1%
DTT	1mM
Nuclear Fractionation Buffer	
Tris-Cl pH 7.4	20 mM
NaCl	150 mM
MgCl2	10 mM
DTT	1 mM
NP40	0.1%
Bacterial lysis buffer (domains)	
Tris-HCl pH 8	20 mM
KCl	500 mM
DTT	1mM
Glycerol	10%
Bacterial Elution buffer (Domains)	
Tris-HCl pH 8	50 mM
KCl	100mM
DTT	1mM
glycerol	10%
reduced glutathione	10mM
Bacterial lysis buffer (Full-length FMRP)	
HEPES pH 8.0	20 mM
NaCl	500 mM
MgCl2	10 mM
β-Mercaptoethanol	10 mM
glycerol	10%
Bacterial elution buffer (Full-length FMRP)	
HEPES pH 8.0	20 mM
NaCl	500 mM
MgCl2	10 mM
β-Mercaptoethanol	10 mM

glycerol	10%
imidazole	500mM
Insect cell lysis buffer	
Tris-HCl pH7.5	20mM
KCl	800mM
BME	5mM
Glycerol	10%
Imidazole	10mM
Insect cell elution buffer	
Tris-HCl pH7.5	20mM
KCl	100mM
BME	5mM
Glycerol	10%
Imidazole	100mM
EMSA Binding buffer	
Tris-HCl pH 8	25 mM
MgCl2	5 mM
glycerol	10%
DTT	2 mM
NaCl	150 mM
***In-vitro* binding buffer**	
HEPES pH7.5	20mM
DTT	1mM
KCl	100mM
MgCl2	2.5mM
glycerol	10%
5X Lamelli buffer	
Tris-HCl pH 6.8	250mM
Glycerol	50% (v/v)
SDS	10% (w/v)
Bromophenol blue	0.1% (w/v)
β-Mercaptoethanol	5% (v/v)
Microtubule enrichment buffer	

KCl	150 mM
MgCl2	2 mM
Tris- HCl, pH 7.5	50 mM
EGTA	2 mM
Glycerol	2%
Paclitaxel	10 nM
Triton X-100,	0.125%
Gradient buffer	
Tris-HCl pH 7.5	20mM
KCl	100mM
MgCl2	5mM
Cycloheximide	0.1mg/ml
Permeabilization buffer for immunostaining	
TBS50	1X
Triton X-100	0.3%
TBST for western blotting	
Tris-HCl pH 7.6	20mM
NaCl	150mM
Tween-20	1%(v/v)
TBS50-T for immunostaining	
Tris-HCl pH 7.4	50mM
NaCl	150mM
TritonX-100	0.3%
Blocking buffer for immunostaining	
TBS50	1X
FBS	2%
BSA	2%
TritonX-100	0.1%
Tris Glycine for western blot	
Tris –HCl pH 7.4	0.5 M
Glycine	0.2 M
Borate buffer for neuronal cultures	
Boric acid	40mM

Borax pH 8.5	10mM

2.21.2 Media Composition

Neural Induction Media	
DMEM- F12 (#21331–020, ThermoFisher Scientific) / Advanced Neurobasal medium (#21103049, ThermoFisher Scientific)	1:1
N2 Supplement (#21103049, ThermoFisher Scientific)	1%
B27 without Retinoic acid (#12587–010, ThermoFisher Scientific)	1%
L-GlutaMAX	1%
Pen/Strep	0.1%
SMAD inhibitor SB431542 (#72232, Stem cell technologies)	10µM
Noggin analog LDN193189 (#72142, Stem cell technologies)	0.1 µM
Neural Expansion Media	
DMEM-F12 / Advanced Neurobasal medium	1:1
N2	1%
B27 without retinoic acid	1%
L-GlutaMAX	1%
Pen/Strep	0.1%
FGF2 (#AF-100-15, Peprotech)	10 ng/ml
EGF (#AF-100-15, Peprotech)	10 ng/ml

2.21.3 Primer details

SDM primer	**Sequence**
SDM I304N forward	GAAAGCTGAATCAGGAGATTGTGGAC
SDM I304N Reverse	CTCCTGATTCAGCTTTCCATTTTTTC
SDM R138Q forward	GTGCCAGAAGACTTACAACAAATGTGTG
SDM R138Q Reverse	CACACATTTGTTGTAAGTCTTCTGGCAC
SDM I241N forward	GCTAATAATCAGCAAGCTAGAAAAGTACC
SDM I241N Reverse	CTGATTATTAGCACCATGAGTACC
SDM S500D forward	CAAATGCTGACGAAACAGAATCTGACCAC
SDM S500D Reverse	CTGTTTCGTCAGCATTTGATGCTTCAG
SDM S500A forward	CAAATGCTGCAGAAACAGAATCTGACCAC

SDM S500A Reverse	CTGTTTCTGCAGCATTTGATGCTTCAG
SDM G266E forward	CATATTTATGAAGAGGATCAGGATGCAGTG
SDM G266E Reverse	GATCCTCTTCATAAATATGAAATGTGCAGGTATC
SDM G482S forward	GGGGGCACTCTAGACGCGGTCCTG
SDM G482S Reverse	CGTCTAGAGTGCCCCCTATTTCTG
SDM G532fs*23 forward	TCCTCTTCCTCCCCCCTCCAC
SDM G532fs*23 Reverse	GGGAGGAAGAGGACAAGGAG
SDM R534H forward	ACGGCGGCATGGAGGGGGAGG
SDM R534H Reverse	CCTCCATGCCGCCGTCCGTCTC

Human snoRNA primer	**Sequence**
SNORD12 Forward	10 GCTGATGATACAGCTTCTTTCC 31
SNORD12 Reverse	72 GTTGATCTCTACACTATTGGCCAGT 48
SNORD88C Forward	TCCCATGATGTCCAGCAC
SNORD88C Reverse	CAGGTGTCAAAGGTCCTGG
SNORD81 Forward	gCAGAATACATGATGATCTCAATCC
SNORD81 Reverse	gcgcCAGAATATCAGATATTTTATTGTC
SNORD32a Forward	GTCAGTGATGAGCAACATTCACC
SNORD32a Reverse	CTCAGAGCGGTGCATGG
SNORD105b Forward	CCACATGCGGCTGATGAC
SNORD105b Reverse	CCACAGTGCGTCAGGG
SNORD80 Forward	cggGATACAATGATGATAACATAGTTC
SNORD80 Reverse	GATACATCAGATAGGAGCGAAAGAC
SNORD33 Forward	GGCCGGTGATGAGAACTTC
SNORD33 Reverse	GTGGCCTCAGATGGTAGTG
SNORD68 Forward	CGCGTGATGACATTCTCCGG
SNORD68 Reverse	GCGCAATCAGATGGAAAAGGGTTC
SNORD99 Forward	gACTGGTCCAGGATGAAACCT
SNORD88 Reverse	GAGCTGGTCTCAGTCCCATATC
SNORD110 Forward	TTGCAGTGATGACTTGCGAATC
SNORD110 Reverse	TGCTCAGAGACATGGAGACATCAG

SNORD25 Forward	TTCCTATGATGAGGACCTTTTCAC
SNORD25 Reverse	CCTCAGAGTTATTTATCCTCACGGAG
SNORD29 Forward	cCTATGATGAATCAAACTAGCTCAC
SNORD29 Reverse	cgCTCAGGTGTTCATGTATTTTCAC
SNORD 43 Forward	CACAGATGATGAACTTATTGACGGG
SNORD43 Reverse	AGAACGTGACAATCAGCACACAG
SNORD44 Forward	CCCTGGATGATGATAAGCAAATGC
SNORD44 Reverse	ccGTCAGTTAGAGCTAATTAAGACC
U6snRNA Forward	CTCGCTTCGGCAGCACATATACTAA
U6snRNA Reverse	AACGCTTCACGAATTTGCGTGTC
U1snRNA Forward	CGCTTCTCGGCCTTTTGGC
U1snRNA Reverse	TGCACCGTTCCTGGAGGTAC

Ribosomal RNA primers	**Sequence**
18S rRNA forward	CAAGACGGACCAGAGCGAAAG
18S rRNA reverse	GAGCCATTCGCAGTTTCA
28S rRNA forward	GAACCTGGCGCTAAACCATTCG
28S rRNA Reverse	CCCTTGTGTCGAGGGCTGAC

2.21.4 Antibody details

Antibodies for western blots	**Dilution**	**Catalog.no**
GST	1:1000	Ab9085, Abcam
6His-Tag	1:3000	SAB4301134, Sigma
HA	1:1000	3724S, CST
RPS6	1:3000	2217S, CST
RPLP0	1:3000	Ab101279, Abcam
FMRP	1:1000	F4055, Sigma
p-FMRP	1:1000	Ab183319, Abcam
α-Tubulin	1:3000	T9026, Sigma
Fibrillarin	1:1000	
Lamin B	1:1000	
Secondary Rabbit HRP	1:5000	A0545, Sigma

Secondary Mouse HRP	1:5000	31430, ThermoFisher Scientific

Antibodies for Immunostaining	**Dilution**	**Catalog.no**
MAP2	1:500	Ab32454, Sigma
HA	1:500	3724S, CST
FMRP-Total	1:500	F4055, Sigma
FMRP- Phospho	1:500	Ab183319, Abcam
Oct-4	1:500	sc-5279, Santa Cruz
Nestin	1:500	MAB5326, Millipore
Alexa Fluor 647 anti-mouse IgG	1:1000	A-21235, ThermoFisher Scientific
Alexa Fluor 488 anti-rabbit IgG	1:1000	A-11008, ThermoFisher Scientific
Alexa Flour 488 anti-mouse IgG	1:1000	A-21206, ThermoFisher Scientific
Alexa Flour 555 anti-rabbit IgG	1:1000	A-21428, ThermoFisher Scientific

CHAPTER 3

REGULATION OF TRANSLATION BY FMRP THROUGH ITS INTERACTION WITH THE RIBOSOME

Introduction:

FMRP is shown to regulate the translation of mRNAs required for synaptic plasticity and neuronal function[87,96,158]. Independent studies have implicated potential structural FMRP recognition motifs on these target mRNAs[17,27,96,97]. However, there is lack of evidence showing the necessity of FMRP binding to these motifs to regulate translation. This has compelled us to look at the mechanism of FMRP-mediated translation regulation beyond its direct interaction with target mRNAs.

FMRP can activate as well as inhibit protein synthesis and at basal state acts as a translational repressor. As introduced in **Chapter 1,** studies have shown that FMRP interacts with components of translation initiation and translation elongation to regulate protein synthesis [19,150]. Majority of FMRP in the cell is found to be associated with polysomes[18,19,27,104]. Interestingly, the pathogenic missense mutation in FMRP's KH2 domain abolishes its ribosome association without affecting its RNA-binding ability which results in a severe form of FXS in the affected individual [18,83]. This suggests that the FMRP's interaction with the ribosome has a significant role in the process of translation regulation.

Although studies have previously indicated the mechanism of translation inhibition by FMRP-ribosome complex, the precise structural and functional contribution of FMRP and its domains in this process is yet to be clearly understood [89,91]. Moreover, there is very little work done in support of the biochemical nature of FMRP-ribosome complex in mammalian system. In this chapter, I will discuss our findings at (i) establishing the biochemical interaction between human FMRP and the ribosome, (ii) the role of FMRP phosphorylation in regulating this interaction and (iii) the functional consequence of this interaction in presence of FMRP phosphorylation.

3.1. Functional contribution of FMRP domains to polysome association.

FMRP is a multi-domain protein and it is essential to determine which of its domains structurally contributes to its interaction with the ribosome. To study this, we used polysome profiling. Polysome profiling is an assay used to separate cellular ribosomes in its subunits, monosomes and polysomes. The process of polysome profiling enables the separation of mRNA, associated ribosomes and their interacting partners based on differential density centrifugation. Previously it is reported that FMRP associates with both monosomes and polysomes thereby modulating the expression of its target mRNAs[83]. To understand the domain contribution in FMRP-ribosome interaction, we fragmented FMRP into three parts: The N-terminal fragment containing Tudor domains (N-term), the middle K-Homology fragment (termed as KH-constituting both KH1 and KH2 domains) and the C-terminal fragment containing the RGG domain (C-term) and performed polysome profiling.

We used two different approaches to examine FMRP's association with ribosomes. First, we monitored the ribosome association of recombinant domains of FMRP in HEK293T cell lysate. Recombinant proteins corresponding to the N-term, KH and C-term of FMRP with N-terminal GST tag were cloned in PGEXP-61 vector and expressed in E.coli Rosetta DE3 cells (**Fig 3.1B**). Full-length FMRP with N-terminal 6XHis tag was initially expressed with E.coli Rosetta DE3 cells. However, this resulted in multiple truncated versions of the purified protein. Then we expressed full-length FMRP in Baculoviral based SF9 insect cell system. The insect cell system provides an advantage of post-translational modifications of the over-expressed proteins and thus we obtained a relatively stable full-length FMRP expression compared to the bacterial system. All *in-vitro* experiments with full-length FMRP have been performed with Baculoviral expressed FMRP.

To study its interaction with ribosomes, purified His-FMRP was incubated with HEK293T cell lysate and subjected to polysome profiling with continuous reading of absorbance at 254nm (**Fig 3.1C)**. Fractions of 1ml each were collected and probed for the presence of the RPLP0 and RPS6 proteins which were used as proxies for distribution of the large subunit and the small subunit along the sucrose gradient respectively (**Fig 3.1D**). Endogenous FMRP was distributed among ribosomal and polysomal fractions (**Fig 3.1D and 3.1H**). A significant part of His-FMRP also fractionated with both ribosomal and polysomal fractions of the gradient (**Fig 3.1E**

and 3.1G). Following this, 150pmoles of each GST-tagged recombinant protein was spiked into HEK293T cell lysate and loaded onto a 15-45% sucrose gradient followed by centrifugation. Fractions of the sucrose gradient were probed with anti-GST antibody to visualize the distribution(**Fig 3.1F).** Purified GST protein alone was also spiked in a similar manner as a negative control (**Fig 3.1F**). Among the three FMRP domain constructs, only the C-term of FMRP showed a distribution among ribosomal and polysomal fractions similar to the distribution of the full-length protein (**Fig 3.1F and 3.1K**). KH domain, which is known to influence the polysome association of FMRP, did not show any ribosomal distribution (**Fig 3.1F and 3.1J**). We also did not capture any significant ribosomal and polysomal association with the N-term and GST alone as well **(Fig 3.1F, 3.1I and 3.1L**).

As a second step, to rule out any artifact from spiked recombinant protein, polysome profiling was performed with HEK293T cells transfected with Flag-HA tagged FMRP constructs (**Fig 3.1M and 3.1N**). Overexpressed Flag-HA FMRP was distributed along all fractions of the gradient similar to endogenous FMRP (**Fig 3.1O and 3.1P**). We observed a similar distribution with HEK293T cells transfected with Flag-HA N-term and Flag-HA KH constructs as compared to distribution of spike GST-N-term and GST-KH (**Fig 3.1O, 3.1Q and 3.1R**). There was no significant improvement in polysome association on fusing N-term to KH domain as well (**Fig 3.1O and 3.1S**). Thus, our results indicate that C-term of FMRP is essential for ribosome/Polysome interaction.

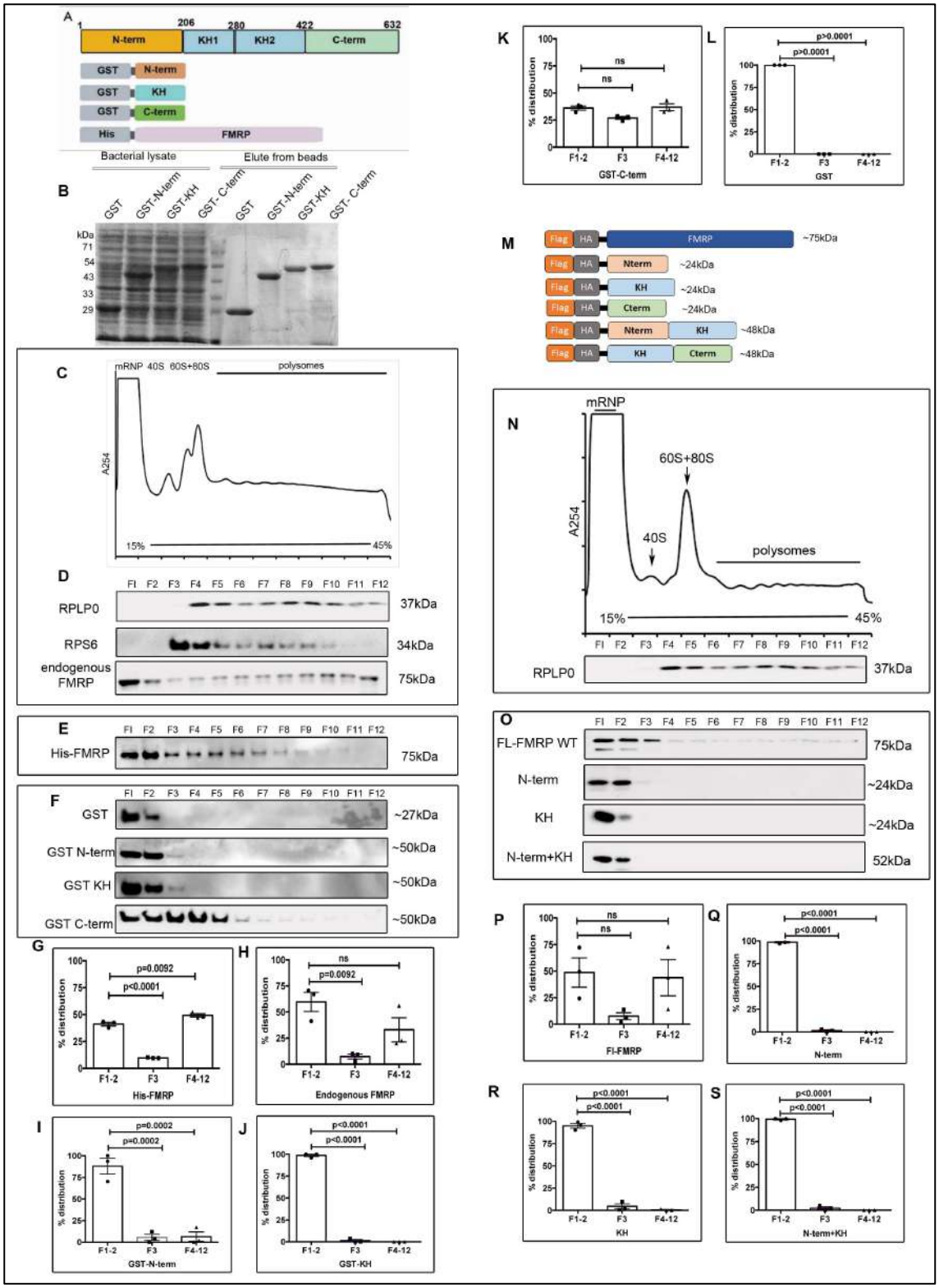

Figure 3.1: C-terminus is essential for FMRP's interaction with ribosomes.

A*-Schematic of recombinant GST-tagged individual domains and full-length His-FMRP proteins.* ***B****-Coomassie stained gel image indicating domains that were bacterially expressed and eluted using Glutathione beads.* ***C****- Representative polysome trace of HEK293T cell lysate on 15%-45% linear sucrose gradient.* ***D****-

Representative immunoblots for endogenous FMRP, RPLP0 and RPS6 distribution in the 12 fractions obtained from polysome profiling (n=3). ***E****-Representative immunoblot for spiked His-tagged full-length FMRP distribution in the 12 fractions obtained from polysome profiling probed with anti-His antibody (n=3).* ***F****-Representative immunoblots indicating the distribution of spiked GST-tagged FMRP domains and purified GST in the 12 fractions obtained from polysome profiling. Blots were probed with anti-GST antibody(n=3).* ***G****-Graph indicating the quantification of His-FMRP among the mRNP (F1-2), ribosomal subunits (F3) and ribosomal fractions (F4-12) n=3, One-Way ANOVA p<0.0001 with Dunnett's multiple comparison test.* ***H****-Quantification of endogenous FMRP among the mRNP (F1-2), ribosomal subunits (F3) and ribosomal fractions (F4-12). n=3, One-Way ANOVA p<0.0149 with Dunnett's multiple comparison test.* ***I****-Quantification of GST-N-term among the mRNP (F1-2), ribosomal subunits (F3) and ribosomal fractions (F4-12). n=3, One-Way ANOVA p=0.0001 with Dunnett's multiple comparison test.* ***J****-Quantification of GST-KH among the mRNP (F1-2), ribosomal subunits (F3) and ribosomal fractions (F4-12). n=3, One-Way ANOVA p<0.0001 with Dunnett's multiple comparison test.* ***K****- Quantification of GST-C-term among the mRNP (F1-2), ribosomal subunits (F3) and ribosomal fractions (F4-12). n=3, One-Way ANOVA p=0.0373 with Dunnett's multiple comparison test.* ***L****- Quantification of GST among the mRNP (F1-2), ribosomal subunits (F3) and ribosomal fractions (F4-12). n=3, One-Way ANOVA p<0.0001 with Dunnett's multiple comparison test.* ***M****-Schematic describing human Flag-HA FMRP constructs alongside truncated versions.* ***N****-Top-Representative trace of HEK293T cell lysate on 15%-45% linear sucrose gradient on transfection with Flag-HA FMRP constructs. Below- Representative immunoblots indicating the distribution of ribosomal protein RPLP0 (probed with anti-RPLP0 antibody) on linear sucrose gradient (n=3).* ***O****-Representative immunoblots indicating the distribution of overexpressed Flag-HA full-length FMRP, N-term, KH and N-term+KH (probed with anti-HA antibody) on linear sucrose gradient (n=3).* ***P****-Graph indicating the quantification of Flag-HA Fl-FMRP among the mRNP (F1-2), ribosomal subunits (F3) and ribosomal fractions (F4-12) n=3, One-Way ANOVA.* ***Q****- Quantification of Flag-HA N-term among the mRNP (F1-2), ribosomal subunits (F3) and ribosomal fractions (F4-12) n=3, One-Way ANOVA p<0.0001 with Dunnett's multiple comparison test.* ***R****-Quantification of Flag-HA KH among the mRNP (F1-2), ribosomal subunits (F3) and ribosomal fractions (F4-12). n=3, One-Way ANOVA p<0.0001 with Dunnett's multiple*

comparison test. ***S****- Quantification of Flag-HA N-term+KH among the mRNP (F1-2), ribosomal subunits (F3) and ribosomal fractions (F4-12). n=3, One-Way ANOVA p<0.0001 with Dunnett's multiple comparison test.*

3.2. Biochemical interaction of FMRP with the ribosome is dependent on its C-terminus domain.

To further validate nature of FMRP-ribosome binding, pull-down assays were performed with recombinant FMRP domains mixed with HEK293T cell lysate or purified human 80S ribosomes. The schematic of the *in-vitro* pulls down assays are described in **Fig 3.2A**. Briefly, HEK293T cell lysates were spiked with 50 pmoles of GST-tagged domains and incubated with glutathione beads. Elutes from the beads were assayed for the presence of 18S and 28S rRNA by qPCR (as a readout for ribosomes). Our results clearly show that 18S and 28S rRNA was significantly pulled down only by C-term of FMRP. In contrast, GST-N-term and GST-KH did not show any significant pull-down of 18S and 28S rRNA. This was similar to control GST as well (**Fig 3.2B and 3.2C**). Simultaneously, elutes were also assayed for the presence of RPS6 and RPLP0 ribosomal proteins. Again, only C-term was associated with ribosomal proteins while N-term, KH and GST were not found to be associated with ribosomes (**Fig 3.2D**).

Next, we performed an *in-vitro* binding assay with purified mRNA-free human 80S ribosomes (from HEK293T cells) and FMRP domains. 80S ribosomes were purified from HEK293T cells and this was incubated with 10X molar excess of GST-tagged domains. Bound 80S-domain complexes were eluted using glutathione beads and elutes were probed for the enrichment of 18S and 28S rRNA as well as ribosomal proteins RPLP0 and RPS6. As seen previously in the pull-down with HEK293T cell lysate, we observed that only C-term of FMRP associated with purified 80S ribosomes (**Fig 3.2E-G**). To confirm the binding between C-term and the remaining ribosomal protein components, we performed an additional pull-down assay. Purified recombinant domains (10X) were incubated with purified HEK293T 80S ribosomes. The 80S ribosome is a mega-Dalton complex and contains around 80 ribosomal proteins. Elutes from the pull-downs were loaded on to an SDS PAGE gel and stained with Coomassie dye to visualize the rest of the ribosomal proteins. As observed, the C-term of FMRP was able to associate with the entire ribosomal complex (**Fig 3.2H).**

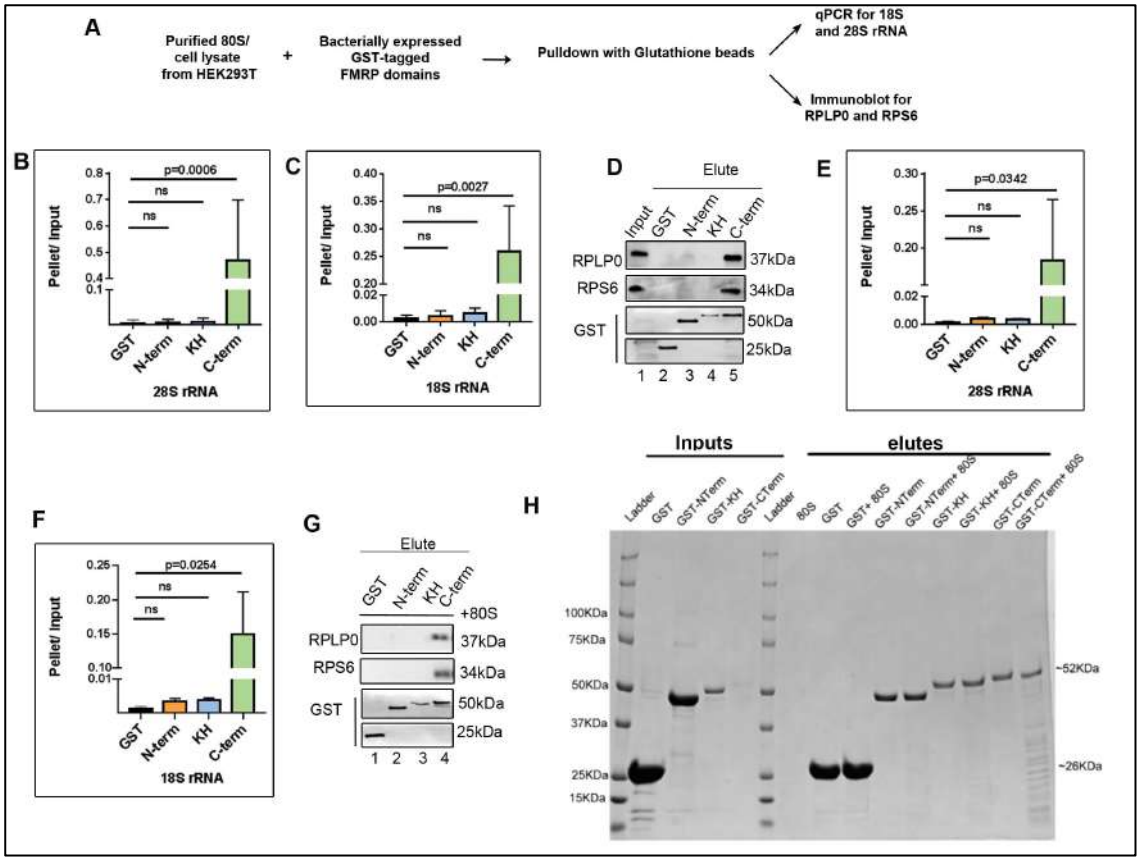

Figure 3.2: C-terminus of FMRP is sufficient to bind to the ribosome.

***A**-Experimental workflow to validate the binding of FMRP domains to ribosomes. **B**-qPCR quantification of 28SrRNA from HEK293T cell lysate bound to GST tagged FMRP domains. Data represented as mean +/- SEM, One-Way ANOVA p=0.0004 followed by Dunnett's multiple comparisons test. **C**-qPCR quantification of 18SrRNA from HEK293T cell lysate bound to GST tagged FMRP domains. Data represented as mean +/- SEM, One-Way ANOVA p=0.0020 followed by Dunnett's multiple comparisons test. **D**-Representative immunoblots for ribosomal proteins RPLP0 and RPS6 obtained from pull downs with GST-tagged FMRP domains incubated with HEK293T cell lysate (n=2). **E**-qPCR quantification of 28SrRNA from purified 80S ribosomes bound to GST tagged FMRP domains. Data represented as mean +/- SEM, One-Way ANOVA p=0.0332 followed by Dunnett's multiple comparisons test. **F**- qPCR quantification of 18SrRNA from purified 80S ribosomes bound to GST tagged FMRP domains. Data represented as mean +/- SEM, One-Way ANOVA p=0.0244 followed by Dunnett's multiple comparisons test. **G**-Representative immunoblots for ribosomal proteins RPLP0 and RPS6 obtained from pull downs with GST-tagged FMRP domains incubated with purified HEK293T 80S ribosomes*

*(n=2).**H**- Coomassie stained gel indicating all ribosomal proteins of the 80S ribosome bound to FMRP domains. (n=1)*

3.3. Inhibition of global protein synthesis in neurons by domains of FMRP.

FMRP is a known modulator of protein synthesis with its primary role as a translational inhibitor at basal levels [20,158]. Our next aim was to test the contribution of individual domains of FMRP in inhibiting global protein synthesis in neurons. Rat primary cortical neurons were transfected at DIV11 with Flag-HA tagged domains (or full length) of FMRP and the neurons were further assayed for changes in de-novo protein synthesis through FUNCAT (**Fig 3.3A**). FUNCAT is a fluorescent-based amino acid tagging system to visualize proteome-wide patterns of newly synthesized proteins. As mentioned previously [20,158], FMRP is an inhibitor of translation and as expected, we observed a significant reduction in the FUNCAT signal in neurons transfected with full-length FMRP in comparison to untransfected neurons **(Fig 3.3B and 3.3C**). Similarly, we observed that the C-term alone could significantly inhibit translation, which was visualized as a decrease in the FUNCAT signal **(Fig 3.3B and 3.3 C**). There was no significant change in the FUNCAT signal in the neurons expressing the KH domains of FMRP **(Fig 3.3B and 3.3C**). This was surprising since the KH domains have been previously implicated to be indispensable for translational regulation[18,27]. Neurons transfected with N-term as well showed no significant change in the FUNCAT signal indicating that N-term also has no effect on global translation regulation **(Fig 3.3B and 3.3C**).

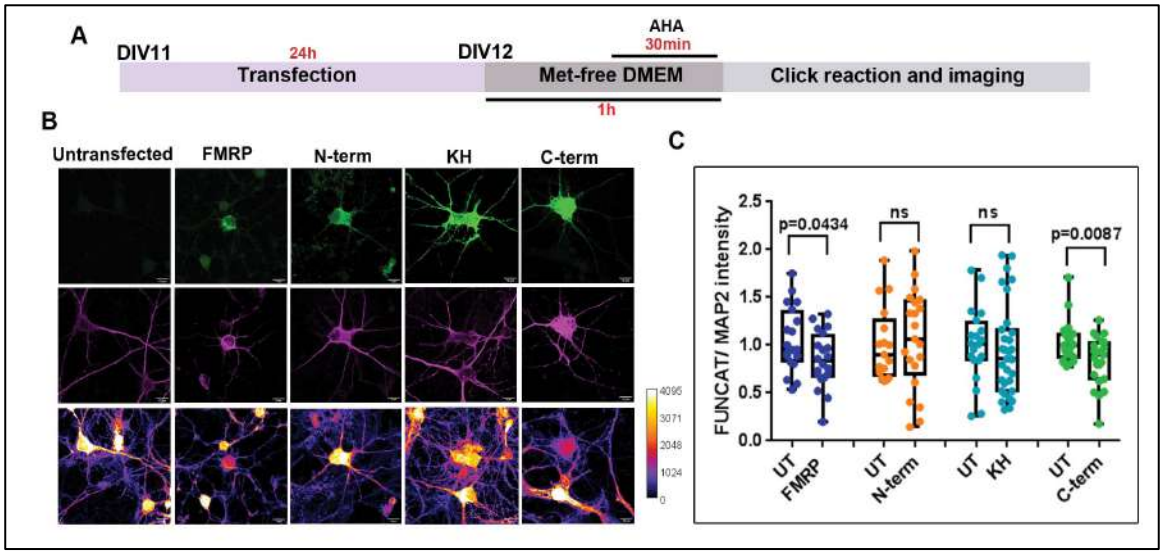

Figure 3.3: C-terminus of FMRP is sufficient to inhibit global protein synthesis in neurons

***A**-Experimental workflow. Primary rat cortical neurons (DIV11) were transfected for 24h with full length and FMRP domains and subjected to fluorescent non-canonical amino acid tagging (FUNCAT) along with immunostaining for HA and MAP2.**B**-Representative images for HA, MAP2 and FUNCAT fluorescent signal in neurons transfected with full length FMRP and FMRP domains (Scale bar - 10µm).**C**-Quantification of the FUNCAT fluorescent intensity normalized to MAP2 fluorescent intensity for full length and domains of FMRP. For each FMRP construct, the FUNCAT signal from the transfected neuron was normalized to the untransfected neuron. Unpaired t-test for each construct, n = 15-30 neurons from 5 independent experiments*

3.4. Phosphorylation of FMRP dictates its polysome association.

FMRP is shown to be a target of various post-translational modifications. Phosphorylation of FMRP, in particular, is known to dynamically regulate its functions like RNA binding and protein-protein interactions[21–23]. The primary site of phosphorylation in human FMRP is Serine 500 located within the C-terminus of FMRP (**Fig 3.4A**). As observed in the polysome profile, FMRP is distributed in non-ribosomal, subunits and ribosomal fractions. On probing the same fractions with an antibody against p-FMRP (targeted at phospho-Serine 500), it was observed that phosphorylated FMRP was accumulated only among the initial fractions of the gradient. Hence it was hypothesized that altering the phosphorylation status of FMRP might alter its distributions across fractions of the sucrose gradients. To test this, HEK293T cells were transfected with Flag-HA tagged WT, phospho (S500D) and de-phosphomimic (S500A) of FMRP. FMRP S500D was present only in the non-ribosomal fractions (Fractions 1-2) of the gradient while FMRP S500A was distributed in all fractions including the polysomal fractions (**Fig 3.4B and 3.4C)**.

Additionally, we transfected HEK293T cells with WT C-term and subjected it to polysome profiling. C-term was restricted to the initial fractions of the gradient. Since the same fractions were probed with an antibody against p-FMRP, it was observed that the majority of the C-term which was in the initial fractions, was phosphorylated (**Fig 3.4D)**. To understand the role of phosphorylation in the distribution of C-term, phospho and de-phosphomimics of C-term were also transfected in HEK293T cells followed by polysome profiling. The over-expression of FMRP and its phospho-mutants were performed in HEK293T cells in the background of existing endogenous FMRP. Since FMRP is known to regulate the expression of its own mRNA, we suspected that there would be a regulation in the expression of the FMRP constructs and thereby a modulation in their association with heavier and lighter ribosomal fractions.

Thus, to dissect out changes in distribution between WT, S500D and S500A C-term, we quantified the amount of overexpressed protein in Fraction 3 (ribosomal subunit) versus Fractions 4-12 (ribosomal) (**Fig 3.4E)**. C-term S500D showed an accumulation in the non-ribosomal fractions and conversely C-term S500A showed an increased association with the ribosomal fractions (**Fig 3.4F and 3.4G**). Finally,

we generated a combination of KH and C-term domains (referred to as KH+C-term here onwards) and examined its ribosomal distribution (**Fig 3.4H)**. KH+C-term was found to be accumulated in the initial fractions of the gradient and these accumulated fractions consisted of phosphorylated KH+C-term when probed with p-FMRP antibody (**Fig 3.4H)**. Further, differences in the ribosomal distribution in WT, S500D and S500A KH+C-term proteins were detectable only when quantified between fractions 3 and fractions 4-12 (**Fig 3.41 and 3.4J)**. Dephosphorylation of KH+C-term clearly increases its association with ribosomes (**Fig 3.4I and 3.4J)**. Thus, confirming that phosphorylation of FMRP at its C-terminus can dictate its ribosome binding ability.

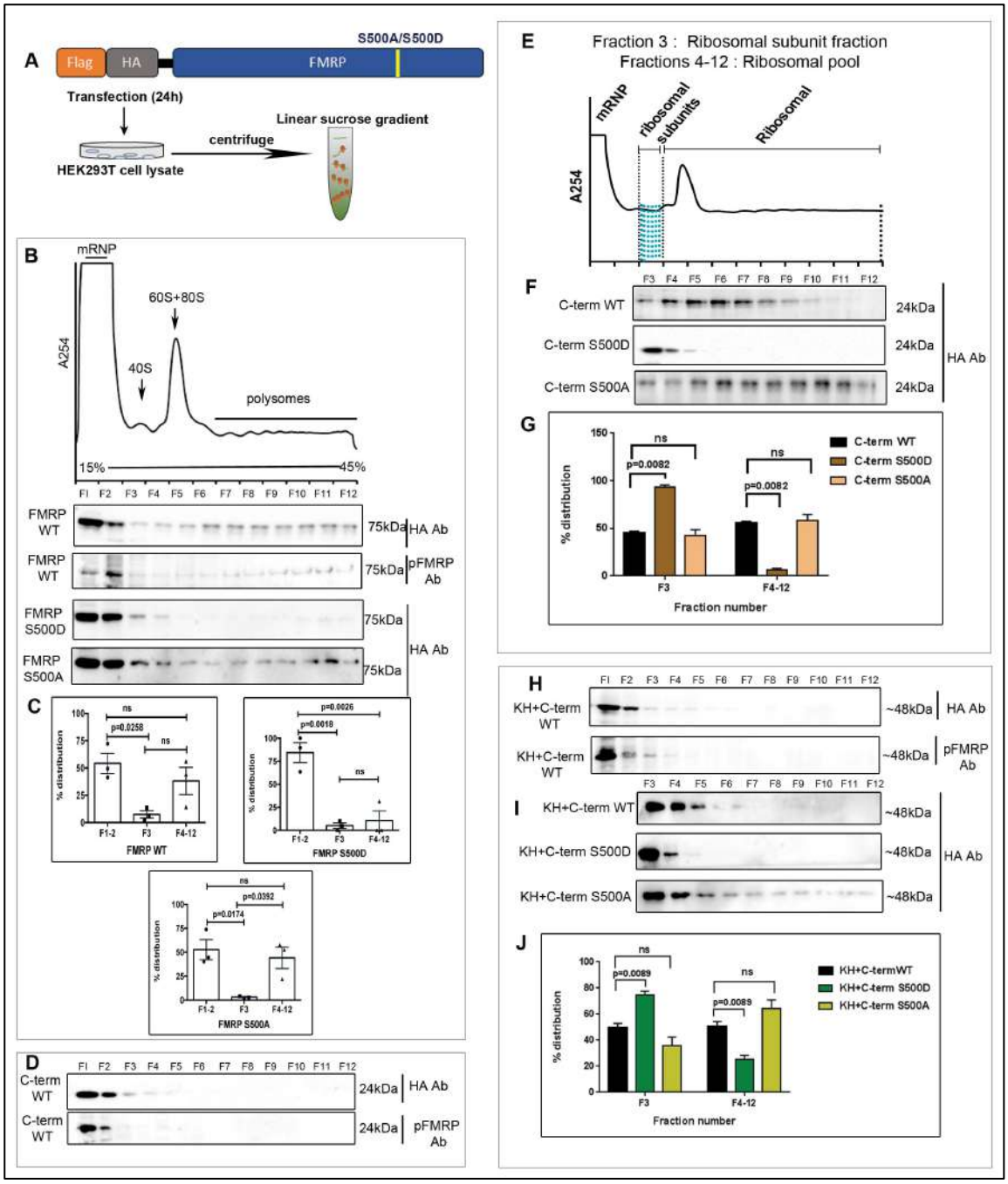

Figure 3.4: Phosphorylation of FMRP dictates its ribosome/polysome distribution

A*-Schematic describing WT FMRP, S500D and S500A mutants of FMRP that were transfected in HEK293T cells for 24h before subjecting it to polysome profiling on a linear sucrose gradient.* ***B****-Top - Representative polysome trace obtained at 254nm indicating the division of fractions into mRNP, 40S, 60S+80S and Polysomes. Bottom – Representative immunoblots indicating the distribution of overexpressed full-length WT FMRP, phosphomimic S500D FMRP and de-phosphomimic S500A FMRP along the 12 fractions of linear sucrose gradient. Fractions with WT FMRP*

were also probed for phospho-FMRP with anti-pFMRP (Serine500) antibody (n=3). ***C****- Top- Quantification of overexpressed FMRP variants among the mRNP (F1-2), ribosomal subunits (F3) and ribosomal fractions (F4-12). n=3, One-Way ANOVA p=0.0291 with Tukey's multiple comparison test for FMRP WT and p=0.0012 with Tukey's multiple comparison test for FMRP S500D. Bottom- Quantification of FMRP S500A among the mRNP (F1-2), ribosomal subunits (F3) and ribosomal fractions (F4-12). n=3, One-Way ANOVA p=0.0158 with Tukey's multiple comparison test.* ***D****- Representative immunoblots indicate the distribution of C-term WT overexpressed in HEK293T cells along the 12 fractions of the linear gradient. Fractions were also probed for phospho (at S500) C-term distribution with anti-pFMRP (Serine500) antibody (n=3).* ***E****-Representative polysome profile with trace obtained at 254nm. Schematic indicates the division of fractions based on the presence of assembled ribosomal subunits. Fraction 3 corresponds to the ribosomal subunit pool. Fractions 4-12 correspond to the ribosomal pool.* ***F****- Representative immunoblots indicating the distribution of overexpressed C-term WT, phospho-mimetic (C-term S500D) and de-phosphomimic (C-term- S500A) along fractions 3 to 12 of a linear sucrose gradient. Blots were probed with anti-HA antibody (n=3).* ***G****- Quantification of overexpressed C-term variants in Ribosomal subunit fraction (F3) versus Ribosomal fractions (F4-12). n=3 for each condition. Data represented as mean +/- SEM, One-Way ANOVA p=0.004 for F3, p=0.004 for F4-12 followed by Bonferroni's Multiple comparisons test.* ***H****- Representative immunoblots indicating the distribution of KH+C-term WT overexpressed in HEK293T cells along all 12 fractions of linear sucrose gradient. Fractions were also probed for phospho KH+C-term distribution using p-FMRP antibody (n=3).* ***I-*** *Representative immunoblots indicating the distribution of overexpressed KH+C-term WT and phospho-mutants along fractions 3 to 12 of linear sucrose gradient. Blots were probed with anti-HA antibody (n=3).* ***J-*** *Graph indicating the quantification of overexpressed KH+C-term variants in ribosomal subunit (F3) versus Ribosomal fractions (F4-12). n=3 for each condition. Data represented as mean +/- SEM, One Way ANOVA p=0.001 for F3, p=0.001 for F4-12, Followed by Bonferroni's Multiple comparisons test*

3.5.Phosphorylation of FMRP modulates its function of global translation regulation.

Since we established that phosphorylation plays a major role in the association of FMRP with ribosomes, we next wanted to test if this post translational modification can influence the translation regulation role of FMRP and its domains. To test this, Rat primary cortical neurons were transfected at DIV11 with WT, S500D (phospho) and S500A (de-phosphomimic) constructs of FMRP for 24h. The neurons were further processed for FUNCAT to measure changes in de-novo protein synthesis. As seen previously, neurons transfected with FMRP WT showed a reduction in FUNCAT intensity indicating an inhibition of total de-novo protein synthesis (**Fig 3.5A and 3.5B**). Similarly, overexpression of FMRP S500D also led to a reduction in FUNCAT signal(**Fig 3.5A and 3.5B**). On the contrary, neurons expressing FMRP S500A showed an increase in FUNCAT signal in comparison to surrounding untransfected neurons(**Fig 3.5A and 3.5B**). In a parallel experiment, rat primary cortical neurons were transfected with WT, S500D and S500A C-term variants and assayed for changes in total protein synthesis. This experiment was performed to confirm that the role of phosphorylation in regulating C-term-ribosome association also extends to corresponding regulation of global protein synthesis. As observed previously, C-term transfected neurons showed a decreased FUNCAT signal and C-term S500A expressing neurons showed a consistent increase in FUNCAT signal (**Fig 3.5C and 3.5D**). Neurons transfected with C-term S500D however, did not show any change in FUNCAT signal in comparison to surrounding untransfected neurons (**Fig 3.5C and 3.5D**). Our results indicate that C-term of FMRP drives translation regulation similar to that of the full-length protein and dephosphorylation mediates translation de-repression of FMRP's C-terminus

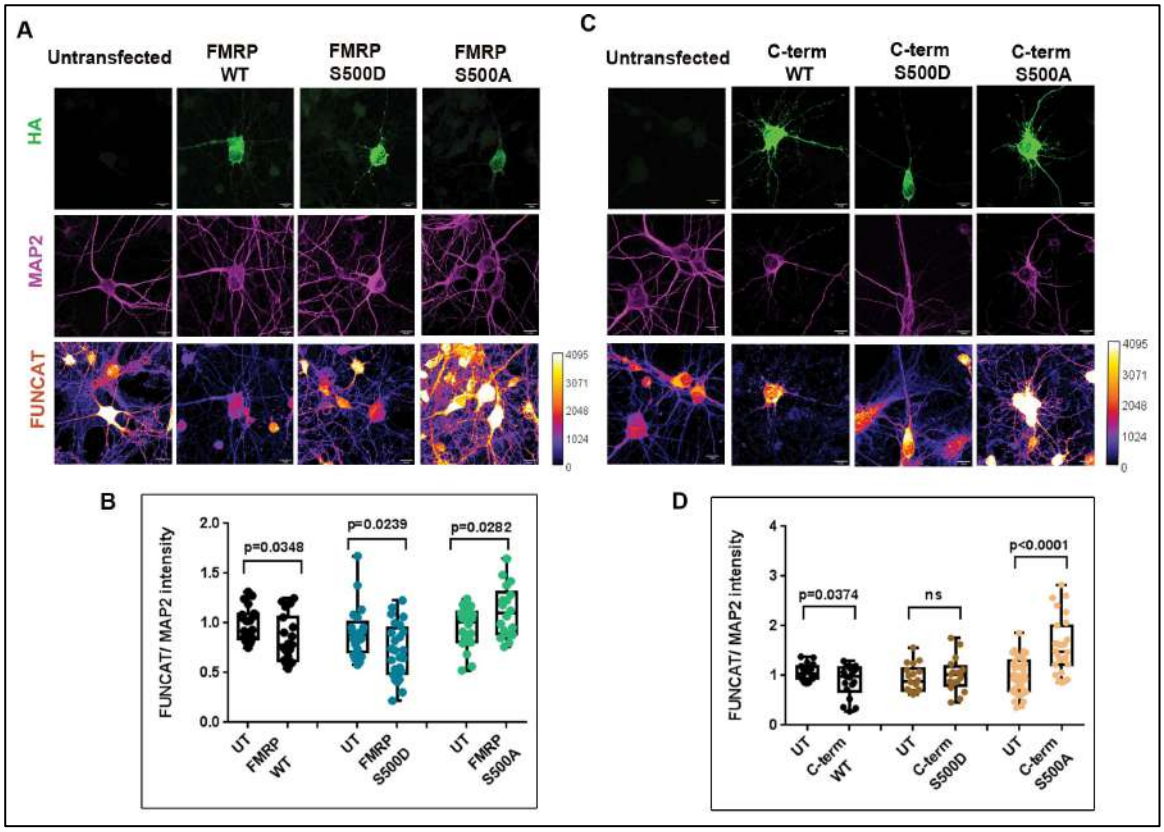

Figure 3.5: Phosphorylation of FMRP modulates in function of global translation regulation

A*-Representative images for HA, MAP2 and FUNCAT fluorescent signals in neurons transfected with full length WT, S500D and S500A FMRP variants (Scale bar - 10µm).* ***B****-Quantification of the FUNCAT fluorescent intensity normalized to MAP2 fluorescent intensity for full length WT, S500D and S500A FMRP. Unpaired t-test for each construct, n = 20-40 neurons from 4 independent experiments.* ***C****-Representative images for HA, MAP2 and FUNCAT fluorescent signals in neurons transfected with C-terminus WT, S500D and S500A variants (Scale bar - 10µm).* ***D****-Quantification of the FUNCAT fluorescent intensity normalized to MAP2 fluorescent intensity for C-terminus WT, S500D and S500A variants. Unpaired t-test for each construct, n = 20-40 neurons from 4 independent experiments*

3.6 Summary:

In this chapter, we have investigated the role of individual domains of FMRP in its primary role of translation regulation and ribosome association. On dissecting FMRP into individual domains and domain combinations, we observe that the C-terminus domain is essential for FMRP's association with the ribosome. To this extent, we observe that the C-terminus alone is essential and sufficient to inhibit protein synthesis in a manner that is similar to full-length FMRP. Although FMRP has been widely associated with translation repression, we also capture its function of activating protein synthesis. Dephosphorylation of serines within the C-terminus of FMRP led to increased association with ribosomes and polysomes. Consequently, this resulted in the up-regulation of protein synthesis in neurons transfected with FMRP S500A which was captured with C-term S500A alone. Through these experiments we elucidate the minimal domain of FMRP that is essential and sufficient for inhibition of neuronal protein synthesis and the role of phosphorylation in modulating the switch between activation and inhibition of neuronal translation.

Chapter 4

Contribution of FMRP domains in regulating puncta formation and microtubule association

Introduction:

Neurons are highly polarized cells with extended cellular processes (axons and dendrites) specializing in information transfer and storage. During development, these processes are dynamically remodeled in response to cues from neurotrophic factors and neuronal activity. Hence there arises the need to dynamically adjust the molecular content within these processes to facilitate plasticity [159,160]. Local translation of mRNAs targeted to axons and dendrites has proven to be an efficient means of regulating the proteome in these compartments[161]. Granules encompassing specific mRNAs are actively transported to synapses via the actin and microtubule cytoskeleton[162]. FMRP is a one such RBP that is known to be a component of membrane-less granules/puncta required for RNA transport both in neuronal dendrites and axon[7,142]. Hence there is a hypothesis that FMRP-granules may play a role in the spatiotemporal control of protein synthesis in presynaptic and post-synaptic compartments[142,149,163].

The process of FMRP-mediated localized translation in neurons is preceded by the canonical processes of granule /puncta formation followed by their directional mobilization through association with microtubules [149]. In the previous chapter, we described the molecular interaction between FMRP and the ribosome. We observe that the primary role of FMRP C-terminus in inhibiting protein synthesis is through its direct association with the ribosome and dephosphorylation is a molecular switch that reverses this function. The formation of FMRP granules *in-vitro* is suggested to be the result of a phase-separation process mediated by the Intrinsically Disordered C-terminus of (IDR) of FMRP[130,164]. But there is lack of physiological evidence showing the involvement of the other domains of FMRP in this process. Moreover, it is unclear which domain of FMRP is responsible for microtubule-dependent transport of these granules. Thus, in this chapter, we investigate the contribution of individual

domains of FMRP in forming neuronal puncta and their association with the microtubule.

4.1.The combinations of FMRP domains synergistically contribute to neuronal puncta formation.

To examine the contribution of FMRP domains in puncta formation, Flag-HA tagged domains of FMRP were overexpressed in rat primary cortical neurons at DIV 11 and the size and relative number of the tagged protein-containing neuronal granules/puncta were quantified (**Fig 4.1A and 4.1B)**. Puncta of all the individual domains of FMRP were smaller in area compared to that of the full-length FMRP protein (**Fig 4.1C)**. Additionally, KH domain containing puncta were lesser in number compared to that of the full-length protein (**Fig 4.1D)**. His-GFP which was also transfected as a control, showed a diffused pattern of expression (**Fig 4.1E and 4.1F).** Interestingly, KH puncta and GFP puncta were not significantly different from each other in terms of size and number indicating that the KH domain alone has the least puncta forming ability among the domains of FMRP (**Fig 4.1G and 4.1H**). Fusion of KH domain to either the N-term or C-term of FMRP increased the relative size and number of puncta in comparison to puncta containing the full-length protein (**Fig 4.1E-F and 4.1I-J).** This indicates that the synergistic contribution of two or more domains of FMRP is required for effective puncta formation in neurons.

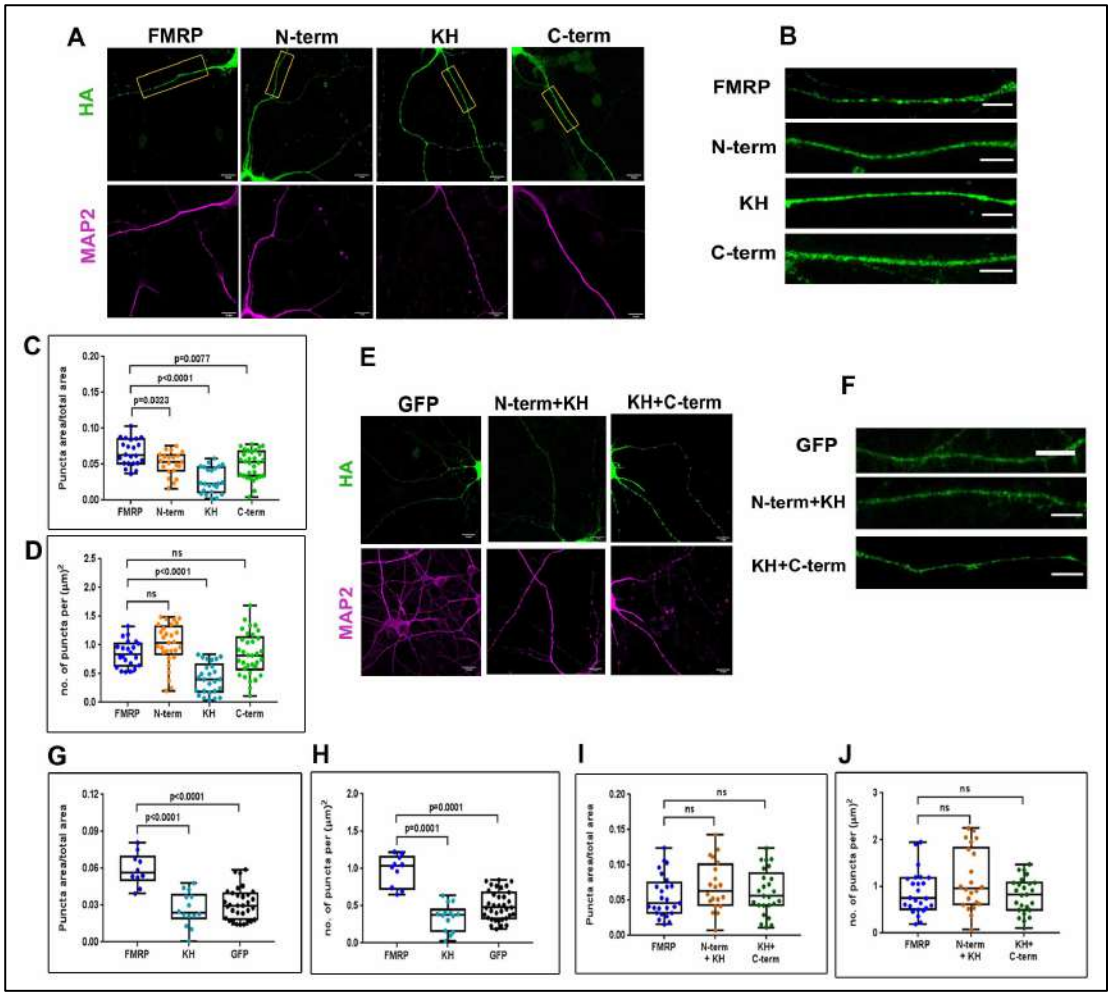

Figure 4.1: Synergistic contribution of FMRP domains contributes to neuronal granule formation

A*. Representative images of Primary rat cortical neurons (DIV11) stained with HA and MAP2 after transfection with full length and FMRP domains for 24h (Scale bar - 10µm)* ***B****. Inserts are enlarged showing dendritic localization of puncta.(Scale bar - 5µm).* ***C****. Box plot represents quantification of puncta area by total dendritic area for full length and FMRP domains. One-way ANOVA p<0.001 followed by Tukey's multiple comparison's test N = 25-35 neurons from 5 independent experiments.* ***D****. Representative images of Primary rat cortical neurons (DIV11) stained with HA and MAP2 after transfection with control His-GFP, N-term+KH and KH+C-term for 24h (Scale bar - 10µm).* ***E****. Inserts are enlarged showing dendritic localization of puncta.(Scale bar - 5µm).* ***F****. Box plot represents quantification of the number of puncta per unit area of the dendrite for full length and FMRP domains. The box extends from 25th to 75th percentile with the middlemost line representing the median of the*

dataset. Whiskers range from minimum to maximum data point. One-way ANOVA p<0.001 followed by Tukey's multiple comparison's test, N = 25-35 neurons from 5 independent experiments. ***G****. Box plot represents quantification of puncta area by total dendritic area for full length FMRP, KH domain and GFP. One-way ANOVA p<0.001 followed by Tukey's multiple comparison's test ,N = 11-35 neurons from 3 independent experiments.* ***H****. Box plot represents quantification of number of puncta per unit area for full length FMRP, KH domain and GFP. One-way ANOVA p<0.001 followed by Tukey's multiple comparison's test ,N = 11-35 neurons from 3 independent experiment****. I****. Box plot represents quantification of puncta area by total dendritic area for full length FMRP , N-term+KH and KH+C-term. One-way ANOVA p=0.3415 followed by Tukey's multiple comparison's test N = 20-25 neurons from 5 independent experiment.* ***J****. Box plot represents quantification of number of puncta per unit area for full length FMRP , N-term+KH and KH +C-term. One-way ANOVA p=0.0566 followed by Tukey's multiple comparison's test N = 20-25 neurons from 5 independent experiment*

4.2.Phosphorylation regulates the dynamics of FMRP puncta

In the previous chapter we described the role of phosphorylation as a molecular switch in modulating ribosomal and polysomal association of FMRP. Furthermore Phosphorylation of FMRP is known to modulate its association with various molecular interactors[20,41,164]. Hence to investigate the role of phosphorylation in puncta formation, we transfected neurons with phospho and de-phosphomimics of FMRP and observed changes in puncta characteristics (**Fig 4.2A and 4.2B**). Rat cortical neurons were transfected with constructs expressing WT, S500D and S500A mutants of full-length FMRP for 24h at DIV11 (**Fig4.2A and 4.2B**). Expression of FMRP S500A in neurons resulted in the formation of significantly larger puncta compared to FMRP WT and FMRP S500D (**Fig 4.2C)**. Dephosphorylation of FMRP also resulted in a significant increase in the overall number of puncta (**Fig 2D)**. Interestingly, there was no significant difference in the size or number of puncta in neurons expressing FMRP WT or FMRP S500D indicating that dephosphosphorylation has a significant influence in increasing the size and number of FMRP puncta (**Fig 4.2C and 4.2D**).

Although FMRP granules are known to harbor RNA, the exact molecular composition of these puncta is yet to be elucidated [16,104]. Dendritically and axonally-localized FMRP granules were observed to contain heterogeneous sets of regulatory proteins and RNAs respectively[14]. Ribosomal subunits were also identified to associate with FMRP granules in multiple brain regions [40]. But it is unclear if FMRP is incorporated into translating ribosomes within these granules. To determine the translation status of these granules, rat cortical neurons were transfected with WT, S500D and S500A FMRP and puncta were analyzed after treatment with the protein synthesis inhibitor Puromycin (**Fig 4.2E and 4.2F**). Puromycin is a tRNA analog that gets incorporated into the C-terminus of the elongating nascent chain causing a premature termination of translation. Hence Puromycin leads to the dissociation of actively translating ribosomes/polysomes. On Puromycin treatment, there was a significant drop in granules containing FMRP WT and FMRP S500A indicating that these granules contain actively translating ribosomes. S500D puncta were insensitive to Puromycin suggesting it to be consisting of stalled ribosomes **(Fig 4.2G and 4.2H**). Together, our data demonstrates that dephosphorylation of FMRP favors increase in puncta size and number and puncta containing dephosphorylated

FMRP contain actively translating polysomes.

Next, we investigated if FMRP positive granules indeed contained actively translating ribosomes. To study this, RPL10-GFP (protein of the larger ribosomal subunit) was overexpressed along with FMRP WT in rat primary cortical neurons and the colocalization of these two proteins was measured with and without Puromycin treatment (**Fig 4.2I**). Our data indicates that FMRP intensities in the puncta also correlate with RPL10 intensities directly demonstrating that ribosomal machinery co-localize to FMRP granules (**Fig 4.2J**). The correlation between FMRP and RPL10 in FMRP puncta reduces on Puromycin treatment indicating that FMRP granules contain actively translating ribosomes (**Fig 4.2K**). Together, our data demonstrates that phosphorylation modulates the characteristics of FMRP-containing granules . Our data also clearly indicates that FMRP associates with actively translation ribosomes within these puncta.

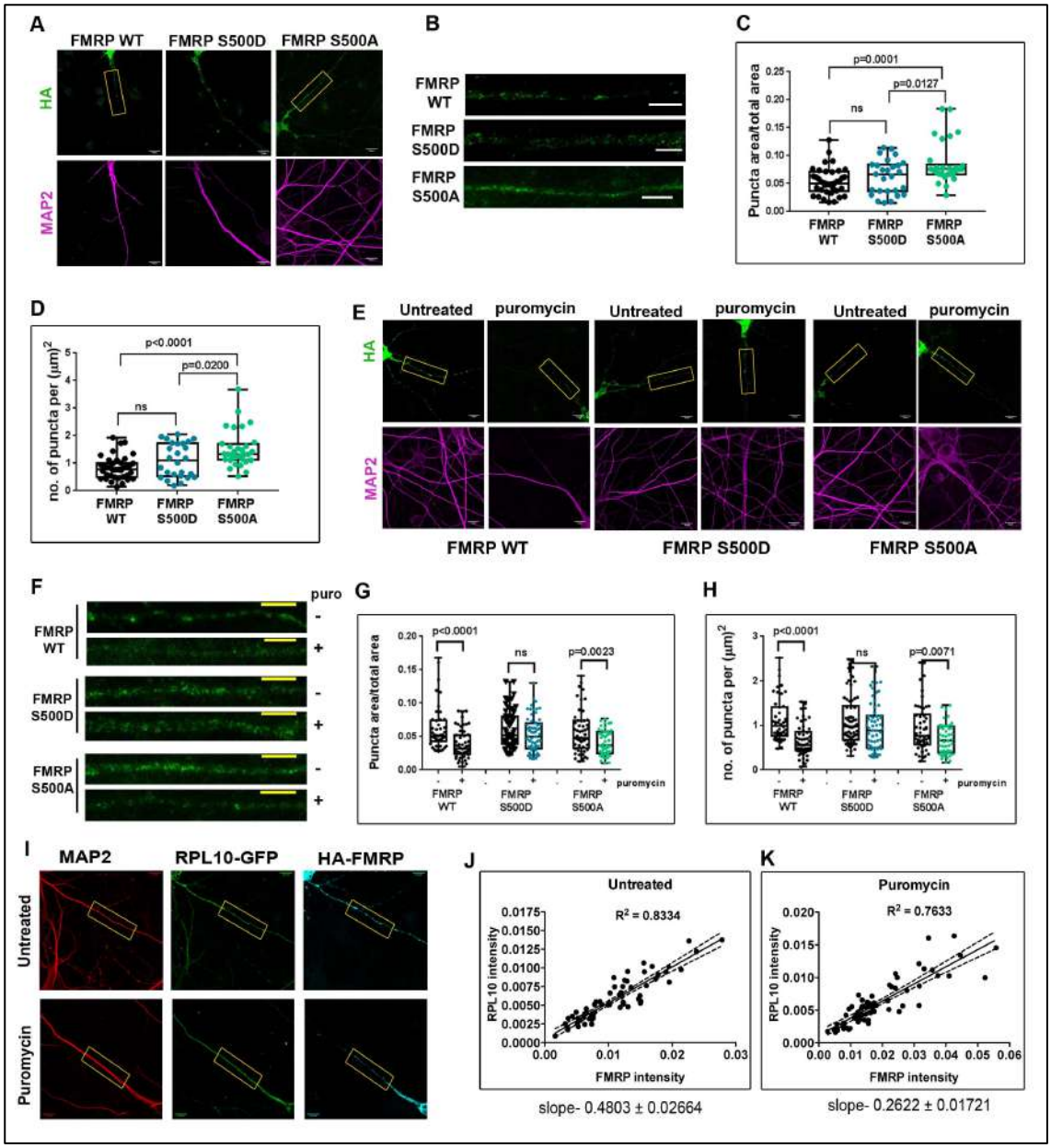

Figure 4.2: FMRP puncta size is regulated by phosphorylation and puncta are sensitive to Puromycin

***A**. Representative images of Primary rat cortical neurons (DIV11) stained with HA and MAP2 after transfection with full length WT, S500D and S500A FMRP variants for 24h (Scale bar - 10µm). **B**. Inserts are enlarged showing dendritic localization of puncta.(Scale bar - 5µm). **C**. Box plot represents quantification of puncta area by total dendritic area for full length WT, S500D and S500A FMRP. N = 20-40 neurons from 5 independent experiments. One-way ANOVA p=0.0002 followed by Tukey's multiple comparison test. **D**. Box plot represents quantification of the number of puncta per unit area of the dendrite for full length and WT, S500D and S500A FMRP. N = 25-40 neurons from 5 independent experiments. One-way ANOVA p<0.0001*

followed by Tukey's multiple comparisons test. ***E*** *.Representative images of Primary rat cortical neurons (DIV11) stained with HA and MAP2 after transfection with full length WT, S500D and S500A FMRP variants for 24h followed by treatment with Puromycin (1mM) for 1hr (Scale bar - 10µm).* ***F****. Inserts are enlarged showing dendritic localization of puncta.(Scale bar - 5µm).* ***G****. Box plot represents quantification of puncta area by total dendritic area for full length WT, S500D and S500A FMRP on Puromycin treatment. Unpaired t-test. N = 40-60 neurons from 3 independent experiments.* ***H****. Box plot represents quantification of the number of puncta per unit area of the dendrite for full length WT, S500D and S500A FMRP on Puromycin treatment. Unpaired t-test. N= 40-60 neurons from 3 independent experiments.* ***I****. MAP2, HA and GFP intensities in primary cortical neurons co-transfected with HA-FMRP and RPL10-GFP followed by Puromycin treatment (1mM) for 1hr (Scale bar - 10µm).* ***J****. Scatter plots indicating distribution of RPL10 intensity and FMRP intensity in FMRP puncta under basal conditions. Dots represent normalized mean intensities of RPL10 and FMRP. n=67 dendrites from 4 independent experiments. Slope= 0.4803 ± 0.02664.* ***K****. Scatter plots indicating distribution of RPL10 intensity and FMRP intensity in FMRP puncta on Puromycin treatment (1mM for 1hr). Dots represent normalized mean intensities of RPL10 and FMRP. n= 74 dendrites from 4 independent experiments. Slope= 0.2622 ± 0.01721*

4.3. Phosphorylation-mediated modulation in FMRP-puncta dynamics is not recapitulated by C-terminus domain of FMRP.

As discussed in Chapter 3, the C-terminus of FMRP played a pivotal role in association with the ribosome and this interaction was enhanced through its dephosphorylation at Serine 500. To reiterate, none of the individual domains of FMRP were capable of forming puncta similar to that of the full-length protein (**Fig 4.1C and 4.1D**). Since the primary phosphorylation site of FMRP (Serine 500) lies within the C-terminus, we postulated that phosphorylation might modulate the characteristics of C-terminus -containing puncta. To investigate this, we transfected rat primary cortical neurons with WT, S500D and S500A mutants of C-term **(Fig 4.3A and 4.3B**). Interestingly there was no significant difference in the puncta characteristics of neurons expressing WT, S500D and S500A mutants of C-term (**Fig 4.3A-D**). Altering the phosphorylation status of C-term alone did not have any effect on the size or number of the puncta (**Fig 4.3C and 4.3D**). As an additional step, we overexpressed WT, S500D and S500A mutants of KH+C-term in rat cortical neurons (**Fig 4.3E and 4.3F**). Similar to the C-term, we did not observe any significant difference between the WT, phospho and de-phospho KH+C-term containing puncta (**Fig 4.3G and 4.3H**).

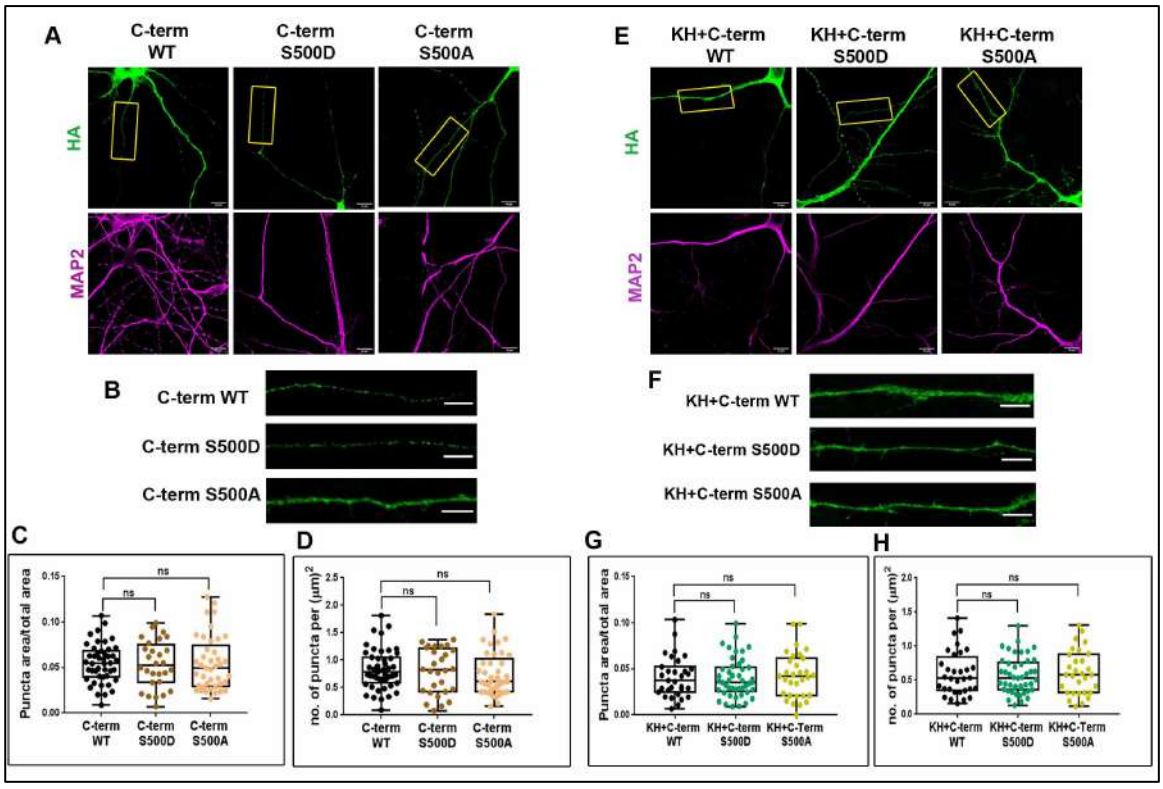

Figure 4.3: Phosphorylation of C-term or KH+Cterm does not alter neuronal

puncta size and number .

A*. Representative images of Primary rat cortical neurons (DIV11) stained with HA and MAP2 after transfection with WT, S500D and S500A C-term variants for 24h (Scale bar - 10µm).* ***B****. Inserts are enlarged showing dendritic localization of puncta.(Scale bar - 5µm).****C****. Box plot represents quantification of puncta area by total dendritic area for full length WT, S500D and S500A C-term. N = 25-45 neurons from 5 independent experiments. One-way ANOVA p=0.02238 followed by Tukey's multiple comparison test.* ***D****. Box plot represents quantification of the number of puncta per unit area of the dendrite for full length and WT, S500D and S500A C-term. N = 25-45 neurons from 5 independent experiments. One-way ANOVA p=0.5737 followed by Tukey's multiple comparisons test.* ***E.*** *Representative images of Primary rat cortical neurons (DIV11) stained with HA and MAP2 after transfection with WT, S500D and S500A KH+C-term variants for 24h (Scale bar - 10µm).****F*** *.Inserts are enlarged showing dendritic localization of puncta.(Scale bar - 5µm).* ***G****. Box plot represents quantification of puncta area by total dendritic area for full length WT, S500D and S500A KH+C-term. N = 30-45 neurons from 5 independent experiments. One-way ANOVA p=0.1518 followed by Tukey's multiple comparison test.* ***H****. Box plot represents quantification of the number of puncta per unit area of the dendrite for full length and WT, S500D and S500A KH+C-term. N = 30-45 neurons from 5 independent experiments. One-way ANOVA p=0.199 followed by Tukey's multiple comparisons test.*

4.4.Domains of FMRP synergistically contribute to microtubule association.

FMRP regulates the translation of its mRNAs in neurons through targeted localization in a microtubule-dependent manner[40]. Our next step was to investigate the biochemical interaction between FMRP domains and microtubules. For this, we employed a previously standardized protocol to stabilize and extract microtubules with its interacting molecular partners **(Fig 4.4A)** [40]**.** This method employs the use of the drug Paclitaxel/Taxol to prevent the disassembly of tubulin polymers and help in the extraction of a stabilized microtubule pellet **(Fig 4.4A)**. With this assay, a significant amount of endogenous FMRP that was present in the microtubule pellet was further enriched on Taxol treatment along with corresponding enrichment in tubulin **(Fig 4.4B).** To confirm that this interaction is microtubule specific, we disrupted the microtubule polymers using the drug Nocodazole and observed a depletion of both endogenous FMRP and tubulin from the microtubule pellet **(Fig 4.4C)**. His-GFP was used as a negative control and it did not show any significant enrichment with the Taxol enriched microtubule pellet **(Fig 4.4D)**. Studies show that that the interaction of FMRP with microtubules is RNA-dependent and to test this, we treated HEK293T cell lysate with an RNase mixture prior to the assay **(Fig 4.4E)**. We observed a loss of FMRP from the microtubule pellet confirming that FMRP-microtubule interaction is RNA dependent **(Fig 4.4E)**.

To dissect out the contribution of the individual domains of FMRP in this interaction, Flag-HA tagged domains of FMRP were transfected in HEK293T cells followed by the microtubule enrichment assay **(Fig 4.4F)**. Surprisingly the microtubule binding ability of all individual domains was significantly lower than that of the full-length protein **(Fig 4.4F)**. Evidently microtubule binding of FMRP requires the participation of more than an individual domain. Hence, we fused KH domain to the N-term and C-term respectively and tested their microtubule interaction **(Fig 4.4G)**. As observed, the combination of domains significantly improved microtubule binding **(Fig 4.4G)** but still significantly lower than the full-length protein.

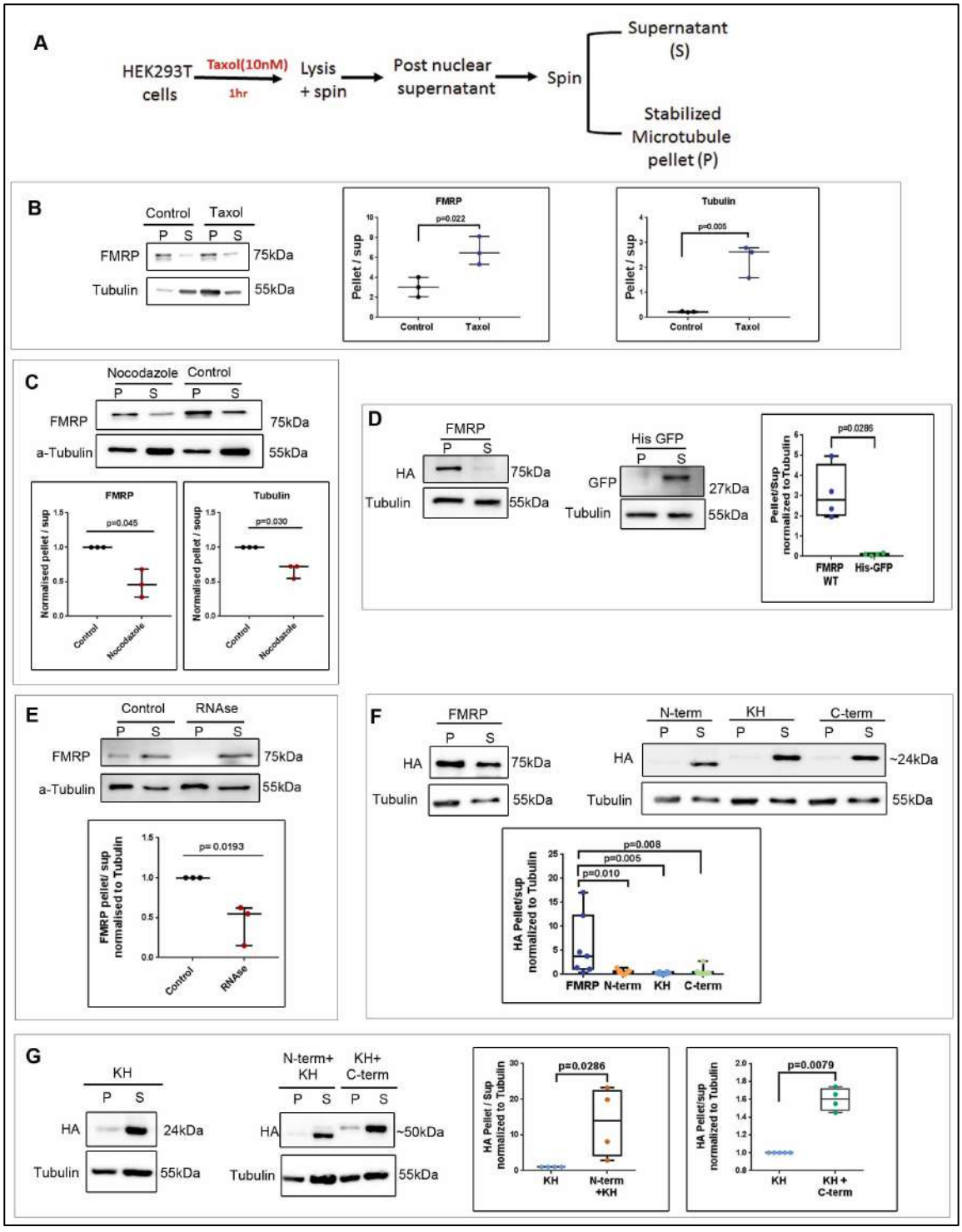

Figure 4.4: Synergistic combination of FMRP domains is necessary for effective FMRP-microtubule association

A*. Schematic for microtubule enrichment assay on Taxol (10nM) treatment.* ***B.*** *Left- Immunoblots indicating the enrichment of endogenous FMRP and tubulin in microtubule pellet on Taxol treatment in HEK293T cells. Middle - Ratio of FMRP enrichment in pellet/supernatant on DMSO (control) and Taxol treatment. Right - Ratio of Tubulin enrichment in pellet/supernatant on DMSO (control) and Taxol*

treatment. Data represented as mean +/- SEM, Unpaired t-test (n=3). ***C****. Top - Representative immunoblots indicating the de-enrichment of endogenous FMRP and Tubulin in microtubule pellet on Nocodazole treatment in HEK293T cells. Bottom – Graphs indicating the pellet to supernatant ratio of endogenous FMRP (left) and Tubulin (right) in Nocodazole versus DMSO (Control) treated cells. Data represented as mean +/- SEM, Unpaired t-test (n=3).* ***D****. Left - Immunoblots indicating enrichment of WT FMRP in microtubule pellet and His-GFP in the supernatant on Taxol treatment. Right – Box plot indicating the ratio of FMRP and His-GFP enrichment in pellet/supernatant on Taxol treatment. Unpaired t-test (n=4).* ***E****. Top – Representative immunoblots indicating the de-enrichment of endogenous FMRP in microtubule pellet on RNase treatment in HEK293T cells. Bottom - Graph indicating the pellet to supernatant ratio of endogenous FMRP in RNase treated cells. Data represented as mean +/- SEM, Unpaired t-test (n=3).* ***F****. Immunoblots of HEK293T cell microtubule pellet enriched on Taxol treatment after transfection with full-length and FMRP domains. Box plots represent the pellet/ supernatant ratio. One-way ANOVA p=0.0053 followed by Dunnett's multiple comparisons test (n=7-8).* ***G****. Immunoblots of HEK293T cell microtubule pellet enriched on Taxol treatment after transfection with KH, N-term+KH and KH+C-term. Box plots represent the pellet/ supernatant ratio. Unpaired t-test (n=4-5).*

4.5. Role of FMRP Phosphorylation in regulating microtubule association.

The role of phosphorylation in modulating neuronal puncta has been studied extensively[20–23,41,130,164]. *In-vitro* studies show that phosphorylation controls mRNA granule assembly and thus modulating the expression of the bound mRNA targets[130,164]. We wanted to test if phosphorylation of FMRP has any effect on microtubule binding. For this, WT, S500D and S500A mutants of full-length FMRP were transfected in HEK293T cells prior to the microtubule-enrichment assay. Interestingly none of the phospho-mutants showed any significant difference compared to WT FMRP in terms of microtubule binding (**Fig 4.5A**). This indicates that phosphorylation has no effect on the association of FMRP with microtubules.

A

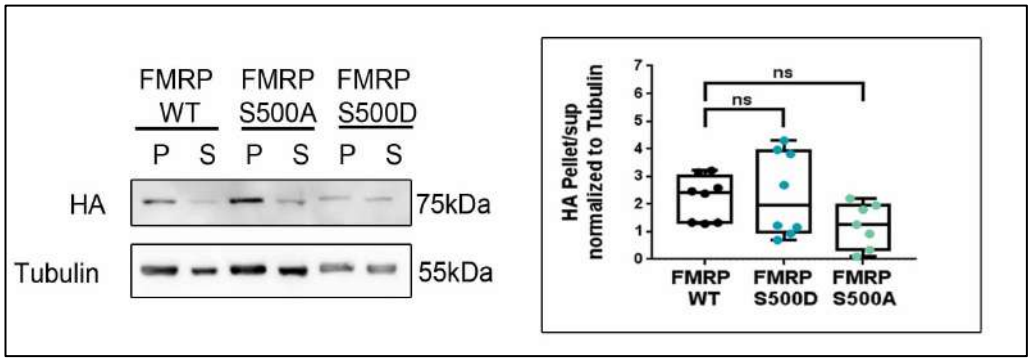

Figure 4.5: Phosphorylation of FMRP does not affect microtubule association

A*. Left- Immunoblots of HEK293T cell microtubule pellet enriched on Taxol treatment after transfection with WT, S500D FMRP and S500A FMRP. Right- Box plots represent the pellet/ supernatant ratio. One-way ANOVA p=0.1325 followed by Dunnett's multiple comparisons test (n=7-8).*

4.6 Summary:

In this chapter, we investigated the contribution of individual domains in the formation of FMRP-containing neuronal granules. Our results support the hypothesis that granule formation is promoted through the involvement of multiple domains of FMRP and not by any individual domain. Synergistic combination of domains enhanced the size and number of FMRP-puncta. Similarly, the contribution of an individual domain was insufficient for optimal microtubule association by FMRP. The efficiency of binding between FMRP and microtubules was strengthened on fusing two domains together. As noted synergistic combination of two domains of FMRP does enhance puncta formation and microtubule association, however this will never be as good as the full-length protein. As observed with ribosome binding, dephosphorylation of full-length FMRP increased the dynamics of FMRP-containing puncta in terms of size and number. However, we did not capture this effect on the size and number of puncta containing C-term or KH+C-term. Our observations also indicate that phosphorylation at Serine 500 has no role in regulating the binding of FMRP to microtubules.

Chapter 5

Validating the role of FMRP domains through pathogenic FMRP mutations

Introduction:

FXS results from the inactivation of the *FMR1* gene (due the expansion of CGG repeats in 5'UTR) leading to the lack of expression of the protein FMRP. The consequence of FMRP's absence is dysregulated translation of its target mRNAs, which is observed as dysregulated synaptic signaling in FXS patient[165,166]. However, recently several FXS-like cases have been reported which are not due to CGG-repeat expansions but resulting from mutations in the coding region of *FMR1* gene[29–32,37]. Advances in high throughput sequencing have made it possible to identify small Indels or point mutations in the *FMR1* gene that can act as potential causes of undiagnosed intellectual disability.

Majority of coding sequence mutations were discovered in individuals with developmental delay exhibiting physical and behavioral features commonly associated with FXS. It is to be noted that these individuals were tested for the typical repeat expansion mutation in the *FMR1* gene but was found to be within the normal range. The most well studied *FMR1* coding sequence mutation I304N, which resides in the RNA-binding KH2 domain, results in the generation of a functionally null FMRP protein [84]. Apart from this mutation, the G266E mutation present in the KH1 domain of FMRP was also found to generate a functionally null protein with respect to RNA-binding and translation regulation [116]. The R534H, G482S and G538fs*23 mutations in the C-terminus domain of FMRP have been predicted to alter RNA-binding and function [30,114]. Although the N-terminus domain of FMRP has been implicated to aid in protein interactions, the R138Q mutation has shown to affect the nuclear localization of FMRP [2,113].

In the previous chapters, we have discussed the contribution of individual domains of FMRP in the cellular processes of puncta formation, microtubule association and ribosome binding which together constitute translation regulation. In

this chapter, I will discuss the molecular impact of coding sequence mutations of FMRP in regulating protein synthesis and how these pathogenic variants confirm the functions of FMRP's domains.

5.1 Effect of pathogenic mutations in domains alters ribosome association of FMRP.

One of the canonical methods of FMRP regulating translation is through its association with polyribosomes whereby it controls the expression of its bound mRNA targets. [167] The absence of FMRP uncouples this translation control over the targets. We made use of relevant pathogenic mutations in the N-term (R138Q), KH domains (I304N, G266E) and C-term (G482S, R534H, G538fs*23) of FMRP that render FMRP non-functional in some aspects. This approach also helps us understand the contribution of individual domains to FMRP's function [29,31,32].

First, we sought to understand the effect of these mutations on ribosome binding through their distribution on a linear sucrose density gradient. For this, we generated Flag-HA tagged full-length FMRP constructs bearing single point mutations in their respective domains. Additionally, we also generated I241N, a functionally relevant mutation in the KH1 domain to mimic the well-studied I304N mutation present in the KH2 domain (**Fig 5.1A**) [17]. All the FMRP mutants showed a similar extent of expression after transfection in HEK293T cells, except for the G538fs*23 mutant (**Fig 5.1B**). Previously, it was found that the G538fs*23 mutation impaired its expression in patient derived cells [32]. To test this observation in our system, we co-transfected equal concentrations FMRP WT with His-GFP and FMRP G538fs*23 with His-GFP separately in HEK293T cells (**Fig 5.1B**). We observed that the levels of FMRP G538fs*23 protein were significantly decreased in comparison to the His-GFP protein whereas there was no significant change in the expression between FMRP WT and His-GFP constructs indicating that this frame shift mutation alters the expression of FMRP (**Fig 5.1C and 5.1D**).

Next, we examined the contribution of pathogenic domain mutations to FMRP –polysome distribution. To test this, Flag-HA FMRP mutants were transfected in HEK293T cells and lysates were separated on a linear sucrose gradient (**Fig 5.1E**). Immunoblots were probed with HA antibody to indicate the distribution of FMRP

mutants and RPLP0 to indicate the distribution of the ribosomes. The distributions of all the FMRP mutants along 12 fractions of the sucrose gradient were quantified (**Fig 5.1D**). Our results indicate that FMRP WT associates with all fractions of the gradient including polysomes (**Fig 5.1E and 5.1G**). We observed that I304N and G266E mutations, residing in the KH domains of FMRP, resulted in decreased association of FMRP with both ribosomes and heavy polysomes (**Fig 5.1E, 5.1J and 5.IK**). Similarly, we observed a decreased association of FMRP I241N mutant with ribosomes and polysomes (**Fig 5.1E and 5.1I**).

R138Q mutation of FMRP, which structurally preserves all the RNA binding domains, did not show any alteration in ribosome and polysome association in comparison to the WT FMRP (**Fig 5.1E and 5.1H**). Similarly, mutations of the C-term R534H and G482S also showed no change in polysome distribution in comparison to WT FMRP (**Fig 5.1E, 5.1L and 5.1M)**. G538fs*23 mutation causes a disruption in the RGG domain generating a premature stop codon with an additional 23 amino acids in the C-term. Consequently, we observed a loss in ribosome and polysome binding of this mutant (**Fig 5.1E and 5.1N).**

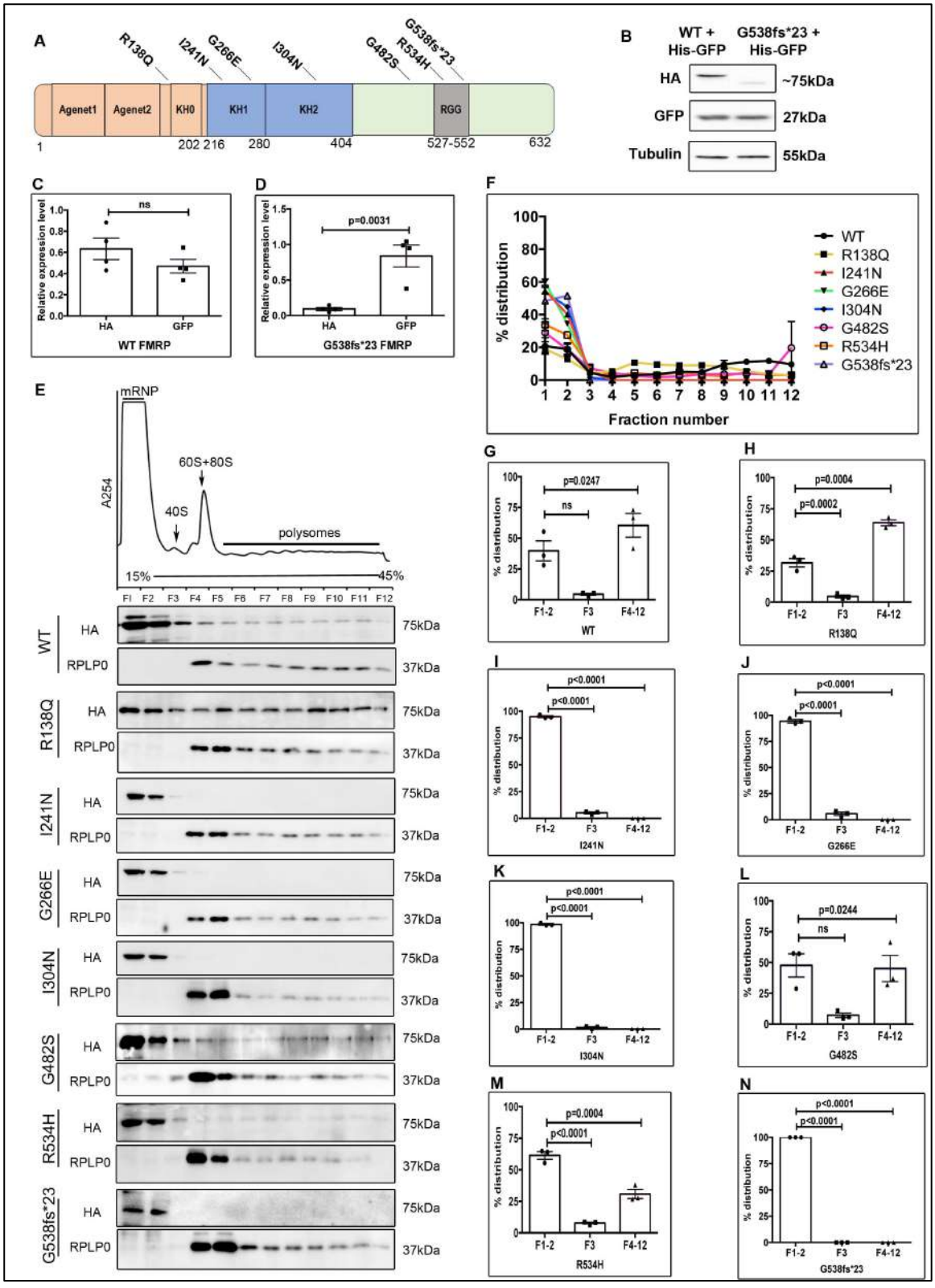

Figure 5.1: KH domain mutations drastically compromise ribosome and polysome binding of FMRP

A*. Schematic depicting position of mutations in FMRP that were identified in patients*

with FXS and intellectual disability. ***B****. Representative blot indicating differential expression of FMRP WT and FMRP G538*fs23 constructs that were co-transfected with control His-GFP.****C****. Quantification of FMRP WT expression efficiency in HEK293T cells after co-transfection with control vector His-GFP. N=4. Unpaired t-test.* ***D****. Quantification of FMRP G538fs*23 expression in HEK293T cells after co-transfection with control vector His-GFP. N=4. Unpaired t-test.* ***E****. Top – Representative polysome trace of HEK293T cell lysate transfected with full-length WT and mutants for 24h. Bottom – Representative immunoblots indicating the distribution of FMRP mutants (probed with HA antibody) with corresponding distribution of ribosome fractions (probed with RPLP0 antibody).****F****. Line graph indicating the distribution of FMRP WT and mutants along 12 fractions of the linear sucrose gradient. N=3. Data points indicate at Mean +/-SEM for each fraction of the overexpressed proteins.* ***G****. Graph indicating the quantification of FMRP WT among the mRNP (F1-2), ribosomal subunits (F3) and ribosomal fractions (F4-12). N=3, One-Way ANOVA p=0.0045 with Dunnett's multiple comparison test.* ***H****. Graph indicating the quantification of FMRP R138Q among the mRNP (F1-2), ribosomal subunits (F3) and ribosomal fractions (F4-12). N=3, One-Way ANOVA p<0.0001 with Dunnett's multiple comparison test.* ***I.*** *Graph indicating the quantification of FMRP I241N among the mRNP (F1-2), ribosomal subunits (F3) and ribosomal fractions (F4-12). N=3, One-Way ANOVA p<0.0001 with Dunnett's multiple comparison test .****J.*** *Graph indicating the quantification of FMRP G266E among the mRNP (F1-2), ribosomal subunits (F3) and ribosomal fractions (F4-12). N=3, One-Way ANOVA p<0.0001 with Dunnett's multiple comparison test* ***K****. Graph indicating the quantification of FMRP I304N among the mRNP (F1-2), ribosomal subunits (F3) and ribosomal fractions (F4-12). N=3, One-Way ANOVA p<0.0001 with Dunnett's multiple comparison test****.*** ***L****. Graph indicating the quantification of FMRP G482S among the mRNP (F1-2), ribosomal subunits (F3) and ribosomal fractions (F4-12). N=3, One-Way ANOVA p=0.0238 with Dunnett's multiple comparison test.* ***M.*** *Graph indicating the quantification of FMRP R534H among the mRNP (F1-2), ribosomal subunits (F3) and ribosomal fractions (F4-12). N=3, One-Way ANOVA p<0.0001 with Dunnett's multiple comparison test.* ***N****. Graph indicating the quantification of FMRP G538fs*23 among the mRNP (F1-2), ribosomal subunits (F3) and ribosomal fractions (F4-12). N=3, One-Way ANOVA p<0.0001 with Dunnett's multiple comparison test*

5.2 Effect of pathogenic FMRP domain mutations on neuronal translation

The next step was to validate the functional effect of these mutations on translation regulation. Rat primary cortical neurons were transfected with Flag-HA FMRP mutants for 24h and changes in global protein synthesis were assayed through FUNCAT (**Fig 5.2A**). Neurons were co-stained for MAP2 whose signal was used to normalize the FUNCAT signal. As seen in previous chapter, FMRP WT showed an overall reduction in the FUNCAT signal in its respective neurons indicating that it inhibits translation (**Fig 5.2B and 5.2C).** On the contrary, KH domain mutations I241N, G266E and I304N failed to inhibit translation in comparison to untransfected neurons. This was visualized as an increase in the FUNCAT signal (**Fig 5.2B and 5.2C)**. Neurons transfected with C-terminus mutants R434H and G482S also showed an increase in FUNCAT signal indicating that these mutations abolish the inhibitory function of FMRP (**Fig 5.2B and 5.2C).** The C-term G538fs*23 mutation also showed an increase in FUNCAT signal **(Fig 5.2B and 5.2C)**. This gain-of-function could be attributed to the insertion of novel amino acids within the C-term. Our initial data indicated that the R138Q mutation does not affect ribosome binding but we observed an increase in FUNCAT signal in comparison to that of untransfected neurons (**Fig 5.2B and 5.2C)**.

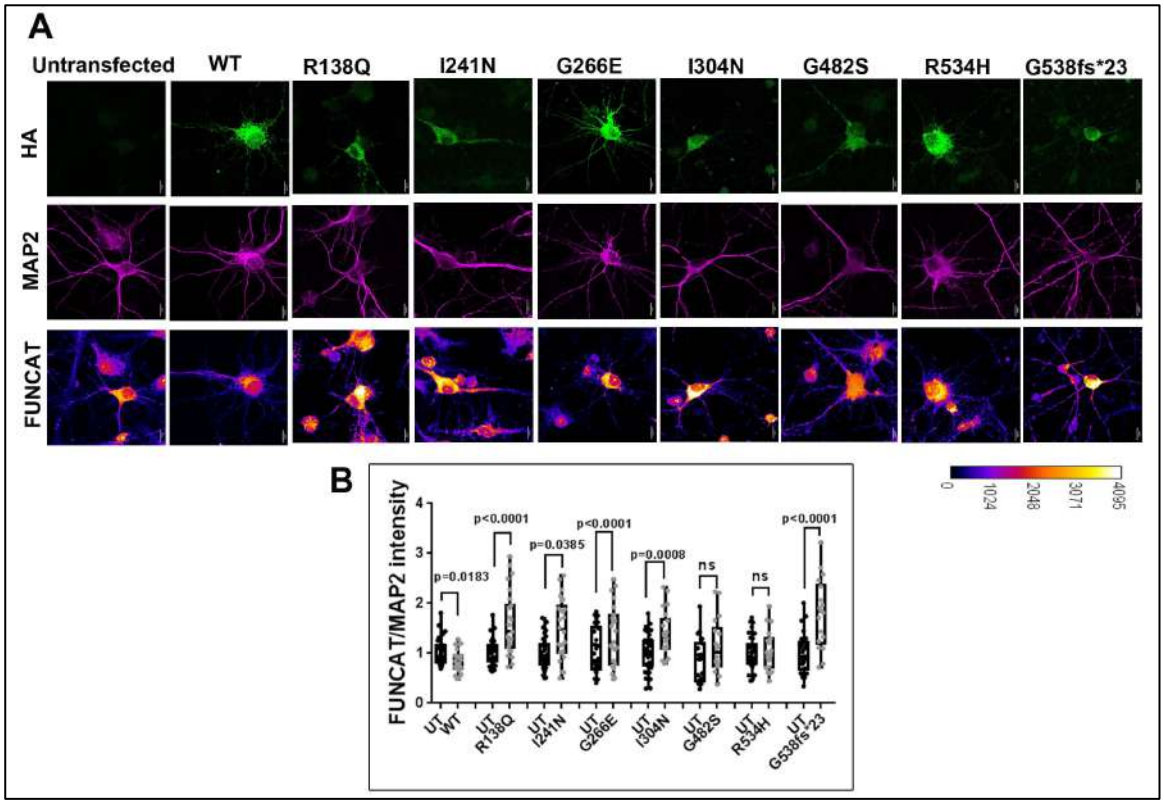

Figure 5.2: KH domain mutations result in loss of translation repression by FMRP.

A. *Representative images for HA, MAP2 and FUNCAT fluorescent intensities in neurons transfected full-length WT and FMRP mutants (Scale bar - 10μM).* ***B.*** *Box plot representing the quantification of the FUNCAT fluorescent intensity normalized to MAP2 fluorescent intensity for WT and mutants of FMRP. For each FMRP construct, the FUNCAT signal from the transfected neuron was normalized to the untransfected neuron. Unpaired t-test, n= 20-35 neurons from 6 independent experiments.*

5.3 Effect of pathogenic FMRP domain mutations in altering puncta characteristics.

Missense mutations in the KH domains (I304N, G266E) have been shown to disrupt the ability of FMRP to bind to RNA and to associate with polysomes [86,116]. But the precise role of these domains in FMRP granule formation, their dynamics and function in neurons is not known. To examine this, we transfected DIV11 rat cortical neurons with FMRP mutants for 24h and measured specific puncta characteristics (**Fig 5.3A and 5.3B**). Neurons were immunostained with HA antibody to identify the puncta containing over-expressed protein and puncta size and number were measured from the proximal dendrites of the neurons. We did not observe any significant changes in puncta size and number among any of the mutants in comparison to FMRP WT (**Fig 5.3C and 5.3D**). This observation is interesting and we speculate that any alteration in puncta characteristics could be captured if they were expressed in neurons lacking endogenous FMRP.

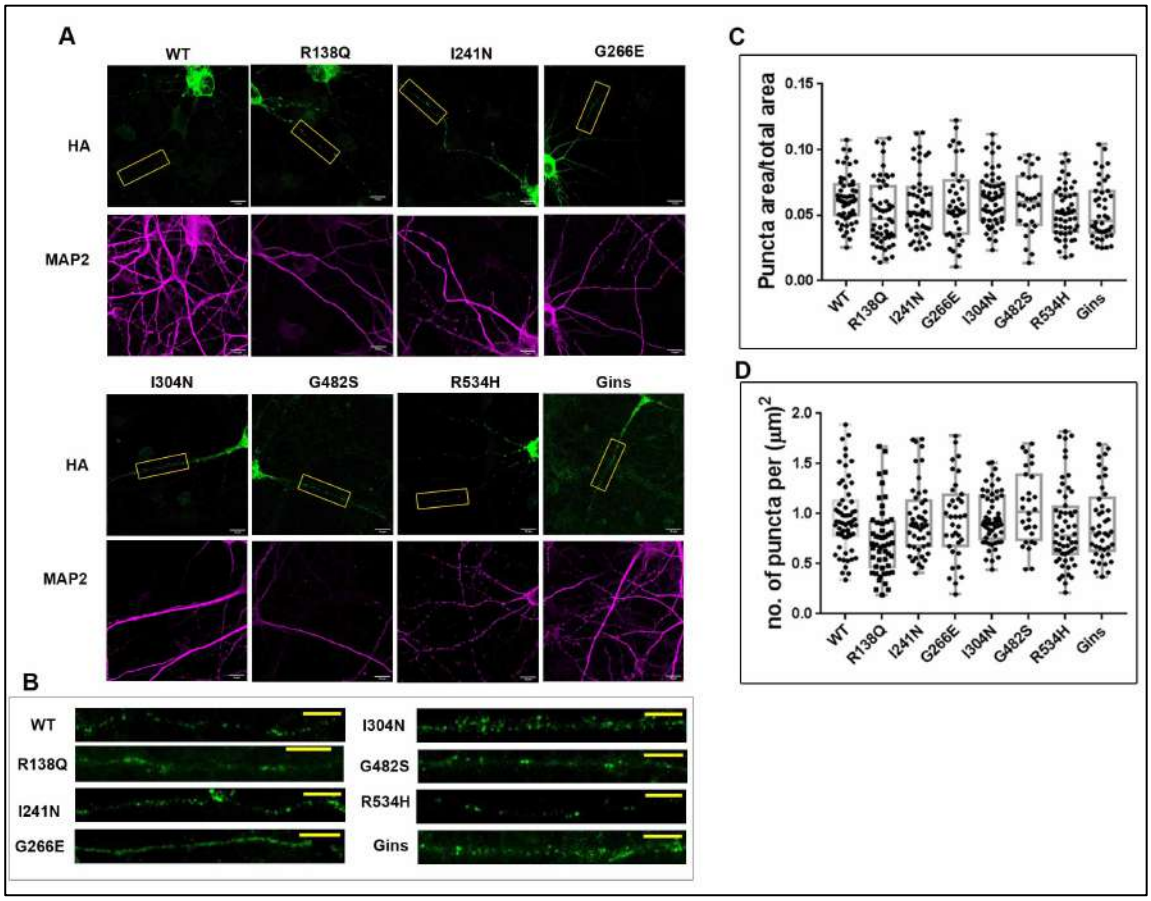

Figure 5.3. Pathogenic mutations of FMRP do not significantly alter puncta size and number in neurons.

***A**. Representative images of HA and MAP2 fluorescent intensities in Primary rat cortical neurons (DIV11) transfected with full-length FMRP mutants for 24h(Scale bar - 10µm).**B**. Inlets shown in panel A are enlarged showing dendritic localization of puncta. (Scale bar - 5µm). **C**. Box plot representing the quantification of puncta area by total dendritic area for full length WT FMRP and mutants of FMRP. n = 30-60 neurons from 5 independent experiments. **D**. Box plot representing the quantification of the number of puncta per unit area of the dendrite for full length FMRP and mutants of FMRP. n = 30-60 neurons from 5 independent experiments*

5.4 Effect of pathogenic FMRP domain mutations on microtubule association.

We show that pathogenic mutations in the KH or C-term domain of FMRP can disrupt ribosome association (**Fig 5.1E, 5.1H-N**). But the influence of these mutations in FMRP-microtubule association is not known. Hence, we sought to examine the effect of these mutations on microtubule binding. We transfected HEK293T cells with Flag-HA FMRP mutants and followed it with a microtubule enrichment assay. KH domain mutations such as I241N, G266E and I304N did not get significantly enriched in the microtubule pellet in comparison to FMRP WT (**Fig 5.4A and 5.4B**). Similarly, C-term mutations R534H and G538fs*23 also significantly hampered FMRP's association with microtubules compared to FMRP WT (**Fig 5.4A and 5.4B**). However, we did not observe any significant effect of R138Q and G482S in FMRP-microtubule association (**Fig 5.4A and 5.4B**). Together, our data concludes that pathogenic mutations identified in the individual domains of FMRP affect their ability to associate with and regulate various components of translation.

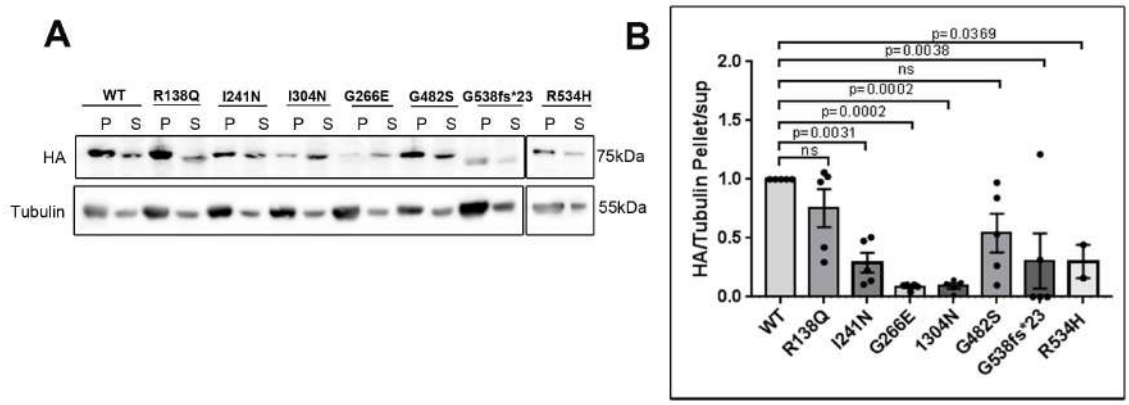

Figure 5.4: KH and C-term domains mutations distinctly affect microtubule association of FMRP but N-term mutations do not.

A*. Representative immunoblots indicating the enrichment of over-expressed WT FMRP, FMRP mutants and tubulin in microtubule pellet and supernatant on Taxol treatment in HEK293T cells (n=3-5).****B****. Box plots indicating the ratio of enrichment of WT and FMRP mutants in pellet/supernatant on Taxol treatment of HEK293T. One-way ANOVA p=0.0002, followed by Dunnett's multiple comparisons test (n=3-5).*

5.5 Summary:

Several point mutations and sequence variants in the coding region of *FMR1* gene have shown to cause FXS- like symptoms. Though most of them have pathophysiological consequences, the molecular functions affected by them are less explored. In this chapter we established the influence of pathogenic domain mutations on the processes of puncta formation, ribosome and microtubule binding by FMRP. We observe a trend of hierarchy among the domains based on effect of the mutations. Our results show that the C-terminus domain is essential for ribosome binding since G482S and R534H mutations are incapable of inhibiting translation. The G538fs*23 mutation alters the reading frame in the C-terminus domain and hence also caused increased translation. Although the C-terminus was intact in proteins containing the R138Q, G266E and I304N mutation, it still resulted in a loss of translation inhibition. Earlier we showed that KH domains alone do not interact with ribosome but mutation of KH domains in full-length protein does affect its ribosome interaction. Likewise, the KH domain mutations also led to a loss in microtubule association. The C-terminus mutations (R534H and G538fs*23) hampered microtubule binding of FMRP as well. Since the KH and C-terminus domains are typical RNA-binding domains, we suspect that pathogenic mutations in these domains could disrupt this property, thereby affecting ribosome and microtubule binding

Chapter 6

Role of nuclear FMRP in regulating protein synthesis

Introduction:

In previous chapters, we focused on the role of FMRP in cellular mechanisms that are predominantly cytoplasmic. However, a significant amount of FMRP also localizes to the nuclear compartments. This can be observed in terminally differentiated cells such as neurons, as well as in cells obtained from early stages of development such as embryonic stem cells (ESCs). While the nuclear localization of FMRP has been reported before, its diverse functions in this compartment are yet to be investigated.

Studies have shown that nuclear FMRP can regulate genomic stability through chromatin remodeling thus impacting developmental stages of FXS[6]. Further due to the presence of a functional Nuclear Localization Signal (NLS) and Nuclear Export Sequence (NES) in FMRP, it is also known to shuttle target mRNAs into the cytoplasm, however there is no clear evidence for this speculation[35,95]. On entering the cytoplasm, the expression of these target mRNAs is regulated by several mechanisms involving FMRP. One such mechanism is through its association with the miRISC complex [10,20,153]. FMRP interacts with a specific set of small RNAs called microRNAs in the cytoplasm to regulate protein synthesis at various stages of development[20,168,169]. We next investigated if FMRP could associate with other small RNA species and the implications of such an association. The findings in this chapter focus on the small-RNA interactome of FMRP and the nature of this interaction. Further we describe the consequences of the interaction between nuclear FMRP with different classes of RNA on protein synthesis and how this can affect neuronal development.

6.1. FMRP localizes to the nucleus in multiple cell types.

Structurally FMRP contains both a NLS and a NES and is localized to both the nucleus and the cytoplasm[36]. We examined the distribution of nuclear of FMRP in rat primary cortical neurons and rat astroglia. Our observations confirm that FMRP localizes to the nucleus of these cell types that we studied (**Fig 6.1A and 6.1B**). FMRP is known to play a role during early stages of development hence we also looked for the distribution of nuclear FMRP in human H9 human embryonic stem cells[169–173] (**Fig 6.1C**). Since ESCs contain relatively larger nuclei, we expected the nuclear: cytoplasmic distribution of FMRP to be higher as compared to other differentiated cell types. Hence to validate this we quantified the distribution of FMRP between these two compartments. On immunostaining H9 human Embryonic Stem Cells with FMRP and DAPI to mark the nucleus, we found the distribution of FMRP to be similar across the nucleus and cytoplasm (**Fig 6.1D**). We next looked at the distribution of phosphorylated FMRP (pFMRP) in human H9 ESCs. H9 ESCs were immunostained with an antibody that recognizes the phospho-Serine 500 epitope of FMRP as well as with DAPI to mark the nucleus (**Fig 6.1E**). We observed that the distribution of pFMRP was the same as that of total-FMRP in the nucleus of ESC indicating that phosphorylation does not dictate the localization of FMRP in ESCs. **(Fig 6.1E and 6.1F**).

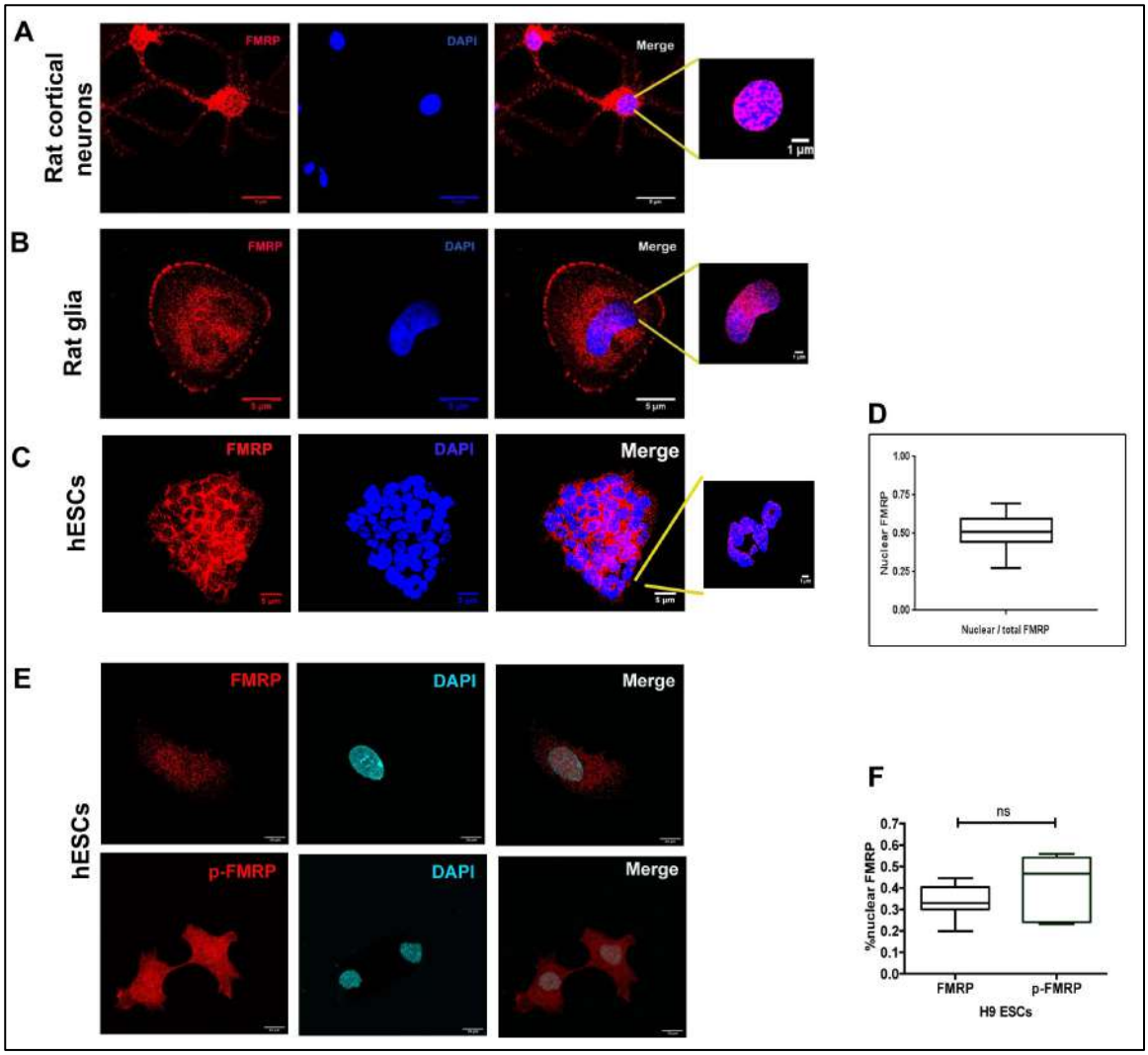

Figure 6.1: FMRP localizes to the nucleus in multiple cell types.

A*. Immunostaining of rat cortical neurons DIV12 (blue-DAPI, red-FMRP, and scale bar, 5 mm) followed by segmented images showing nuclear distribution of FMRP (scale bar, 1 mm).****B****. Immunostaining of rat glia DIV12 (blue-DAPI, red-FMRP, and scale bar, 5 mm) followed by segmented images showing nuclear distribution of FMRP (scale bar, 1 mm).****C****. Immunostaining of human H9 ESCs (blue-DAPI, red-FMRP, and scale bar, 5 mm) followed by segmented images showing nuclear distribution of FMRP (scale bar, 1 mm).****D****. Quantification of nuclear FMRP in H9 hESCs, n = 29 cells.* ***E*** *.Immunostaining of human H9 ESCs (blue-DAPI, red-FMRP/ p-FMRP, and scale bar, 5 mm) showing nuclear distribution of FMRP and p-FMRP (scale bar, 1 mm).****F****. Quantification of nuclear FMRP and p-FMRP in H9 hESCs, n = 8-9 cells.*

6.2. FMRP interacts with C/D box snoRNA in the nucleus.

Multiple studies have emphasized the role of FMRP in translation regulation through its interaction with components of the miRISC complex including microRNAs[10,42]. Initially we investigated the microRNAs that interact with FMRP during neuronal development. For this, we made use of H9 ESCs and H9 NPCs as our model system. Additionally, we also investigated the other types of small RNA species that could interact with FMRP. First, H9 ESCs were characterized for the presence of the pluripotency marker OCT4 (**Figure 6.2A**). H9 ESCs were later differentiated into Neural Precursor Cells through the inhibition of the SMAD signaling pathway[174]. These NPCs were characterized for the expression of Nestin (**Figure 6.2A**). Through immunoprecipitation experiments with H9 ESCs, we show that FMRP interacts with AGO2 and vice versa (**Figure 6.2B**). AGO2 is a primary component of the microRNA Induced Silencing Complex (miRISC) and our results indicate that FMRP interacts with components of the microRNA machinery (**Figure 6.2B).**

We next isolated FMRP bound RNA from H9 ESCs and H9 NPCs after FMRP immunoprecipitation and subjected them to small RNA sequencing. An AGO2-IP was performed simultaneously from H9 ESCs as a positive control to profile microRNAs. Libraries were prepared for the small RNAs and were separated on 6% Polyacrylamide gel (**Figure 6.2C**). The library bands corresponding to 140bp represents the microRNAs which are approximately 35nt in length and this was prominent in the AGO2 IP sample (**Figure 6.2C).** In our initial observation from the FMRP immunoprecipitants, we found an additional band at 200bp that contained a class of RNA likely other than microRNA (**Figure 6.2C**). This additional band at 200bp, which corresponds to RNA species of 80-100nt length, was absent in the AGO2-IP samples (**Figure 6.2C**). The cDNA library bands corresponding to both 140bp and 200bp in the FMRP IP and AGO2 IP samples were isolated and sequenced separately.

The cDNA library band corresponding to 140bp consisted primarily of microRNA as expected (data not shown). However the major component of the 200bp cDNA library band corresponding to 80-100nt RNA species was C/D Box snoRNA[9]. AGO2 IP from H9 ESCs and H9 NPCs showed negligible amount of C/D Box snoRNA in comparison to the input. Our data indicates C/D Box snoRNA

association is specific to FMRP and that the profile of FMRP-bound snoRNA were similar in both H9 ESCs and H9 NPCs [9]. Top C/D Box snoRNAs associated with FMRP in H9 ESCs and H9 NPCs are predicted to target and methylate specific sites on 18S and 28S ribosomal RNA[9]. Although we did identify FMRP-bound microRNA candidates, we focused on understanding the FMRP-bound snoRNA candidates and their function.

We next validated the interaction of FMRP with snoRNA by performing qPCR for C/D Box snoRNA that were enriched in FMRP IP from H9 ESC lysate (**Figure 6.2D**). qPCR primers were designed such that the entire length of the snoRNA was amplified form the FMRP IP, indicating that FMRP interacts with mature snoRNA and not with their shorter processed forms[175]. All target snoRNA showed significant enrichment in the FMRP IP compared to the IgG control (**Figure 6.2D**). Finally, to confirm that this interaction of FMRP with C/D Box snoRNA occurs only within the nucleus, we performed FMRP IP from nuclear and cytoplasmic fractions of H9 ESCs and followed this by qPCR for the top target snoRNA candidates (**Figure 6.2E**). Our data indicates that these snoRNA are significantly enriched in the FMRP immunoprecipitants from nuclear fractions compared to cytoplasmic fractions (**Figure 6.2E**). Thus, FMRP interacts with C/D Box snoRNA in the nucleus and this interaction is conserved even in Neuronal Precursor cells (NPCs).

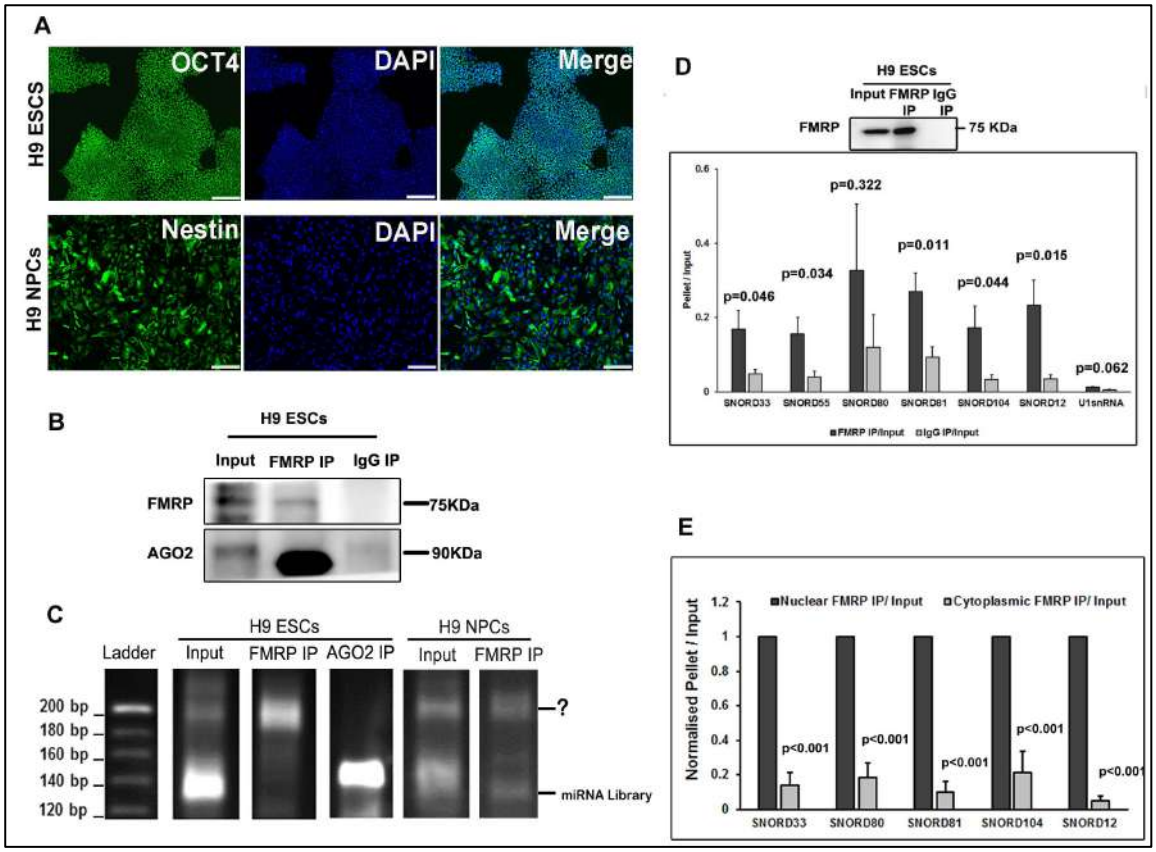

Figure 6.2: FMRP interacts with C/D Box snoRNA in the nucleus.

A*. Characterization of H9 hESCs with pluripotency marker OCT4 and nuclear marker DAPI (scale bar, 100μm) and characterization of H9 hNPCs with differentiation marker Nestin and nuclear marker DAPI (scale bar 100μm).****B.*** *Representative immunoblot for FMRP and AGO2 from H9 hESC lysate after FMRP and IgG immunoprecipitation. Representative of 3 independent experiments.* ***C.*** *Polyacrylamide gels showing mobility of cDNA libraries prepared from RNA extracted after immunoprecipitation with FMRP and AGO2 from H9 hESC and hNPCs lysate. Band corresponding to 120bp indicates the microRNA library and band corresponding to 200bp indicates the snoRNA library.* ***D****. Validation of FMRP-interacting snoRNA in human H9 hESCs by qPCR with representative immunoblot for FMRP IP (n = 6, unpaired Student's t test, mean+/- SEM).****E****. qPCR for selected snoRNAs after immunoprecipitation with FMRP from nuclear and cytoplasmic lysates of H9 hESCs. Values are the ratio of pellet/input of the cytoplasmic fraction normalized to the pellet/input ratio of the nuclear fraction (n = 3, unpaired Student's t test, mean+/-SEM).*

6.3. FMRP-snoRNA complex is devoid of Fibrillarin.

C/D Box snoRNA along with H/ACA Box snoRNA are the two major classes of snoRNAs that are responsible for the post-transcriptional modification on rRNAs, snRNAs and other types of RNAs. C/D Box snoRNA are shown to guide the generation of a 2'O Methylation through complementary binding with ribosomal RNA[176,177]. However, the extent to which 2'O Methylations can alter rRNA folding, dynamics and interactions with other RNA species is unclear. 2'O Methylations do not directly alter the Watson-Crick base pairing however they are known to protect rRNA from hydrolytic cleavage and stabilize the nucleotide conformation[178–180]. Fibrillarin is the nucleolar specific methyltransferase, which associates with the snoRNP complex to generate a 2'O Methylation on a specific site on rRNA [179–181]. Since we observed that FMRP can localize to the nucleus and can interact with C/D Box snoRNA, we hypothesized that FMRP might associate with Fibrillarin to regulate rRNA 2'O Methylation.

To test this, we probed for the presence of Fibrillarin in FMRP immunoprecipitants from H9 ESC nuclear fractions. Surprisingly, we did not observe any co-precipitation of Fibrillarin with FMRP-IP in H9 ESC nuclear lysate (**Figure 6.3A and 6.3B**). We also did not observe any co-precipitation of FMRP with Fibrillarin-IP in H9 ESC nuclear lysates either (**Figure 6.3A and 6.3B).** To validate this finding in another system, we chose HeLa cells. Again, we did not observe the co-precipitation of Fibrillarin with FMRP-IP or the co-precipitation of FMRP with Fibrillarin-IP in HeLa nuclear lysates (**Figure 6.3C and 6.3D**). These results strongly suggest that although FMRP and Fibrillarin interact with C/D Box snoRNA, they are likely to be present in separate RNP complexes.

Our next objective was to investigate if FMRP directly interacts with C/D Box snoRNAs. We performed an Electrophoretic Mobility Shift Assay (EMSA) with purified full-length FMRP and SNORD80, one of the top snoRNA candidates associated with FMRP from the high-throughput analysis (**Figure 6.3E**). SNORD80 was radiolabeled with γ-P-ATP and was incubated with increasing concentrations of FMRP (from 100 nM to 14.6 mM). A clear shift in SNORD80 mobility was observed even with 500nM of purified FMRP (**Figure 6.3E).** This shift in mobility was further

enhanced in a concentration-dependent manner indicating a direct interaction of SNORD80 with FMRP (**Figure 6.3E**). The shift in SNORD80 mobility was completely reversed by incubating the complex with molar excess of unlabeled SNORD80 while there was no shift observed with non-specific bacterial RNA **(Figure 6.3E**). This demonstrates the direct interaction of FMRP with C/D Box snoRNAs.

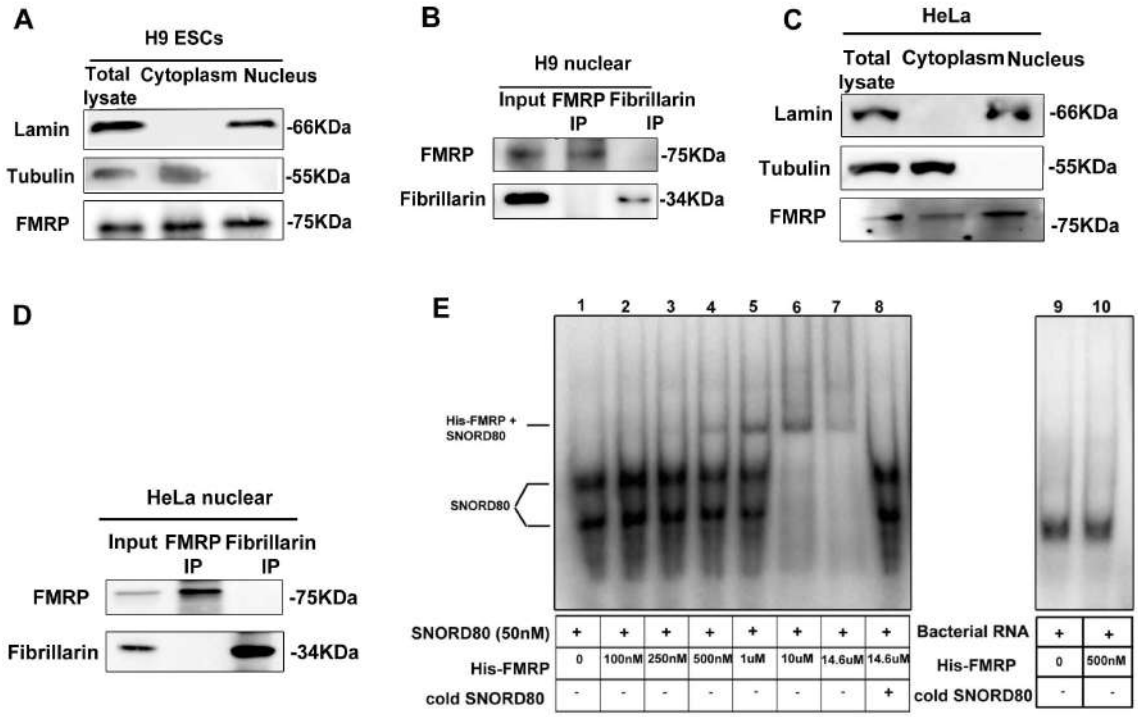

Figure 6.3: FMRP interacts directly with snoRNA independent of Fibrillarin

A*. Representative immunoblots showing the distribution of FMRP in H9 hESC nuclear and cytoplasmic fractions, Lamin B1 as nuclear marker and Tubulin as cytoplasmic marker. N=3.****B****. Representative immunoblots for FMRP and Fibrillarin followed by FMRP or Fibrillarin immunoprecipitation from nuclear fractions of H9 hESCs. N=3.* ***C****. Representative immunoblots showing the distribution of FMRP in HeLa nuclear and cytoplasmic fractions with Lamin as nuclear marker and Tubulin as cytoplasmic marker.* ***D****. Representative immunoblots for FMRP and Fibrillarin followed by FMRP or Fibrillarin immunoprecipitation from nuclear fractions of HeLa cells. N=3.* ***E****. Electrophoretic mobility shift assay showing shift in mobility of radiolabeled SNORD80 by increasing concentration of His-FMRP. Lane 8 shows a complete abolishment of shift with molar excess of unlabeled (cold) SNORD80 RNA. Lanes 9 and 10 indicated no change in the mobility of His-FMRP with radiolabeled non-specific bacterial RNA. Samples in lanes 9 and 10 were run on a separate gel.*

6.4. Absence of FMRP alters differential 2'O Methylation pattern of rRNA in ESCs.

Approximately 100 sites have been identified on human rRNA that are known to be 2'O Methylated[182]. The differential methylation of these designated sites are presumed to generate ribosome heterogeneity as demonstrated in HeLa cells[176,182–184]. To test the levels of ribosome heterogeneity in human ESCs we measured the extent of 2-OMethylation of known sites in Shef4 human ESCs using a previously described high-throughput RiboMeth Sequencing protocol [185,186]. Briefly, ribosomal RNA was extracted from ESCs and subjected to alkaline hydrolysis followed by library preparation and sequencing (*refer to Materials and methods*). Sequenced data was analyzed using a previously described pipeline to estimate the extent of methylation[182]

A total of 97 sites were detected in our sequencing analysis of Shef4 ESC rRNA. A majority of the sites were completely methylated showing a Methylation Index (MI) of 1 or close to 1 (**Figure 6.4A and 6.4B**). However , 9 sites on 18S rRNA and 15 sites on 28S rRNA were only partially methylated (i.e., MI significantly less than 1) (**Figure 6.4A and 6.4B**). These sites showed a MI ranging from 0.6 -0.9 indicating that these sites are methylated only in 60%- 90% of ribosomes whereas the remaining 10%-40% ribosomes are unmethylated at these positions. Our data indicates that the heterogeneity observed in Shef4 ESC ribosomes is distinct from that of the ribosomes in HeLa as previously reported [182]

Since the interaction of FMRP with C/D Box snoRNA resulted in a distinct 2'O Methylation pattern of rRNA, we wanted to measure the changes in this pattern in the absence of FMRP. For this we subjected RNA from WT and *FMR1* KO Shef ESCs to RiboMethSeq. On comparing the profiles between WT and KO cells, we observed that the sites that were completely methylated in the WT were unaffected in the KO. However, the sites that were partially methylated in the WT were significantly altered in the absence of FMRP (**Figure 6.4C).** We collectively found 13 such sites on 18S and 28S rRNA that displayed altered methylation in *FMR1* KO ESCs as compared to the WT (**Figure 6.4C**). This was an interesting observation

since the absence of FMRP had no effect on the steady state levels of the corresponding FMRP-bound C/D Box snoRNA yet there was a significant alteration in corresponding 2'O Methylation pattern of rRNA (**Figure 6.4D**). Our results so far confirm FMRP can contribute to the generation of ribosome heterogeneity in various cell types and that the absence of FMRP has a significant impact on the methylation status of specific rRNA sites.

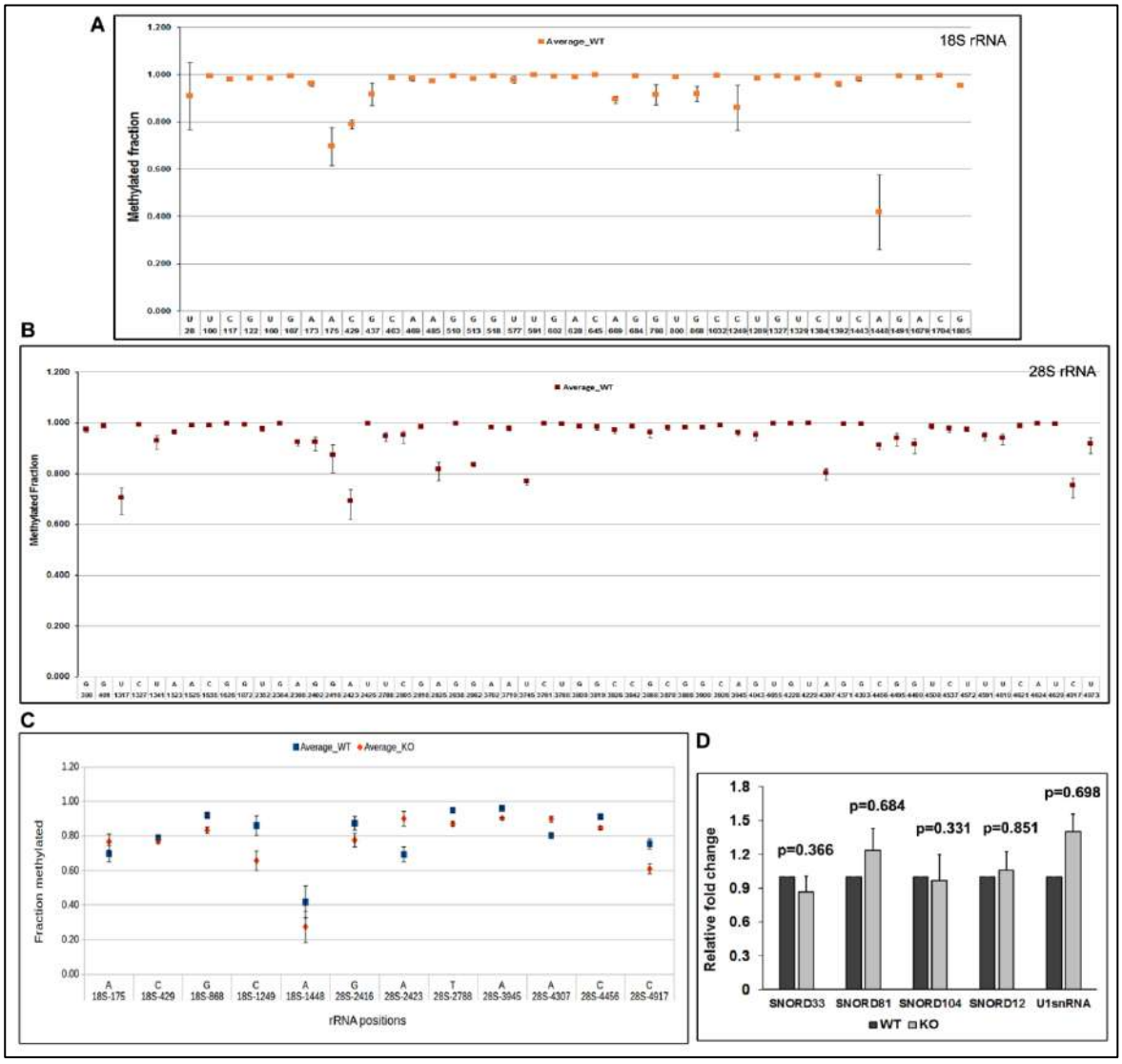

Figure 6.4: Differential 2'O-methylation of rRNA in WT and FMR1KO ESCs.

***A**. Methylation index of the sites on 18S rRNA in Shef4 hESCs. The x axis represents the respective methylation position on 18S rRNA, and y axis represents the fraction methylated, n = 3. **B**. Methylation index of the sites on 28S rRNA in Shef4 hESCs. The x axis represents the respective methylation position on 28S rRNA, and y axis represents the fraction methylated, n = 3.**C**. Change in levels of top snoRNA candidates in Shef4WT and Shef4 FMR1 KO hESCs by qPCR (n = 5,*

*unpaired Student's t test, mean+/- SEM).**D**. Sites in 18S and 28S rRNA that show 5% or more difference in the methylation index between Shef4 hESCs and Shef4 FMR1 KO hESCs (n = 3, mean+/-SEM).*

6.5 Summary:

FMRP as an RNA-binding protein localizes to both cytoplasm and in the nucleus. Here, we observe that a significant amount of FMRP localizes to the nucleus of Embryonic Stem Cells (ESCs) and phosphorylation of FMRP does not appear influence its cellular distribution. Nevertheless, we speculate that the percentage of nuclear FMRP will reduce along differentiation with a clear reduction in nuclear/cytoplasmic ratio in differentiated cells.

In this chapter we investigated the small RNA interactome of FMRP in ESCs. While our small-RNA sequencing did reveal a distinct set of FMRP target microRNAs, we identified novel class of RNAs (C/D box snoRNA) that interact with FMRP. Then we directed our focus to understanding the function of FMRP target snoRNAs and the nature of their interaction. The small-RNA interactome of cytoplasmic FMRP has been extensively studied, but our finding was interesting since the it revealed a novel function of nuclear FMRP. To this extent, we identified that FMRP interacts with a specific set of C/D box snoRNAs in the nucleus. C/D box snoRNAs guide 2'O methylations of ribosomal RNA (rRNA) on defined sites, and this modification regulates rRNA folding and assembly of ribosomes[182,187]. Interestingly, FMRP was found to regulate rRNA 2'Omethylation through an indirect mechanism. We observed that although FMRP interacts directly with C/D Box snoRNA, this complex is devoid of the primary methyltransferase, Fibrillarin. Hence FMRP-bound snoRNA affect the epi-transcriptome of rRNA independently of Fibrillarin.

FMRP-target C/D Box snoRNA were found to guide the 2'O methylation of 18S and 28SrRNA on several sites leading to ribosome heterogeneity. A majority of the sites on both 18S and 28S rRNA were completely 2'O-methylated in all ribosomes, whereas a distinct set of sites were only partially methylated/ hypomethylated. In the absence of FMRP ,we have demonstrated that the 2'Omethylation pattern of rRNA is altered. Sites that were completely methylated in the WT were unaffected in the

FMR1 KO cells but most importantly, sites that were partially methylated in the WT seemed to be further affected in the absence of FMRP. This suggests that nuclear FMRP has a contribution in generating ribosome heterogeneity , a phenomenon which is severely affected when FMRP is absent.

References

1. Santoro, M. R., Bray, S. M. & Warren, S. T. Molecular Mechanisms of Fragile X Syndrome: A Twenty-Year Perspective. *Annu. Rev. Pathol. Mech. Dis.* **7**, 219–245 (2012).
2. Myrick, L. K., Hashimoto, H., Cheng, X. & Warren, S. T. Human FMRP contains an integral tandem Agenet (Tudor) and KH motif in the amino terminal domain. *Hum. Mol. Genet.* **24**, 1733–1740 (2015).
3. Siomi, H., Siomi, M. C., Nussbaum, R. L. & Dreyfuss, G. The protein product of the fragile X gene, FMR1, has characteristics of an RNA-binding protein. *Cell* **74**, 291–298 (1993).
4. Nelson, D. L., Orr, H. T. & Warren, S. T. The Unstable Repeats—Three Evolving Faces of Neurological Disease. *Neuron* **77**, 825–843 (2013).
5. Hu, Y. *et al.* The amino-terminal structure of human fragile X mental retardation protein obtained using precipitant-immobilized imprinted polymers. *Nat. Commun.* **6**, 6634 (2015).
6. Alpatov, R. *et al.* A Chromatin-Dependent Role of the Fragile X Mental Retardation Protein FMRP in the DNA Damage Response. *Cell* **157**, 869–881 (2014).
7. Antar, L. N. Metabotropic Glutamate Receptor Activation Regulates Fragile X Mental Retardation Protein and Fmr1 mRNA Localization Differentially in Dendrites and at Synapses. *J. Neurosci.* **24**, 2648–2655 (2004).
8. Darnell, J. C. *et al.* FMRP Stalls Ribosomal Translocation on mRNAs Linked to Synaptic Function and Autism. *Cell* **146**, 247–261 (2011).
9. D'Souza, M. N. *et al.* FMRP Interacts with C/D Box snoRNA in the Nucleus and Regulates Ribosomal RNA Methylation. *iScience* **9**, 399–411 (2018).
10. Kute, P. M., Ramakrishna, S., Neelagandan, N., Chattarji, S. & Muddashetty, Ravi. S. NMDAR mediated translation at the synapse is regulated by MOV10 and FMRP. *Mol. Brain* **12**, 65 (2019).
11. Muddashetty, R. S., Kelic, S., Gross, C., Xu, M. & Bassell, G. J. Dysregulated Metabotropic Glutamate Receptor-Dependent Translation of AMPA Receptor and Postsynaptic Density-95 mRNAs at Synapses in a Mouse Model of Fragile X Syndrome. *J. Neurosci.* **27**, 5338–5348 (2007).

12. Pasciuto, E. & Bagni, C. SnapShot: FMRP Interacting Proteins. *Cell* **159**, 218-218.e1 (2014).
13. Huber, K. M., Gallagher, S. M., Warren, S. T. & Bear, M. F. Altered synaptic plasticity in a mouse model of fragile X mental retardation. *Proc. Natl. Acad. Sci.* **99**, 7746–7750 (2002).
14. Sidorov, M. S., Auerbach, B. D. & Bear, M. F. Fragile X mental retardation protein and synaptic plasticity. *Mol. Brain* **6**, 15 (2013).
15. Bear, M. F., Huber, K. M. & Warren, S. T. The mGluR theory of fragile X mental retardation. *Trends Neurosci.* **27**, 370–377 (2004).
16. Antar, L. N., Dictenberg, J. B., Plociniak, M., Afroz, R. & Bassell, G. J. Localization of FMRP-associated mRNA granules and requirement of microtubules for activity-dependent trafficking in hippocampal neurons. *Genes Brain Behav.* **4**, 350–359 (2005).
17. Darnell, J. C. Kissing complex RNAs mediate interaction between the Fragile-X mental retardation protein KH2 domain and brain polyribosomes. *Genes Dev.* **19**, 903–918 (2005).
18. Feng, Y. *et al.* FMRP Associates with Polyribosomes as an mRNP, and the I304N Mutation of Severe Fragile X Syndrome Abolishes This Association. *Mol. Cell* **1**, 109–118 (1997).
19. Stefani, G. Fragile X Mental Retardation Protein Is Associated with Translating Polyribosomes in Neuronal Cells. *J. Neurosci.* **24**, 7272–7276 (2004).
20. Muddashetty, R. S. *et al.* Reversible Inhibition of PSD-95 mRNA Translation by miR-125a, FMRP Phosphorylation, and mGluR Signaling. *Mol. Cell* **42**, 673–688 (2011).
21. Narayanan, U. *et al.* S6K1 Phosphorylates and Regulates Fragile X Mental Retardation Protein (FMRP) with the Neuronal Protein Synthesis-dependent Mammalian Target of Rapamycin (mTOR) Signaling Cascade. *J. Biol. Chem.* **283**, 18478–18482 (2008).
22. Ceman, S. *et al.* Phosphorylation influences the translation state of FMRP-associated polyribosomes. *Hum. Mol. Genet.* **12**, 3295–3305 (2003).
23. Nalavadi, V. C., Muddashetty, R. S., Gross, C. & Bassell, G. J. Dephosphorylation-Induced Ubiquitination and Degradation of FMRP in Dendrites: A Role in Immediate Early mGluR-Stimulated Translation. *J. Neurosci.* **32**, 2582–2587 (2012).

24. Ferron, L. *et al.* FMRP regulates presynaptic localization of neuronal voltage gated calcium channels. *Neurobiol. Dis.* **138**, 104779 (2020).
25. Zhan, X. *et al.* FMRP(1–297)-tat restores ion channel and synaptic function in a model of Fragile X syndrome. *Nat. Commun.* **11**, 2755 (2020).
26. Athar, Y. M. & Joseph, S. The Human Fragile X Mental Retardation Protein Inhibits the Elongation Step of Translation through Its RGG and C-Terminal Domains. *Biochemistry* **59**, 3813–3822 (2020).
27. Phan, A. T. *et al.* Structure-function studies of FMRP RGG peptide recognition of an RNA duplex-quadruplex junction. *Nat. Struct. Mol. Biol.* **18**, 796–804 (2011).
28. Laggerbauer, B. Evidence that fragile X mental retardation protein is a negative regulator of translation. *Hum. Mol. Genet.* **10**, 329–338 (2001).
29. Tekcan, A. In Silico Analysis of FMR1 Gene Missense SNPs. *Cell Biochem. Biophys.* **74**, 109–127 (2016).
30. Collins, S. C. *et al.* Identification of novel FMR1 variants by massively parallel sequencing in developmentally delayed males. *Am. J. Med. Genet. A.* **152A**, 2512–2520 (2010).
31. Handt, M. *et al.* Point mutation frequency in the FMR1 gene as revealed by fragile X syndrome screening. *Mol. Cell. Probes* **28**, 279–283 (2014).
32. Okray, Z. *et al.* A novel fragile X syndrome mutation reveals a conserved role for the carboxy-terminus in FMRP localization and function. *EMBO Mol. Med.* **7**, 423–437 (2015).
33. Eberhart, D. The fragile X mental retardation protein is a ribonucleoprotein containing both nuclear localization and nuclear export signals. *Hum. Mol. Genet.* **5**, 1083–1091 (1996).
34. Fridell, R. A., Benson, R. E., Hua, J., Bogerd, H. P. & Cullen, B. R. A nuclear role for the Fragile X mental retardation protein. *EMBO J.* **15**, 5408–5414 (1996).
35. Kim, M., Bellini, M. & Ceman, S. Fragile X mental retardation protein FMRP binds mRNAs in the nucleus. *Mol. Cell. Biol.* **29**, 214–228 (2009).
36. Taha, M. S. *et al.* Subcellular fractionation and localization studies reveal a direct interaction of the fragile X mental retardation protein (FMRP) with nucleolin. *PloS One* **9**, e91465 (2014).
37. Diaz, J., Scheiner, C. & Leon, E. Presentation of a recurrent FMR1 missense mutation (R138Q) in an affected female. *Transl. Sci. Rare Dis.* **3**, 139–144 (2018).

38. Suvrathan, A., Hoeffer, C. A., Wong, H., Klann, E. & Chattarji, S. Characterization and reversal of synaptic defects in the amygdala in a mouse model of fragile X syndrome. *Proc. Natl. Acad. Sci.* **107**, 11591–11596 (2010).
39. Pfeiffer, B. E. & Huber, K. M. Fragile X Mental Retardation Protein Induces Synapse Loss through Acute Postsynaptic Translational Regulation. *J. Neurosci.* **27**, 3120–3130 (2007).
40. Wang, H. *et al.* Dynamic Association of the Fragile X Mental Retardation Protein as a Messenger Ribonucleoprotein between Microtubules and Polyribosomes. *Mol. Biol. Cell* **19**, 105–114 (2008).
41. Cheever, A. & Ceman, S. Phosphorylation of FMRP inhibits association with Dicer. *RNA* **15**, 362–366 (2009).
42. Kenny, P. J. *et al.* MOV10 and FMRP Regulate AGO2 Association with MicroRNA Recognition Elements. *Cell Rep.* **9**, 1729–1741 (2014).
43. Xing, L. & Bassell, G. J. mRNA Localization: An Orchestration of Assembly, Traffic and Synthesis: mRNA Transport and Localization. *Traffic* **14**, 2–14 (2013).
44. Pichon, X. *et al.* RNA Binding Protein/RNA Element Interactions and the Control of Translation. *Curr. Protein Pept. Sci.* **13**, 294–304 (2012).
45. Änkö, M.-L. & Neugebauer, K. M. RNA–protein interactions in vivo: global gets specific. *Trends Biochem. Sci.* **37**, 255–262 (2012).
46. Martignetti, J. A. & Brosius, J. BC200 RNA: a neural RNA polymerase III product encoded by a monomeric Alu element. *Proc. Natl. Acad. Sci.* **90**, 11563–11567 (1993).
47. Cléry, A., Blatter, M. & Allain, F. H.-T. RNA recognition motifs: boring? Not quite. *Curr. Opin. Struct. Biol.* **18**, 290–298 (2008).
48. Bolognani, F. & Perrone-Bizzozero, N. I. RNA–protein interactions and control of mRNA stability in neurons. *J. Neurosci. Res.* **86**, 481–489 (2008).
49. Hinman, M. N. & Lou, H. Diverse molecular functions of Hu proteins. *Cell. Mol. Life Sci.* **65**, 3168–3181 (2008).
50. Szabo, A. *et al.* HuD, a paraneoplastic encephalomyelitis antigen, contains RNA-binding domains and is homologous to Elav and sex-lethal. *Cell* **67**, 325–333 (1991).
51. Weskamp, K. & Barmada, S. J. TDP43 and RNA instability in amyotrophic lateral sclerosis. *Brain Res.* **1693**, 67–74 (2018).

52. Lefebvre, S. *et al.* Identification and characterization of a spinal muscular atrophy-determining gene. *Cell* **80**, 155–165 (1995).
53. Dormann, D. *et al.* ALS-associated fused in sarcoma (FUS) mutations disrupt Transportin-mediated nuclear import. *EMBO J.* **29**, 2841–2857 (2010).
54. Fang, M. Y. *et al.* Small-Molecule Modulation of TDP-43 Recruitment to Stress Granules Prevents Persistent TDP-43 Accumulation in ALS/FTD. *Neuron* **103**, 802-819.e11 (2019).
55. Patel, A. *et al.* A Liquid-to-Solid Phase Transition of the ALS Protein FUS Accelerated by Disease Mutation. *Cell* **162**, 1066–1077 (2015).
56. Gandelman, M. *et al.* Staufen 1 amplifies proapoptotic activation of the unfolded protein response. *Cell Death Differ.* **27**, 2942–2951 (2020).
57. Verkerk, A. J. M. H. *et al.* Identification of a gene (FMR-1) containing a CGG repeat coincident with a breakpoint cluster region exhibiting length variation in fragile X syndrome. *Cell* **65**, 905–914 (1991).
58. Sutcliffe, J. S. *et al.* DNA methylation represses *FMR-1* transcription in fragile X syndrome. *Hum. Mol. Genet.* **1**, 397–400 (1992).
59. Hunter, J. *et al.* Epidemiology of fragile X syndrome: A systematic review and meta-analysis. *Am. J. Med. Genet. A.* **164**, 1648–1658 (2014).
60. Hartley, S. L. *et al.* Exploring the adult life of men and women with fragile X syndrome: results from a national survey. *Am. J. Intellect. Dev. Disabil.* **116**, 16–35 (2011).
61. Ashley, C. T., Wilkinson, K. D., Reines, D. & Warren, S. T. *FMR1* Protein: Conserved RNP Family Domains and Selective RNA Binding. *Science* **262**, 563–566 (1993).
62. Hinds, H. L. *et al.* Tissue specific expression of FMR–1 provides evidence for a functional role in fragile X syndrome. *Nat. Genet.* **3**, 36–43 (1993).
63. Li, Y. & Zhao, X. Concise Review: Fragile X Proteins in Stem Cell Maintenance and Differentiation. *Stem Cells* **32**, 1724–1733 (2014).
64. Liu, B. *et al.* Regulatory discrimination of mRNAs by FMRP controls mouse adult neural stem cell differentiation. *Proc. Natl. Acad. Sci.* **115**, (2018).
65. Garber, K. B., Visootsak, J. & Warren, S. T. Fragile X syndrome. *Eur. J. Hum. Genet.* **16**, 666–672 (2008).

66. Irwin, S. A. *et al.* Abnormal dendritic spine characteristics in the temporal and visual cortices of patients with fragile-X syndrome: A quantitative examination. *Am. J. Med. Genet.* **98**, 161–167 (2001).
67. Jin, P. *et al.* Biochemical and genetic interaction between the fragile X mental retardation protein and the microRNA pathway. *Nat. Neurosci.* **7**, 113–117 (2004).
68. Lacoux, C. *et al.* BC1-FMRP interaction is modulated by 2′-O-methylation: RNA-binding activity of the tudor domain and translational regulation at synapses. *Nucleic Acids Res.* **40**, 4086–4096 (2012).
69. Zalfa, F. *et al.* The Fragile X Syndrome Protein FMRP Associates with BC1 RNA and Regulates the Translation of Specific mRNAs at Synapses. *Cell* **112**, 317–327 (2003).
70. Kao, D.-I., Aldridge, G. M., Weiler, I. J. & Greenough, W. T. Altered mRNA transport, docking, and protein translation in neurons lacking fragile X mental retardation protein. *Proc. Natl. Acad. Sci.* **107**, 15601–15606 (2010).
71. Dictenberg, J. B., Swanger, S. A., Antar, L. N., Singer, R. H. & Bassell, G. J. A Direct Role for FMRP in Activity-Dependent Dendritic mRNA Transport Links Filopodial-Spine Morphogenesis to Fragile X Syndrome. *Dev. Cell* **14**, 926–939 (2008).
72. Zhang, Y. *et al.* The fragile X mental retardation syndrome protein interacts with novel homologs FXR1 and FXR2. *EMBO J.* **14**, 5358–5366 (1995).
73. Adinolfi, S. *et al.* The N-Terminus of the Fragile X Mental Retardation Protein Contains a Novel Domain Involved in Dimerization and RNA Binding. *Biochemistry* **42**, 10437–10444 (2003).
74. Ramos, A. *et al.* The Structure of the N-Terminal Domain of the Fragile X Mental Retardation Protein: A Platform for Protein-Protein Interaction. *Structure* **14**, 21–31 (2006).
75. Bardoni, B. 82-FIP, a novel FMRP (Fragile X Mental Retardation Protein) interacting protein, shows a cell cycle-dependent intracellular localization. *Hum. Mol. Genet.* **12**, 1689–1698 (2003).
76. Bardoni, B., Schenck, A. & Louis Mandel, J. A Novel RNA-binding Nuclear Protein That Interacts With the Fragile X Mental Retardation (FMR1) Protein. *Hum. Mol. Genet.* **8**, 2557–2566 (1999).

77. Deng, P.-Y. *et al.* FMRP Regulates Neurotransmitter Release and Synaptic Information Transmission by Modulating Action Potential Duration via BK Channels. *Neuron* **77**, 696–711 (2013).
78. Deng, P.-Y. & Klyachko, V. A. Genetic upregulation of BK channel activity normalizes multiple synaptic and circuit defects in a mouse model of fragile X syndrome: BK channels in synaptic and circuit defects in FXS. *J. Physiol.* **594**, 83–97 (2016).
79. Kshatri, A. *et al.* Differential regulation of BK channels by fragile X mental retardation protein. *J. Gen. Physiol.* **152**, e201912502 (2020).
80. Clifton, N. E., Thomas, K. L., Wilkinson, L. S., Hall, J. & Trent, S. FMRP and CYFIP1 at the Synapse and Their Role in Psychiatric Vulnerability. *Complex Psychiatry* **6**, 5–19 (2020).
81. Nicastro, G., Taylor, I. A. & Ramos, A. KH–RNA interactions: back in the groove. *Curr. Opin. Struct. Biol.* **30**, 63–70 (2015).
82. Valverde, R., Edwards, L. & Regan, L. Structure and function of KH domains: Structure and function of KH domains. *FEBS J.* **275**, 2712–2726 (2008).
83. De Boulle, K. *et al.* A point mutation in the FMR-1 gene associated with fragile X mental retardation. *Nat. Genet.* **3**, 31–35 (1993).
84. Feng, Y. *et al.* FMRP Associates with Polyribosomes as an mRNP, and the I304N Mutation of Severe Fragile X Syndrome Abolishes This Association. *Mol. Cell* **1**, 109–118 (1997).
85. Di Marino, D., Achsel, T., Lacoux, C., Falconi, M. & Bagni, C. Molecular dynamics simulations show how the FMRP Ile304Asn mutation destabilizes the KH2 domain structure and affects its function. *J. Biomol. Struct. Dyn.* **32**, 337–350 (2014).
86. Zang, J. B. *et al.* A Mouse Model of the Human Fragile X Syndrome I304N Mutation. *PLoS Genet.* **5**, e1000758 (2009).
87. Ascano, M. *et al.* FMRP targets distinct mRNA sequence elements to regulate protein expression. *Nature* **492**, 382–386 (2012).
88. Suhl, J. A., Chopra, P., Anderson, B. R., Bassell, G. J. & Warren, S. T. Analysis of FMRP mRNA target datasets reveals highly associated mRNAs mediated by G-quadruplex structures formed via clustered WGGA sequences. *Hum. Mol. Genet.* **23**, 5479–5491 (2014).

89. Athar, Y. M. & Joseph, S. RNA-Binding Specificity of the Human Fragile X Mental Retardation Protein. *J. Mol. Biol.* **432**, 3851–3868 (2020).
90. Zhang, G. *et al.* Dynamic FMR1 granule phase switch instructed by m6A modification contributes to maternal RNA decay. *Nat. Commun.* **13**, 859 (2022).
91. Chen, E., Sharma, M. R., Shi, X., Agrawal, R. K. & Joseph, S. Fragile X Mental Retardation Protein Regulates Translation by Binding Directly to the Ribosome. *Mol. Cell* **54**, 407–417 (2014).
92. Starke, E. L., Zius, K. & Barbee, S. A. FXS causing missense mutations disrupt FMRP granule formation, dynamics, and function. *PLOS Genet.* **18**, e1010084 (2022).
93. Calabretta, S. & Richard, S. Emerging Roles of Disordered Sequences in RNA-Binding Proteins. *Trends Biochem. Sci.* **40**, 662–672 (2015).
94. Vasilyev, N. *et al.* Crystal structure reveals specific recognition of a G-quadruplex RNA by a β-turn in the RGG motif of FMRP. *Proc. Natl. Acad. Sci. U. S. A.* **112**, E5391-5400 (2015).
95. Eberhart, D. The fragile X mental retardation protein is a ribonucleoprotein containing both nuclear localization and nuclear export signals. *Hum. Mol. Genet.* **5**, 1083–1091 (1996).
96. Brown, V. *et al.* Microarray Identification of FMRP-Associated Brain mRNAs and Altered mRNA Translational Profiles in Fragile X Syndrome. *Cell* **107**, 477–487 (2001).
97. Darnell, J. C. *et al.* Fragile X Mental Retardation Protein Targets G Quartet mRNAs Important for Neuronal Function. *Cell* **107**, 489–499 (2001).
98. Schaeffer, C. The fragile X mental retardation protein binds specifically to its mRNA via a purine quartet motif. *EMBO J.* **20**, 4803–4813 (2001).
99. Menon, L., Mader, S. A. & Mihailescu, M.-R. Fragile X mental retardation protein interactions with the microtubule associated protein 1B RNA. *RNA* **14**, 1644–1655 (2008).
100. Menon, L. & Mihailescu, M.-R. Interactions of the G quartet forming semaphorin 3F RNA with the RGG box domain of the fragile X protein family. *Nucleic Acids Res.* **35**, 5379–5392 (2007).
101. Zalfa, F. *et al.* A new function for the fragile X mental retardation protein in regulation of PSD-95 mRNA stability. *Nat. Neurosci.* **10**, 578–587 (2007).

102. Zalfa, F. *et al.* Fragile X Mental Retardation Protein (FMRP) Binds Specifically to the Brain Cytoplasmic RNAs BC1/BC200 via a Novel RNA-binding Motif. *J. Biol. Chem.* **280**, 33403–33410 (2005).

103. Blackwell, E., Zhang, X. & Ceman, S. Arginines of the RGG box regulate FMRP association with polyribosomes and mRNA. *Hum. Mol. Genet.* **19**, 1314–1323 (2010).

104. Mazroui, R. Fragile X Mental Retardation protein determinants required for its association with polyribosomal mRNPs. *Hum. Mol. Genet.* **12**, 3087–3096 (2003).

105. Athar, Y. M. & Joseph, S. The Human Fragile X Mental Retardation Protein Inhibits the Elongation Step of Translation through Its RGG and C-Terminal Domains. *Biochemistry* **59**, 3813–3822 (2020).

106. Blice-Baum, A. C. & Mihailescu, M.-R. Biophysical characterization of G-quadruplex forming *FMR1* mRNA and of its interactions with different fragile X mental retardation protein isoforms. *RNA* **20**, 103–114 (2014).

107. Mestre-Fos, S. *et al.* G-Quadruplexes in Human Ribosomal RNA. *J. Mol. Biol.* **431**, 1940–1955 (2019).

108. Taha, M. S. *et al.* Novel FMRP interaction networks linked to cellular stress. *FEBS J.* **288**, 837–860 (2021).

109. Musco, G. *et al.* Three-Dimensional Structure and Stability of the KH Domain: Molecular Insights into the Fragile X Syndrome. *Cell* **85**, 237–245 (1996).

110. Pozdnyakova, I. & Regan, L. New insights into Fragile X syndrome: Relating genotype to phenotype at the molecular level. *FEBS J.* **272**, 872–878 (2005).

111. Leffers, H., Dejgaard, K. & Celis, J. E. Characterisation of two major cellular poly(rC)-binding human proteins, each containing three K-homologous (KH) domains. *Eur. J. Biochem.* **230**, 447–453 (1995).

112. Castrén, M., Haapasalo, A., Oostra, B. A. & Castrén, E. Subcellular Localization of Fragile X Mental Retardation Protein with the I304N Mutation in the RNA-Binding Domain in Cultured Hippocampal Neurons. *Cell. Mol. Neurobiol.* **21**, 29–38 (2001).

113. Myrick, L. K. *et al.* Independent role for presynaptic FMRP revealed by an *FMR1* missense mutation associated with intellectual disability and seizures. *Proc. Natl. Acad. Sci.* **112**, 949–956 (2015).

114. Suhl, J. A. & Warren, S. T. Single-Nucleotide Mutations in *FMR1* Reveal Novel Functions and Regulatory Mechanisms of the Fragile X Syndrome Protein FMRP. *J. Exp. Neurosci.* **9s2**, JEN.S25524 (2015).

115. Santorelli, D. *et al.* Folding Mechanism and Aggregation Propensity of the KH0 Domain of FMRP and Its R138Q Pathological Variant. *Int. J. Mol. Sci.* **23**, 12178 (2022).

116. Myrick, L. K. *et al.* Fragile X syndrome due to a missense mutation. *Eur. J. Hum. Genet.* **22**, 1185–1189 (2014).

117. Bear, M. F., Huber, K. M. & Warren, S. T. The mGluR theory of fragile X mental retardation. *Trends Neurosci.* **27**, 370–377 (2004).

118. Martin, L., Latypova, X. & Terro, F. Post-translational modifications of tau protein: Implications for Alzheimer's disease. *Neurochem. Int.* **58**, 458–471 (2011).

119. Xu, H. *et al.* PTMD: A Database of Human Disease-associated Post-translational Modifications. *Genomics Proteomics Bioinformatics* **16**, 244–251 (2018).

120. Coffee, R. L. *et al.* In vivo neuronal function of the fragile X mental retardation protein is regulated by phosphorylation. *Hum. Mol. Genet.* **21**, 900–915 (2012).

121. Pronot, M. *et al.* Bidirectional regulation of synaptic SUMOylation by Group 1 metabotropic glutamate receptors. *Cell. Mol. Life Sci.* **79**, 378 (2022).

122. Huber, K. M., Roder, J. C. & Bear, M. F. Chemical Induction of mGluR5- and Protein Synthesis–Dependent Long-Term Depression in Hippocampal Area CA1. *J. Neurophysiol.* **86**, 321–325 (2001).

123. Weiler, I. J. *et al.* Fragile X mental retardation protein is translated near synapses in response to neurotransmitter activation. *Proc. Natl. Acad. Sci.* **94**, 5395–5400 (1997).

124. Huang, J., Ikeuchi, Y., Malumbres, M. & Bonni, A. A Cdh1-APC/FMRP Ubiquitin Signaling Link Drives mGluR-Dependent Synaptic Plasticity in the Mammalian Brain. *Neuron* **86**, 726–739 (2015).

125. Niere, F., Wilkerson, J. R. & Huber, K. M. Evidence for a Fragile X Mental Retardation Protein-Mediated Translational Switch in Metabotropic Glutamate Receptor-Triggered Arc Translation and Long-Term Depression. *J. Neurosci.* **32**, 5924–5936 (2012).

126. Muddashetty, R. S. *et al.* Reversible inhibition of PSD-95 mRNA translation by miR-125a, FMRP phosphorylation, and mGluR signaling. *Mol. Cell* **42**, 673–688 (2011).

127. Bartley, C. M., O'Keefe, R. A. & Bordey, A. FMRP S499 Is Phosphorylated Independent of mTORC1-S6K1 Activity. *PLoS ONE* **9**, e96956 (2014).

128. Bartley, C. M. *et al.* Mammalian FMRP S499 Is Phosphorylated by CK2 and Promotes Secondary Phosphorylation of FMRP. *eneuro* **3**, ENEURO.0092-16.2016 (2016).

129. Siomi, M. C., Higashijima, K., Ishizuka, A. & Siomi, H. Casein kinase II phosphorylates the fragile X mental retardation protein and modulates its biological properties. *Mol. Cell. Biol.* **22**, 8438–8447 (2002).

130. Tsang, B. *et al.* Phosphoregulated FMRP phase separation models activity-dependent translation through bidirectional control of mRNA granule formation. *Proc. Natl. Acad. Sci.* **116**, 4218–4227 (2019).

131. Bedford, M. T. & Clarke, S. G. Protein Arginine Methylation in Mammals: Who, What, and Why. *Mol. Cell* **33**, 1–13 (2009).

132. Henley, J. M., Craig, T. J. & Wilkinson, K. A. Neuronal SUMOylation: Mechanisms, Physiology, and Roles in Neuronal Dysfunction. *Physiol. Rev.* **94**, 1249–1285 (2014).

133. Schorova, L. & Martin, S. Sumoylation in Synaptic Function and Dysfunction. *Front. Synaptic Neurosci.* **8**, (2016).

134. Khayachi, A. *et al.* Sumoylation regulates FMRP-mediated dendritic spine elimination and maturation. *Nat. Commun.* **9**, 757 (2018).

135. Kerscher, O. SUMO junction—what's your function?: New insights through SUMO-interacting motifs. *EMBO Rep.* **8**, 550–555 (2007).

136. Meulmeester, E. & Melchior, F. SUMO. *Nature* **452**, 709–711 (2008).

137. Zhang, J. *et al.* Expression and Characterization of Human Fragile X Mental Retardation Protein Isoforms and Interacting Proteins in Human Cells. *Proteomics Insights* **10**, 117864181882526 (2019).

138. Polevoda, B. & Sherman, F. Nα-terminal Acetylation of Eukaryotic Proteins. *J. Biol. Chem.* **275**, 36479–36482 (2000).

139. Khandjian, E. W. *et al.* Biochemical evidence for the association of fragile X mental retardation protein with brain polyribosomal ribonucleoparticles. *Proc. Natl. Acad. Sci.* **101**, 13357–13362 (2004).

140. Khandjian, E. W., Corbin, F., Woerly, S. & Rousseau, F. The fragile X mental retardation protein is associated with ribosomes. *Nat. Genet.* **12**, 91–93 (1996).

141. Zalfa, F., Achsel, T. & Bagni, C. mRNPs, polysomes or granules: FMRP in neuronal protein synthesis. *Curr. Opin. Neurobiol.* **16**, 265–269 (2006).

142. Antar, L. N., Li, C., Zhang, H., Carroll, R. C. & Bassell, G. J. Local functions for FMRP in axon growth cone motility and activity-dependent regulation of filopodia and spine synapses. *Mol. Cell. Neurosci.* **32**, 37–48 (2006).

143. De Diego Otero, Y. *et al.* Transport of Fragile X Mental Retardation Protein via Granules in Neurites of PC12 Cells. *Mol. Cell. Biol.* **22**, 8332–8341 (2002).

144. Davidovic, L. *et al.* The fragile X mental retardation protein is a molecular adaptor between the neurospecific KIF3C kinesin and dendritic RNA granules. *Hum. Mol. Genet.* **16**, 3047–3058 (2007).

145. Huang, Y.-S., Carson, J. H., Barbarese, E. & Richter, J. D. Facilitation of dendritic mRNA transport by CPEB. *Genes Dev.* **17**, 638–653 (2003).

146. Kanai, Y., Dohmae, N. & Hirokawa, N. Kinesin Transports RNA. *Neuron* **43**, 513–525 (2004).

147. Lindsay, A. J. & McCaffrey, M. W. Myosin Va is required for the transport of fragile X mental retardation protein (FMRP) granules: Myosin Va transports FMRP. *Biol. Cell* **106**, 57–71 (2014).

148. Ling, S.-C., Fahrner, P. S., Greenough, W. T. & Gelfand, V. I. Transport of *Drosophila* fragile X mental retardation protein-containing ribonucleoprotein granules by kinesin-1 and cytoplasmic dynein. *Proc. Natl. Acad. Sci.* **101**, 17428–17433 (2004).

149. Akins, M. R. *et al.* Axonal ribosomes and mRNAs associate with fragile X granules in adult rodent and human brains. *Hum. Mol. Genet.* ddw381 (2017) doi:10.1093/hmg/ddw381.

150. Napoli, I. *et al.* The Fragile X Syndrome Protein Represses Activity-Dependent Translation through CYFIP1, a New 4E-BP. *Cell* **134**, 1042–1054 (2008).

151. Matsuo, H. *et al.* Structure of translation factor eIF4E bound to m7GDP and interaction with 4E-binding protein. *Nat. Struct. Biol.* **4**, 717–724 (1997).

152. Buchan, J. R. & Stansfield, I. Halting a cellular production line: responses to ribosomal pausing during translation. *Biol. Cell* **99**, 475–487 (2007).

153. Nawalpuri, B., Ravindran, S. & Muddashetty, R. S. The Role of Dynamic miRISC During Neuronal Development. *Front. Mol. Biosci.* **7**, 8 (2020).

154. Lin, S.-L. microRNAs and Fragile X Syndrome. in *microRNA: Medical Evidence* (ed. Santulli, G.) vol. 888 107–121 (Springer International Publishing, 2015).

155. Richter, J. D. & Zhao, X. The molecular biology of FMRP: new insights into fragile X syndrome. *Nat. Rev. Neurosci.* **22**, 209–222 (2021).

156. Shi, Y., Kirwan, P. & Livesey, F. J. Directed differentiation of human pluripotent stem cells to cerebral cortex neurons and neural networks. *Nat. Protoc.* **7**, 1836–1846 (2012).

157. Khatter, H., Myasnikov, A. G., Natchiar, S. K. & Klaholz, B. P. Structure of the human 80S ribosome. *Nature* **520**, 640–645 (2015).

158. Darnell, J. C. *et al.* FMRP Stalls Ribosomal Translocation on mRNAs Linked to Synaptic Function and Autism. *Cell* **146**, 247–261 (2011).

159. Runge, K., Cardoso, C. & de Chevigny, A. Dendritic Spine Plasticity: Function and Mechanisms. *Front. Synaptic Neurosci.* **12**, 36 (2020).

160. Kasai, H., Fukuda, M., Watanabe, S., Hayashi-Takagi, A. & Noguchi, J. Structural dynamics of dendritic spines in memory and cognition. *Trends Neurosci.* **33**, 121–129 (2010).

161. Rangaraju, V., tom Dieck, S. & Schuman, E. M. Local translation in neuronal compartments: how local is local? *EMBO Rep.* **18**, 693–711 (2017).

162. Kiebler, M. A. & Bassell, G. J. Neuronal RNA Granules: Movers and Makers. *Neuron* **51**, 685–690 (2006).

163. Christie, S. B., Akins, M. R., Schwob, J. E. & Fallon, J. R. The FXG: A Presynaptic Fragile X Granule Expressed in a Subset of Developing Brain Circuits. *J. Neurosci.* **29**, 1514–1524 (2009).

164. Kim, T. H. *et al.* Phospho-dependent phase separation of FMRP and CAPRIN1 recapitulates regulation of translation and deadenylation. *Science* **365**, 825–829 (2019).

165. Bassell, G. J. & Warren, S. T. Fragile X Syndrome: Loss of Local mRNA Regulation Alters Synaptic Development and Function. *Neuron* **60**, 201–214 (2008).

166. Chen, J., Yu, S., Fu, Y. & Li, X. Synaptic proteins and receptors defects in autism spectrum disorders. *Front. Cell. Neurosci.* **8**, (2014).

167. Darnell, J. C. *et al.* FMRP Stalls Ribosomal Translocation on mRNAs Linked to Synaptic Function and Autism. *Cell* **146**, 247–261 (2011).
168. DeMarco, B. *et al.* FMRP - G-quadruplex mRNA - miR-125a interactions: Implications for miR-125a mediated translation regulation of PSD-95 mRNA. *PloS One* **14**, e0217275 (2019).
169. Didiot, M.-C., Subramanian, M., Flatter, E., Mandel, J.-L. & Moine, H. Cells lacking the fragile X mental retardation protein (FMRP) have normal RISC activity but exhibit altered stress granule assembly. *Mol. Biol. Cell* **20**, 428–437 (2009).
170. Till, S. M. The developmental roles of FMRP. *Biochem. Soc. Trans.* **38**, 507–510 (2010).
171. Khalfallah, O. *et al.* Depletion of the Fragile X Mental Retardation Protein in Embryonic Stem Cells Alters the Kinetics of Neurogenesis. *Stem Cells Dayt. Ohio* **35**, 374–385 (2017).
172. Telias, M., Segal, M. & Ben-Yosef, D. Neural differentiation of fragile X human embryonic stem cells reveals abnormal patterns of development despite successful neurogenesis. *Dev. Biol.* **374**, 32–45 (2013).
173. Luo, Y. *et al.* Fragile X Mental Retardation Protein Regulates Proliferation and Differentiation of Adult Neural Stem/Progenitor Cells. *PLoS Genet.* **6**, e1000898 (2010).
174. Shi, Y., Kirwan, P. & Livesey, F. J. Directed differentiation of human pluripotent stem cells to cerebral cortex neurons and neural networks. *Nat. Protoc.* **7**, 1836–1846 (2012).
175. Brameier, M., Herwig, A., Reinhardt, R., Walter, L. & Gruber, J. Human box C/D snoRNAs with miRNA like functions: expanding the range of regulatory RNAs. *Nucleic Acids Res.* **39**, 675–686 (2011).
176. Falaleeva, M., Welden, J. R., Duncan, M. J. & Stamm, S. C/D-box snoRNAs form methylating and non-methylating ribonucleoprotein complexes: Old dogs show new tricks. *BioEssays* **39**, 1600264 (2017).
177. Henras, A. K., Plisson-Chastang, C., O'Donohue, M.-F., Chakraborty, A. & Gleizes, P.-E. An overview of pre-ribosomal RNA processing in eukaryotes: Pre-ribosomal RNA processing in eukaryotes. *Wiley Interdiscip. Rev. RNA* **6**, 225–242 (2015).

178. Prusiner, P., Yathindra, N. & Sundaralingam, M. Effect of ribose O(2′)-methylation on the conformation of nucleosides and nucleotides. *Biochim. Biophys. Acta BBA - Nucleic Acids Protein Synth.* **366**, 115–123 (1974).
179. Bachellerie, J.-P. & Cavaillé, J. Guiding ribose methylation of rRNA. *Trends Biochem. Sci.* **22**, 257–261 (1997).
180. Kiss-László, Z., Henry, Y., Bachellerie, J.-P., Caizergues-Ferrer, M. & Kiss, T. Site-Specific Ribose Methylation of Preribosomal RNA: A Novel Function for Small Nucleolar RNAs. *Cell* **85**, 1077–1088 (1996).
181. Shubina, M. Y., Musinova, Y. R. & Sheval, E. V. Nucleolar methyltransferase fibrillarin: Evolution of structure and functions. *Biochem. Mosc.* **81**, 941–950 (2016).
182. Krogh, N. *et al.* Profiling of 2′- *O* -Me in human rRNA reveals a subset of fractionally modified positions and provides evidence for ribosome heterogeneity. *Nucleic Acids Res.* **44**, 7884–7895 (2016).
183. Incarnato, D. *et al.* High-throughput single-base resolution mapping of RNA 2′-O-methylated residues. *Nucleic Acids Res.* **45**, 1433–1441 (2017).
184. Machnicka, M. A. *et al.* MODOMICS: a database of RNA modification pathways—2013 update. *Nucleic Acids Res.* **41**, D262–D267 (2012).
185. *RNA methylation: methods and protocols*. (Humana Press, 2017).
186. Marchand, V. *et al.* High-Throughput Mapping of 2′-O-Me Residues in RNA Using Next-Generation Sequencing (Illumina RiboMethSeq Protocol). in *RNA Methylation* (ed. Lusser, A.) vol. 1562 171–187 (Springer New York, 2017).
187. Lafontaine, D. L. J. Noncoding RNAs in eukaryotic ribosome biogenesis and function. *Nat. Struct. Mol. Biol.* **22**, 11–19 (2015).
188. Narayanan, U. *et al.* FMRP Phosphorylation Reveals an Immediate-Early Signaling Pathway Triggered by Group I mGluR and Mediated by PP2A. *J. Neurosci.* **27**, 14349–14357 (2007).
189. Baumann, K. mRNA translation in stress granules is not uncommon. *Nat. Rev. Mol. Cell Biol.* **22**, 164–164 (2021).
190. El Fatimy, R. *et al.* Tracking the Fragile X Mental Retardation Protein in a Highly Ordered Neuronal RiboNucleoParticles Population: A Link between Stalled Polyribosomes and RNA Granules. *PLOS Genet.* **12**, e1006192 (2016).
191. Willemsen, R. *et al.* Association of FMRP with Ribosomal Precursor Particles in the Nucleolus. *Biochem. Biophys. Res. Commun.* **225**, 27–33 (1996).

192. Mateju, D. *et al.* Single-Molecule Imaging Reveals Translation of mRNAs Localized to Stress Granules. *Cell* **183**, 1801-1812.e13 (2020).
193. Bechara, E. G. *et al.* A Novel Function for Fragile X Mental Retardation Protein in Translational Activation. *PLoS Biol.* **7**, e1000016 (2009).
194. Cavaillé, J., Nicoloso, M. & Bachellerie, J.-P. Targeted ribose methylation of RNA in vivo directed by tailored antisense RNA guides. *Nature* **383**, 732–735 (1996).
195. Ojha, S., Malla, S. & Lyons, S. M. snoRNPs: Functions in Ribosome Biogenesis. *Biomolecules* **10**, 783 (2020).
196. Genuth, N. R. & Barna, M. The Discovery of Ribosome Heterogeneity and Its Implications for Gene Regulation and Organismal Life. *Mol. Cell* **71**, 364–374 (2018).
197. Shi, Z. *et al.* Heterogeneous Ribosomes Preferentially Translate Distinct Subpools of mRNAs Genome-wide. *Mol. Cell* **67**, 71-83.e7 (2017).
198. Motorin, Y., Quinternet, M., Rhalloussi, W. & Marchand, V. Constitutive and variable 2'-O-methylation (Nm) in human ribosomal RNA. *RNA Biol.* **18**, 88–97 (2021).
199. Prieto, M., Folci, A. & Martin, S. Post-translational modifications of the Fragile X Mental Retardation Protein in neuronal function and dysfunction. *Mol. Psychiatry* **25**, 1688–1703 (2020).
200. Basu, S. & Bahadur, R. P. A structural perspective of RNA recognition by intrinsically disordered proteins. *Cell. Mol. Life Sci.* **73**, 4075–4084 (2016).
201. Fuxreiter, M., Simon, I., Friedrich, P. & Tompa, P. Preformed Structural Elements Feature in Partner Recognition by Intrinsically Unstructured Proteins. *J. Mol. Biol.* **338**, 1015–1026 (2004).

List of publications

1. Function of FMRP Domains in Regulating Distinct Roles of Neuronal Protein Synthesis. **D'Souza MN**, Ramakrishna S, Radhakrishna BK, Jhaveri V, Ravindran S, Yeramala L, Nair D, Palakodeti D, Muddashetty RS.Mol Neurobiol. 2022 Oct 1. doi: 10.1007/s12035-022-03049-1. Online ahead of print. PMID: 36181660.
2. A perspective on molecular signalling dysfunction, its clinical relevance and therapeutics in autism spectrum disorder. Purushotham SS, Reddy NMN, **D'Souza MN**, Choudhury NR, Ganguly A, Gopalakrishna N, Muddashetty R, Clement JP.Exp Brain Res. 2022 Oct;240(10):2525-2567. doi: 10.1007/s00221-022-06448-x. Epub 2022 Sep 5.PMID: 36063192 Review.
3. FMRP Interacts with C/D Box snoRNA in the Nucleus and Regulates Ribosomal RNA Methylation. **D'Souza MN**, Gowda NKC, Tiwari V, Babu RO, Anand P, Dastidar SG, Singh R, James OG, Selvaraj B, Pal R, Ramesh A, Chattarji S, Chandran S, Gulyani A, Palakodeti D, Muddashetty RS.iScience. 2019 Feb 22;12:368. doi: 10.1016/j.isci.2019.01.026. Epub 2019 Feb 11.PMID: 30763793